Chapter 3

Mass Transfer and Diffusion

§3.0 INSTRUCTIONAL OBJECTIVES

After completing this chapter, you should be able to:

- Explain the relationship between mass transfer and phase equilibrium, and why models for both are useful.
- Discuss mechanisms of mass transfer, including bulk flow.
- State Fick's law of diffusion for binary mixtures and discuss its analogy to Fourier's law of heat conduction.
- Estimate, in the absence of data, diffusivities for gas, liquid, and solid mixtures.
- Calculate multidimensional, unsteady-state molecular diffusion by analogy to heat conduction.
- Calculate rates of mass transfer by molecular diffusion in laminar flow for three common cases.
- Define a mass-transfer coefficient and explain its analogy to the heat-transfer coefficient.
- Use analogies, particularly those of Chilton and Colburn, and Churchill et al., to calculate rates of mass transfer in turbulent flow.
- Calculate rates of mass transfer across fluid–fluid interfaces using two-film theory and penetration theory.
- Relate molecular motion to potentials arising from chemical, pressure, thermal, gravitational, electrostatic, and friction forces.
- Compare the Maxwell–Stefan formulation with Fick's law for mass transfer.
- Use simplified forms of the Maxwell–Stefan relations to characterize mass transport due to chemical, pressure, thermal, centripetal, electrostatic, and friction forces.
- Use a linearized form of the Maxwell–Stefan relations to describe film mass transfer in stripping and membrane polarization.

M*ass transfer* is the net movement of a species in a mixture from one location to another. In separation operations, the transfer often takes place across an interface between phases. Absorption by a liquid of a solute from a carrier gas involves transfer of the solute through the gas to the gas–liquid interface, across the interface, and into the liquid. Mathematical models for this process—as well as others such as mass transfer of a species through a gas to the surface of a porous, adsorbent particle—are presented in this book.

Two mechanisms of mass transfer are: (1) *molecular diffusion* by random and spontaneous microscopic movement of molecules as a result of thermal motion; and (2) *eddy* (turbulent) *diffusion* by random, macroscopic fluid motion. Both molecular and eddy diffusion may involve the movement of different species in opposing directions. When a bulk flow occurs, the total rate of mass transfer of individual species is increased or decreased by this *bulk flow*, which is a third mechanism of mass transfer.

Molecular diffusion is extremely slow; eddy diffusion is orders of magnitude more rapid. Therefore, if industrial separation processes are to be conducted in equipment of reasonable size, the fluids must be agitated and interfacial areas maximized. For solids, the particle size is decreased to increase the area for mass transfer and decrease the distance for diffusion.

In multiphase systems the extent of the separation is limited by phase equilibrium because, with time, concentrations equilibrate by mass transfer. When mass transfer is rapid, equilibration takes seconds or minutes, and design of separation equipment is based on phase equilibrium, not mass transfer. For separations involving barriers such as membranes, mass-transfer rates govern equipment design.

Diffusion of species A with respect to B occurs because of driving forces, which include gradients of species concentration (ordinary diffusion), pressure, temperature (thermal diffusion), and external force fields that act unequally on different species. Pressure diffusion requires a large gradient, which is achieved for gas mixtures with a centrifuge. Thermal diffusion columns can be employed to separate mixtures by establishing a temperature gradient. More widely applied is forced diffusion of ions in an electrical field.

This chapter begins by describing only molecular diffusion driven by concentration gradients, which is the most common type of diffusion in chemical separation processes.

Emphasis is on binary systems, for which molecular-diffusion theory is relatively simple and applications are straightforward. The other types of diffusion are introduced in §3.8 because of their importance in bioseparations. Multicomponent ordinary diffusion is considered briefly in Chapter 12. It is a more appropriate topic for advanced study using texts such as Taylor and Krishna [1].

Molecular diffusion occurs in fluids that are stagnant, or in laminar or turbulent motion. Eddy diffusion occurs in fluids when turbulent motion exists. When both molecular diffusion and eddy diffusion occur, they are additive. When mass transfer occurs under bulk turbulent flow but across an interface or to a solid surface, flow is generally laminar or stagnant near the interface or solid surface. Thus, the eddy-diffusion mechanism is dampened or eliminated as the interface or solid surface is approached.

Mass transfer can result in a total net rate of bulk flow or flux in a direction relative to a fixed plane or stationary coordinate system. When a net flux occurs, it carries all species present. Thus, the molar flux of a species is the sum of all three mechanisms. If N_i is the molar flux of i with mole fraction x_i, and N is the total molar flux in moles per unit time per unit area in a direction perpendicular to a stationary plane across which mass transfer occurs, then

$$\begin{aligned} N_i = {} & \text{molecular diffusion flux of } i \\ & + \text{eddy diffusion flux of } i + x_i N \end{aligned} \tag{3-1}$$

where $x_i N$ *is* the bulk-flow flux. Each term in (3-1) is positive or negative depending on the direction of the flux relative to the direction selected as positive. When the molecular and eddy-diffusion fluxes are in one direction and N is in the opposite direction (even though a gradient of i exists), the net species mass-transfer flux, N_i, can be zero.

This chapter covers eight areas: (1) steady-state diffusion in stagnant media, (2) estimation of diffusion coefficients, (3) unsteady-state diffusion in stagnant media, (4) mass transfer in laminar flow, (5) mass transfer in turbulent flow, (6) mass transfer at fluid–fluid interfaces, (7) mass transfer across fluid–fluid interfaces, and (8) molecular mass transfer in terms of different driving forces in bioseparations.

§3.1 STEADY-STATE, ORDINARY MOLECULAR DIFFUSION

Imagine a cylindrical glass vessel partly filled with dyed water. Clear water is carefully added on top so that the dyed solution on the bottom is undisturbed. At first, a sharp boundary exists between layers, but as mass transfer of the dye occurs, the upper layer becomes colored and the layer below less colored. The upper layer is more colored near the original interface and less colored in the region near the top. During this color change, the motion of each dye molecule is random, undergoing collisions with water molecules and sometimes with dye molecules, moving first in one direction and then in another, with no one direction preferred. This type of motion is sometimes called a *random-walk process*, which yields a mean-square distance of travel in a time interval but not in a direction interval. At a given horizontal plane through the solution, it is not possible to determine whether, in a given time interval, a molecule will cross the plane or not. On the average, a fraction of all molecules in the solution below the plane cross over into the region above and the same fraction will cross over in the opposite direction. Therefore, if the concentration of dye in the lower region is greater than that in the upper region, a net rate of mass transfer of dye takes place from the lower to the upper region. Ultimately, a dynamic equilibrium is achieved and the dye concentration will be uniform throughout. Based on these observations, it is clear that:

1. Mass transfer by ordinary molecular diffusion in a binary mixture occurs because of a concentration gradient; that is, a species diffuses in the direction of decreasing concentration.
2. The mass-transfer rate is proportional to the area normal to the direction of mass transfer. Thus, the rate can be expressed as a flux.
3. Net transfer stops when concentrations are uniform.

§3.1.1 Fick's Law of Diffusion

The three observations above were quantified by Fick in 1855. He proposed an analogy to Fourier's 1822 first law of heat conduction,

$$q_z = -k\frac{dT}{dz} \tag{3-2}$$

where q_z is the heat flux by conduction in the z-direction, k is the thermal conductivity, and dT/dz is the temperature gradient, which is negative in the direction of heat conduction. Fick's first law also features a proportionality between a flux and a gradient. For a mixture of A and B,

$$\boxed{J_{A_z} = -D_{AB}\frac{dc_A}{dz}} \tag{3-3a}$$

and

$$\boxed{J_{B_z} = -D_{BA}\frac{dc_B}{dz}} \tag{3-3b}$$

where J_{A_z} is the molar flux of A by ordinary molecular diffusion relative to the molar-average velocity of the mixture in the z-direction, D_{AB} is the *mutual diffusion coefficient* or *diffusivity* of A in B, c_A is the molar concentration of A, and dc_A/dz the concentration gradient of A, which is negative in the direction of diffusion. Similar definitions apply to (3-3b). The fluxes of A and B are in opposite directions. If the medium through which diffusion occurs is isotropic, then values of k and D_{AB} are independent of direction. Nonisotropic (anisotropic) materials include fibrous and composite solids as well as noncubic crystals.

Alternative driving forces and concentrations can be used in (3-3a) and (3-3b). An example is

$$J_A = -cD_{AB}\frac{dx_A}{dz} \tag{3-4}$$

where the z subscript on J has been dropped, c = total molar concentration, and x_A = mole fraction of A.

Equation (3-4) can also be written in an equivalent mass form, where j_A is the mass flux of A relative to the mass-average velocity of the mixture in the positive z-direction, ρ is the mass density, and w_A is the mass fraction of A:

$$j_A = -\rho D_{AB} \frac{dw_A}{dz} \tag{3-5}$$

§3.1.2 Species Velocities in Diffusion

If velocities are based on the molar flux, N, and the molar diffusion flux, J, then the molar average mixture velocity, v_M, relative to stationary coordinates for the binary mixture, is

$$v_M = \frac{N}{c} = \frac{N_A + N_B}{c} \tag{3-6}$$

Similarly, the velocity of species i in terms of N_i, relative to stationary coordinates, is:

$$v_i = \frac{N_i}{c_i} \tag{3-7}$$

Combining (3-6) and (3-7) with $x_i = c_i/c$ gives

$$v_M = x_A v_A + x_B v_B \tag{3-8}$$

Diffusion velocities, v_{i_D}, defined in terms of J_i, are relative to molar-average velocity and are defined as the difference between the species velocity and the molar-average mixture velocity:

$$v_{i_D} = \frac{J_i}{c_i} = v_i - v_M \tag{3-9}$$

When solving mass-transfer problems involving net mixture movement (bulk flow), fluxes and flow rates based on v_M as the frame of reference are inconvenient to use. It is thus preferred to use mass-transfer fluxes referred to stationary coordinates. Thus, from (3-9), the total species velocity is

$$v_i = v_M + v_{i_D} \tag{3-10}$$

Combining (3-7) and (3-10),

$$N_i = c_i v_M + c_i v_{i_D} \tag{3-11}$$

Combining (3-11) with (3-4), (3-6), and (3-7),

$$\boxed{N_A = \frac{n_A}{A} = x_A N - cD_{AB}\left(\frac{dx_A}{dz}\right)} \tag{3-12}$$

and

$$\boxed{N_B = \frac{n_B}{A} = x_B N - cD_{BA}\left(\frac{dx_B}{dz}\right)} \tag{3-13}$$

In (3-12) and (3-13), n_i is the molar flow rate in moles per unit time, A is the mass-transfer area, the first right-hand side terms are the fluxes resulting from bulk flow, and the second terms are the diffusion fluxes. Two cases are important: (1) equimolar counterdiffusion (EMD); and (2) unimolecular diffusion (UMD).

§3.1.3 Equimolar Counterdiffusion (EMD)

In EMD, the molar fluxes in (3-12) and (3-13) are equal but opposite in direction, so

$$N = N_A + N_B = 0 \tag{3-14}$$

Thus, from (3-12) and (3-13), the diffusion fluxes are also equal but opposite in direction:

$$J_A = -J_B \tag{3-15}$$

This idealization is approached in distillation of binary mixtures, as discussed in Chapter 7. From (3-12) and (3-13), in the absence of bulk flow,

$$N_A = J_A = -cD_{AB}\left(\frac{dx_A}{dz}\right) \tag{3-16}$$

and

$$N_B = J_B = -cD_{BA}\left(\frac{dx_B}{dz}\right) \tag{3-17}$$

If the total concentration, pressure, and temperature are constant and the mole fractions are constant (but different) at two sides of a stagnant film between z_1 and z_2, then (3-16) and (3-17) can be integrated from z_1 to any z between z_1 and z_2 to give

$$J_A = \frac{cD_{AB}}{z - z_1}(x_{A_1} - x_A) \tag{3-18}$$

and

$$J_B = \frac{cD_{BA}}{z - z_1}(x_{B_1} - x_B) \tag{3-19}$$

At steady state, the mole fractions are linear in distance, as shown in Figure 3.1a. Furthermore, because total

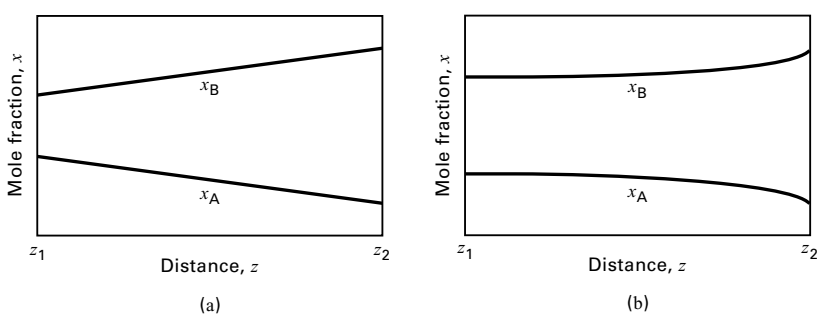

Figure 3.1 Concentration profiles for limiting cases of ordinary molecular diffusion in binary mixtures across a stagnant film: (a) equimolar counterdiffusion (EMD); (b) unimolecular diffusion (UMD).

concentration c is constant through the film, where

$$c = c_A + c_B \tag{3-20}$$

by differentiation,

$$dc = 0 = dc_A + dc_B \tag{3-21}$$

Thus,

$$dc_A = -dc_B \tag{3-22}$$

From (3-3a), (3-3b), (3-15), and (3-22),

$$\frac{D_{AB}}{dz} = \frac{D_{BA}}{dz} \tag{3-23}$$

Therefore, $D_{AB} = D_{BA}$. This equality of diffusion coefficients is always true in a binary system.

EXAMPLE 3.1 EMD in a Tube.

Two bulbs are connected by a straight tube, 0.001 m in diameter and 0.15 m in length. Initially the bulb at End 1 contains N_2 and the bulb at End 2 contains H_2. Pressure and temperature are constant at 25°C and 1 atm. At a time after diffusion starts, the nitrogen content of the gas at End 1 of the tube is 80 mol% and at End 2 is 25 mol%. If the binary diffusion coefficient is 0.784 cm^2/s, determine:

(a) The rates and directions of mass transfer in mol/s

(b) The species velocities relative to stationary coordinates, in cm/s

Solution

(a) Because the gas system is closed and at constant pressure and temperature, no bulk flow occurs and mass transfer in the connecting tube is EMD.

The area for mass transfer through the tube, in cm^2, is $A = 3.14(0.1)^2/4 = 7.85 \times 10^{-3}$ cm^2. By the ideal gas law, the total gas concentration (molar density) is $c = \frac{P}{PT} = \frac{1}{(82.06)(298)} = 4.09 \times 10^{-5}$ mol/cm^3. Take as the reference plane End 1 of the connecting tube. Applying (3-18) to N_2 over the tube length,

$$\begin{aligned} n_{N_2} &= \frac{cD_{N_2,H_2}}{z_2 - z_1}\left[(x_{N_2})_1 - (x_{N_2})_2\right]A \\ &= \frac{(4.09 \times 10^{-5})(0.784)(0.80 - 0.25)}{15}(7.85 \times 10^{-3}) \\ &= 9.23 \times 10^{-9} \text{ mol/s in the positive } z\text{-direction} \\ n_{H_2} &= 9.23 \times 10^{-9} \text{ mol/s in the negative } z\text{-direction} \end{aligned}$$

(b) For EMD, the molar-average velocity of the mixture, υ_M, is 0. Therefore, from (3-9), species velocities are equal to species diffusion velocities. Thus,

$$\begin{aligned} \upsilon_{N_2} &= (\upsilon_{N_2})_D = \frac{J_{N_2}}{c_{N_2}} = \frac{n_{N_2}}{Acx_{N_2}} \\ &= \frac{9.23 \times 10^{-9}}{[(7.85 \times 10^{-3})(4.09 \times 10^{-5})x_{N_2}]} \\ &= \frac{0.0287}{x_{N_2}} \quad \text{in the positive } z\text{-direction} \end{aligned}$$

Similarly, $\upsilon_{H_2} = \dfrac{0.0287}{x_{H_2}}$ in the negative z-direction

Thus, species velocities depend on mole fractions, as follows:

z, cm	x_{N_2}	x_{H_2}	υ_{N_2},cm/s	υ_{H_2},cm/s
0 (End 1)	0.800	0.200	0.0351	−0.1435
5	0.617	0.383	0.0465	−0.0749
10	0.433	0.567	0.0663	−0.0506
15 (End 2)	0.250	0.750	0.1148	−0.0383

Note that species velocities vary along the length of the tube, but at any location z, $\upsilon_M = 0$. For example, at $z = 10$ cm, from (3-8),

$$\upsilon_M = (0.433)(0.0663) + (0.567)(-0.0506) = 0$$

§3.1.4 Unimolecular Diffusion (UMD)

In UMD, mass transfer of component A occurs through stagnant B, resulting in a bulk flow. Thus,

$$N_B = 0 \tag{3-24}$$

and

$$N = N_A \tag{3-25}$$

Therefore, from (3-12),

$$N_A = x_A N_A - cD_{AB}\frac{dx_A}{dz} \tag{3-26}$$

which can be rearranged to a Fick's-law form by solving for N_A,

$$\boxed{N_A = -\frac{cD_{AB}}{(1 - x_A)}\frac{dx_A}{dz} = -\frac{cD_{AB}}{x_B}\frac{dx_A}{dz}} \tag{3-27}$$

The factor $(1 - x_A)$ accounts for the bulk-flow effect. For a mixture dilute in A, this effect is small. But in an equimolar mixture of A and B, $(1 - x_A) = 0.5$ and, because of bulk flow, the molar mass-transfer flux of A is twice the ordinary molecular-diffusion flux.

For the stagnant component, B, (3-13) becomes

$$0 = x_B N_A - cD_{BA}\frac{dx_B}{dz} \tag{3-28}$$

or

$$x_B N_A = cD_{BA}\frac{dx_B}{dz} \tag{3-29}$$

Thus, the bulk-flow flux of B is equal to but opposite its diffusion flux.

At quasi-steady-state conditions (i.e., no accumulation of species with time) and with constant molar density, (3-27) in integral form is:

$$\int_{z_1}^{z} dz = -\frac{cD_{AB}}{N_A}\int_{x_{A_1}}^{x_A}\frac{dx_A}{1 - x_A} \tag{3-30}$$

which upon integration yields

$$N_A = \frac{cD_{AB}}{z - z_1}\ln\left(\frac{1 - x_A}{1 - x_{A_1}}\right) \tag{3-31}$$

Thus, the mole-fraction variation as a function of z is

$$x_A = 1 - (1 - x_{A_1})\exp\left[\frac{N_A(z - z_1)}{cD_{AB}}\right] \tag{3-32}$$

Figure 3.1b shows that the mole fractions are thus nonlinear in z.

A more useful form of (3-31) can be derived from the definition of the log mean. When $z = z_2$, (3-31) becomes

$$N_A = \frac{cD_{AB}}{z_2 - z_1} \ln\left(\frac{1 - x_{A_2}}{1 - x_{A_1}}\right) \tag{3-33}$$

The log mean (LM) of $(1 - x_A)$ at the two ends of the stagnant layer is

$$\begin{aligned}(1 - x_A)_{LM} &= \frac{(1 - x_{A_2}) - (1 - x_{A_1})}{\ln[(1 - x_{A_2})/(1 - x_{A_1})]} \\ &= \frac{x_{A_1} - x_{A_2}}{\ln[(1 - x_{A_2})/(1 - x_{A_1})]}\end{aligned} \tag{3-34}$$

Combining (3-33) with (3-34) gives

$$\begin{aligned}N_A &= \frac{cD_{AB}}{z_2 - z_1}\frac{(x_{A_1} - x_{A_2})}{(1 - x_A)_{LM}} = \frac{cD_{AB}}{(1 - x_A)_{LM}}\frac{(-\Delta x_A)}{\Delta z} \\ &= \frac{cD_{AB}}{(x_B)_{LM}}\frac{(-\Delta x_A)}{\Delta z}\end{aligned} \tag{3.35}$$

EXAMPLE 3.2 Evaporation from an Open Beaker.

In Figure 3.2, an open beaker, 6 cm high, is filled with liquid benzene (A) at 25°C to within 0.5 cm of the top. Dry air (B) at 25°C and 1 atm is blown across the mouth of the beaker so that evaporated benzene is carried away by convection after it transfers through a stagnant air layer in the beaker. The vapor pressure of benzene at 25°C is 0.131 atm. Thus, as shown in Figure 3.2, the mole fraction of benzene in the air at the top of the beaker is zero and is determined by Raoult's law at the gas–liquid interface. The diffusion coefficient for benzene in air at 25°C and 1 atm is 0.0905 cm^2/s. Compute the: (a) initial rate of evaporation of benzene as a molar flux in mol/cm^2-s; (b) initial mole-fraction profiles in the stagnant air layer; (c) initial fractions of the mass-transfer fluxes due to molecular diffusion; (d) initial diffusion velocities, and the species velocities (relative to stationary coordinates) in the stagnant layer; (e) time for the benzene level in the beaker to drop 2 cm if the specific gravity of benzene is 0.874.

Neglect the accumulation of benzene and air in the stagnant layer with time as it increases in height (quasi-steady-state assumption).

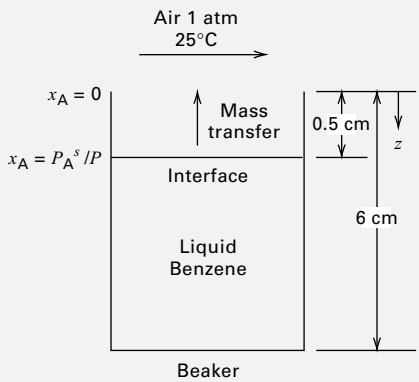

Figure 3.2 Evaporation of benzene from a beaker—Example 3.2.

Solution

The total vapor concentration by the ideal-gas law is:

$$c = \frac{P}{RT} = \frac{1}{(82.06)(298)} = 4.09 \times 10^{-5} \text{ mol/cm}^3$$

(a) With z equal to the distance down from the top of the beaker, let $z_1 = 0$ at the top of beaker and $z_2 =$ the distance from the top of the beaker to gas–liquid interface. Then, initially, the stagnant gas layer is $z_2 - z_1 = \Delta z = 0.5$ cm. From Dalton's law, assuming equilibrium at the liquid benzene–air interface,

$$x_{A_1} = \frac{p_{A_1}}{P} = \frac{0.131}{1} = 0.131, \quad x_{A_2} = 0$$

$$(1 - x_A)_{LM} = \frac{0.131}{\ln[(1 - 0)/(1 - 0.131)]} = 0.933 = (x_B)_{LM}$$

From (3-35),

$$N_A = \frac{(4.09 \times 10^{-6})(0.0905)}{0.5}\left(\frac{0.131}{0.933}\right) = 1.04 \times 10^{-6} \text{ mol/cm}^2\text{-s}$$

(b) $$\frac{N_A(z - z_1)}{cD_{AB}} = \frac{(1.04 \times 10^{-6})(z - 0)}{(4.09 \times 10^{-5})(0.0905)} = 0.281\, z$$

From (3-32),

$$x_A = 1 - 0.869 \exp(0.281\, z) \tag{1}$$

Using (1), the following results are obtained:

z, cm	x_A	x_B
0.0	0.1310	0.8690
0.1	0.1060	0.8940
0.2	0.0808	0.9192
0.3	0.0546	0.9454
0.4	0.0276	0.9724
0.5	0.0000	1.0000

These profiles are only slightly curved.

(c) Equations (3-27) and (3-29) yield the bulk-flow terms, $x_A N_A$ and $x_B N_A$, from which the molecular-diffusion terms are obtained.

	$x_i N$ Bulk-Flow Flux, mol/cm^2-s $\times 10^6$		J_i Molecular-Diffusion Flux, mol/cm^2-s $\times 10^6$	
z, cm	A	B	A	B
0.0	0.1360	0.9040	0.9040	−0.9040
0.1	0.1100	0.9300	0.9300	−0.9300
0.2	0.0840	0.9560	0.9560	−0.9560
0.3	0.0568	0.9832	0.9832	−0.9832
0.4	0.0287	1.0113	1.0113	−1.0113
0.5	0.0000	1.0400	1.0400	−1.0400

Note that the molecular-diffusion fluxes are equal but opposite and that the bulk-flow flux of B is equal but opposite to its molecular diffusion flux; thus N_B is zero, making B (air) stagnant.

(d) From (3-6),

$$v_M = \frac{N}{c} = \frac{N_A}{c} = \frac{1.04 \times 10^{-6}}{4.09 \times 10^{-5}} = 0.0254 \text{ cm/s} \tag{2}$$

From (3-9), the diffusion velocities are given by

$$v_{i_d} = \frac{J_i}{c_i} = \frac{J_i}{x_i c} \tag{3}$$

From (3-10), species velocities relative to stationary coordinates are

$$v_i = v_{i_d} + v_M \tag{4}$$

Using (2) to (4), there follows

	v_{i_d} Molecular-Diffusion Velocity, cm/s		J_i Species Velocity, cm/s	
z, cm	A	B	A	B
0.0	0.1687	−0.0254	0.1941	0
0.1	0.2145	−0.0254	0.2171	0
0.2	0.2893	−0.0254	0.3147	0
0.3	0.4403	−0.0254	0.4657	0
0.4	0.8959	−0.0254	0.9213	0
0.5	∞	−0.0254	∞	0

Note that v_A is zero everywhere, because its molecular-diffusion velocity is negated by the molar-mean velocity.

(e) The mass-transfer flux for benzene evaporation equals the rate of decrease in the moles of liquid benzene per unit cross section area of the beaker.

Using (3-35) with $\Delta z = z$,

$$N_A = \frac{cD_{AB}}{z}\frac{(-\Delta x_A)}{(1-x_A)_{LM}} = \frac{\rho_L}{M_L}\frac{dz}{dt} \tag{5}$$

Separating variables and integrating,

$$\int_0^t dt = t = \frac{\rho_L (1-x_A)_{LM}}{M_L c D_{AB}(-\Delta x_A)} \int_{z_1}^{z_2} z\, dz \tag{6}$$

where now z_1 = initial location of the interface and z_2 = location of the interface after it drops 2 cm.

The coefficient of the integral on the RHS of (6) is constant at

$$\frac{0.874(0.933)}{78.11(4.09 \times 10^{-5})(0.0905)(0.131)} = 21{,}530 \text{ s/cm}^2$$

$$\int_{z_1}^{z_2} z\, dz = \int_{0.5}^{2.5} z\, dz = 3 \text{ cm}^2$$

From (6), $t = 21{,}530(3) = 64{,}590$ s or 17.94 h, which is a long time because of the absence of turbulence.

§3.2 DIFFUSION COEFFICIENTS (DIFFUSIVITIES)

Diffusion coefficients (diffusivities) are defined for a binary mixture by (3-3) to (3-5). Measurement of diffusion coefficients involve a correction for bulk flow using (3-12) and (3-13), with the reference plane being such that there is no net molar bulk flow.

The binary diffusivities, D_{AB} and D_{BA}, are called mutual or binary diffusion coefficients. Other coefficients include D_{i_M}, the diffusivity of i in a multicomponent mixture; D_{ii}, the self-diffusion coefficient; and the tracer or interdiffusion coefficient.

In this chapter and throughout this book, the focus is on the mutual diffusion coefficient, which will be referred to as the diffusivity or diffusion coefficient.

§3.2.1 Diffusivity in Gas Mixtures

As discussed by Poling, Prausnitz, and O'Connell [2], equations are available for estimating the value of $D_{AB} = D_{BA}$ in gases at low to moderate pressures. The theoretical equations based on Boltzmann's kinetic theory of gases, the theorem of corresponding states, and a suitable intermolecular energy-potential function, as developed by Chapman and Enskog, predict D_{AB} to be inversely proportional to pressure, to increase significantly with temperature, and to be almost independent of composition. Of greater accuracy and ease of use is the empirical equation of Fuller, Schettler, and Giddings [3], which retains the form of the Chapman–Enskog theory but utilizes empirical constants derived from experimental data:

$$D_{AB} = D_{BA} = \frac{0.00143T^{1.75}}{P M_{AB}^{1/2}[(\sum_V)_A^{1/3} + (\sum_V)_B^{1/3}]^2} \tag{3-36}$$

where D_{AB} is in cm^2/s, P is in atm, T is in K,

$$M_{AB} = \frac{2}{(1/M_A) + (1/M_B)} \tag{3-37}$$

and $\sum_V$ = summation of atomic and structural diffusion volumes from Table 3.1, which includes diffusion volumes of simple molecules.

Table 3.1 Diffusion Volumes from Fuller, Ensley, and Giddings [*J. Phys. Chem.*,**73,** 3679–3685 (1969)] for Estimating Binary Gas Diffusivities by the Method of Fuller et al. [3]

Atomic Diffusion Volumes and Structural Diffusion-Volume Increments			
C	15.9	F	14.7
H	2.31	Cl	21.0
O	6.11	Br	21.9
N	4.54	I	29.8
Aromatic ring	−18.3	S	22.9
Heterocyclic ring	−18.3		
Diffusion Volumes of Simple Molecules			
He	2.67	CO	18.0
Ne	5.98	CO_2	26.7
Ar	16.2	N_2O	35.9
Kr	24.5	NH_3	20.7
Xe	32.7	H_2O	13.1
H_2	6.12	SF_6	71.3
D_2	6.84	Cl_2	38.4
N_2	18.5	Br_2	69.0
O_2	16.3	SO_2	41.8
Air	19.7		

Table 3.2 Experimental Binary Diffusivities of Gas Pairs at 1 atm

Gas pair, A-B	Temperature, K	D_{AB}, cm^2/s
Air—carbon dioxide	317.2	0.177
Air—ethanol	313	0.145
Air—helium	317.2	0.765
Air—*n*-hexane	328	0.093
Air—water	313	0.288
Argon—ammonia	333	0.253
Argon—hydrogen	242.2	0.562
Argon—hydrogen	806	4.86
Argon—methane	298	0.202
Carbon dioxide—nitrogen	298	0.167
Carbon dioxide—oxygen	293.2	0.153
Carbon dioxide—water	307.2	0.198
Carbon monoxide—nitrogen	373	0.318
Helium—benzene	423	0.610
Helium—methane	298	0.675
Helium—methanol	423	1.032
Helium—water	307.1	0.902
Hydrogen—ammonia	298	0.783
Hydrogen—ammonia	533	2.149
Hydrogen—cyclohexane	288.6	0.319
Hydrogen—methane	288	0.694
Hydrogen—nitrogen	298	0.784
Nitrogen—benzene	311.3	0.102
Nitrogen—cyclohexane	288.6	0.0731
Nitrogen—sulfur dioxide	263	0.104
Nitrogen—water	352.1	0.256
Oxygen—benzene	311.3	0.101
Oxygen—carbon tetrachloride	296	0.0749
Oxygen—cyclohexane	288.6	0.0746
Oxygen—water	352.3	0.352

From Marrero, T. R., and E. A. Mason, *J. Phys. Chem. Ref. Data*, **1,** 3–118 (1972).

Experimental values of binary gas diffusivity at 1 atm and near-ambient temperature range from about 0.10 to 10.0 cm^2/s. Poling et al. [2] compared (3-36) to experimental data for 51 different binary gas mixtures at low pressures over a temperature range of 195–1,068 K. The average deviation was only 5.4%, with a maximum deviation of 25%.

Equation (3-36) indicates that D_{AB} is proportional to $T^{1.75}/P$, which can be used to adjust diffusivities for T and P. Representative experimental values of binary gas diffusivity are given in Table 3.2.

EXAMPLE 3.3 Estimation of a Gas Diffusivity.

Estimate the diffusion coefficient for oxygen (A)/benzene (B) at 38°C and 2 atm using the method of Fuller et al.

Solution

From (3-37), $$M_{AB} = \frac{2}{(1/32) + (1/78.11)} = 45.4$$

From Table 3.1, $(\sum_V)_A = 16.3$ and $(\sum_V)_B = 6(15.9) + 6(2.31) - 18.3 = 90.96$

From (3-36), at 2 atm and 311.2 K,

$$D_{AB} = D_{BA} = \frac{0.00143(311.2)^{1.75}}{(2)(45.4)^{1/2}[16.3^{1/3} + 90.96^{1/3}]^2} = 0.0495\ \text{cm}^2/\text{s}$$

At 1 atm, the predicted diffusivity is 0.0990 cm^2/s, which is about 2% below the value in Table 3.2. The value for 38°C can be corrected for temperature using (3-36) to give, at 200°C:

$$D_{AB} \text{ at } 200°\text{C and 1 atm} = 0.102\left(\frac{200 + 273.2}{38 + 273.2}\right)^{1.75} = 0.212\ \text{cm}^2/\text{s}$$

For light gases, at pressures to about 10 atm, the pressure dependence on diffusivity is adequately predicted by the inverse relation in (3-36); that is, $PD_{AB} =$ a constant. At higher pressures, deviations are similar to the modification of the ideal-gas law by the compressibility factor based on the theorem of corresponding states. Takahashi [4] published a corresponding-states correlation, shown in Figure 3.3, patterned after a correlation by Slattery [5]. In the Takahashi plot, $D_{AB}P/(D_{AB}P)_{LP}$ is a function of reduced temperature and pressure, where $(D_{AB}P)_{LP}$ is at low pressure when (3-36) applies. Mixture critical temperature and pressure are molar-average values. Thus, a finite effect of composition is predicted at high pressure. The effect of high pressure on diffusivity is important in supercritical extraction, discussed in Chapter 11.

EXAMPLE 3.4 Estimation of a Gas Diffusivity at High Pressure.

Estimate the diffusion coefficient for a 25/75 molar mixture of argon and xenon at 200 atm and 378 K. At this temperature and 1 atm, the diffusion coefficient is 0.180 cm^2/s. Critical constants are:

	T_c, K	P_c, atm
Argon	151.0	48.0
Xenon	289.8	58.0

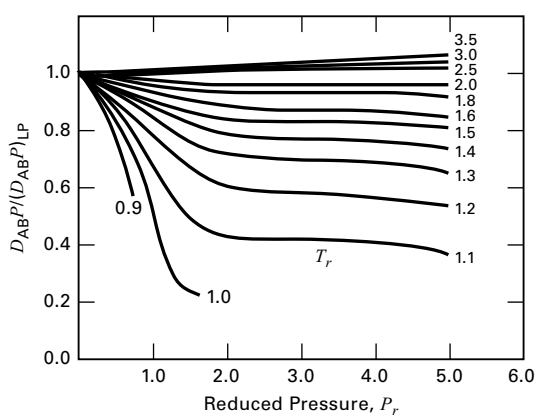

Figure 3.3 Takahashi [4] correlation for effect of high pressure on binary gas diffusivity.

Solution

Calculate reduced conditions:

$T_c = 0.25(151) + 0.75(289.8) = 255.1$ K

$T_r = T/T_c = 378/255.1 = 1.48$

$P_c = 0.25(48) + 0.75(58) = 55.5$

$P_r = P/P_c = 200/55.5 = 3.6$

From Figure 3.3, $\dfrac{D_{AB}P}{(D_{AB}P)_{LP}} = 0.82$

$$D_{AB} = \frac{(D_{AB}P)_{LP}}{P}\left[\frac{D_{AB}P}{(D_{AB}P)_{LP}}\right] = \frac{(0.180)(1)}{200}(0.82)$$
$$= 7.38 \times 10^{-4}\text{cm/s}$$

§3.2.2 Diffusivity in Nonelectrolyte Liquid Mixtures

For liquids, diffusivities are difficult to estimate because of the lack of a rigorous model for the liquid state. An exception is a dilute solute (A) of large, rigid, spherical molecules diffusing through a solvent (B) of small molecules with no slip at the surface of the solute molecules. The resulting relation, based on the hydrodynamics of creeping flow to describe drag, is the Stokes–Einstein equation:

$$(D_{AB})_\infty = \frac{RT}{6\pi\mu_B R_A N_A} \tag{3-38}$$

where R_A is the solute-molecule radius and N_A is Avogadro's number. Equation (3-38) has long served as a starting point for more widely applicable empirical correlations for liquid diffusivity. Unfortunately, unlike for gas mixtures, where $D_{AB} = D_{BA}$, in liquid mixtures diffusivities can vary with composition, as shown in Example 3.7. The Stokes–Einstein equation is restricted to dilute binary mixtures of not more than 10% solutes.

An extension of (3-38) to more concentrated solutions for small solute molecules is the empirical Wilke–Chang [6] equation:

$$(D_{AB})_\infty = \frac{7.4 \times 10^{-8}(\phi_B M_B)^{1/2} T}{\mu_B \upsilon_A^{0.6}} \tag{3-39}$$

where the units are cm^2/s for D_{AB}; cP (centipoises) for the solvent viscosity, μ_B; K for T; and cm^3/mol for υ_A, the solute molar volume, at its normal boiling point. The parameter ϕ_B is a solvent association factor, which is 2.6 for water, 1.9 for methanol, 1.5 for ethanol, and 1.0 for unassociated solvents such as hydrocarbons. The effects of temperature and viscosity in (3-39) are taken identical to the prediction of the Stokes–Einstein equation, while the radius of the solute molecule is replaced by υ_A, which can be estimated by summing atomic contributions tabulated in Table 3.3. Some

Table 3.3 Molecular Volumes of Dissolved Light Gases and Atomic Contributions for Other Molecules at the Normal Boiling Point

	Atomic Volume $(m^3/kmol) \times 10^3$		Atomic Volume $(m^3/kmol) \times 10^3$
C	14.8	Ring	
H	3.7	Three-membered, as in ethylene oxide	−6
O (except as below)	7.4		
Doubly bonded as carbonyl	7.4	Four-membered	−8.5
Coupled to two other elements:		Five-membered	−11.5
In aldehydes, ketones	7.4	Six-membered	−15
In methyl esters	9.1	Naphthalene ring	−30
In methyl ethers	9.9	Anthracene ring	−47.5
In ethyl esters	9.9		
In ethyl ethers	9.9		Molecular Volume $(m^3/kmol) \times 10^3$
In higher esters	11.0		
In higher ethers	11.0	Air	29.9
In acids (—OH)	12.0	O_2	25.6
Joined to S, P, N	8.3	N_2	31.2
N		Br_2	53.2
Doubly bonded	15.6	Cl_2	48.4
In primary amines	10.5	CO	30.7
In secondary amines	12.0	CO_2	34.0
Br	27.0	H_2	14.3
Cl in RCHClR′	24.6	H_2O	18.8
Cl in RCl (terminal)	21.6	H_2S	32.9
F	8.7	NH_3	25.8
I	37.0	NO	23.6
S	25.6	N_2O	36.4
P	27.0	SO_2	44.8

Source: G. Le Bas, *The Molecular Volumes of Liquid Chemical Compounds*, David McKay, New York (1915).

Table 3.4 Experimental Binary Liquid Diffusivities for Solutes, A, at Low Concentrations in Solvents, B

Solvent, B	Solute, A	Temperature, K	Diffusivity, D_{AB}, $cm^2/s \times 10^5$
Water	Acetic acid	293	1.19
	Aniline	293	0.92
	Carbon dioxide	298	2.00
	Ethanol	288	1.00
	Methanol	288	1.26
Ethanol	Allyl alcohol	293	0.98
	Benzene	298	1.81
	Oxygen	303	2.64
	Pyridine	293	1.10
	Water	298	1.24
Benzene	Acetic acid	298	2.09
	Cyclohexane	298	2.09
	Ethanol	288	2.25
	n-heptane	298	2.10
	Toluene	298	1.85
n-hexane	Carbon tetrachloride	298	3.70
	Methyl ethyl ketone	303	3.74
	Propane	298	4.87
	Toluene	298	4.21
Acetone	Acetic acid	288	2.92
	Formic acid	298	3.77
	Nitrobenzene	293	2.94
	Water	298	4.56

From Poling et al. [2].

representative experimental values of solute diffusivity in dilute binary liquid solutions are given in Table 3.4.

EXAMPLE 3.5 Estimation of a Liquid Diffusivity.

Use the Wilke–Chang equation to estimate the diffusivity of aniline (A) in a 0.5 mol% aqueous solution at 20°C. The solubility of aniline in water is 4 g/100 g or 0.77 mol%. Compare the result to the experimental value in Table 3.4.

Solution

$$\mu_B = \mu_{H_2O} = 1.01 \text{ cP at } 20^\circ\text{C}$$

υ_A = liquid molar volume of aniline at its normal boiling point of 457.6 K = 107 cm^3/mol

$$\phi_B = 2.6 \text{ for water}, \quad M_B = 18 \text{ for water}, \quad T = 293 \text{ K}$$

From (3-39),

$$D_{AB} = \frac{(7.4 \times 10^{-8})[2.6(18)]^{0.5}(293)}{1.01(107)^{0.6}} = 0.89 \times 10^{-5} \text{cm}^2/\text{s}$$

This value is about 3% less than the experimental value of 0.92×10^{-5} cm^2/s for an infinitely dilute solution of aniline in water.

More recent liquid diffusivity correlations due to Hayduk and Minhas [7] give better agreement than the Wilke–Chang equation with experimental values for nonaqueous solutions. For a dilute solution of one normal paraffin (C_5 to C_{32}) in another (C_5 to C_{16}),

$$(D_{AB})_\infty = 13.3 \times 10^{-8} \frac{T^{1.47} \mu_B^{\epsilon}}{\upsilon_A^{0.71}} \tag{3-40}$$

where

$$\epsilon = \frac{10.2}{\upsilon_A} - 0.791 \tag{3-41}$$

and the other variables have the same units as in (3-39). For nonaqueous solutions in general,

$$(D_{AB})_\infty = 1.55 \times 10^{-8} \frac{T^{1.29}(\mathscr{P}_B^{0.5}/\mathscr{P}_A^{0.42})}{\mu_B^{0.92} \upsilon_B^{0.23}} \tag{3-42}$$

where $\mathscr{P}$ is the parachor, which is defined as

$$\mathscr{P} = \upsilon \sigma^{1/4} \tag{3-43}$$

When units of liquid molar volume, υ, are cm^3/mol and surface tension, σ, are g/s^2 (dynes/cm), then the units of the parachor are $cm^3\text{-}g^{1/4}/s^{1/2}$-mol. Normally, at near-ambient conditions, $\mathscr{P}$ is treated as a constant, for which a tabulation is given in Table 3.5 from Quayle [8], who also provides in Table 3.6 a group-contribution method for estimating the parachor for compounds not listed.

The restrictions that apply to (3-42) are:

1. Solvent viscosity should not exceed 30 cP.
2. For organic acid solutes and solvents other than water, methanol, and butanols, the acid should be treated as a dimer by doubling the values of $\mathscr{P}_A$ and υ_A.
3. For a nonpolar solute in monohydroxy alcohols, values of υ_B and $\mathscr{P}_B$ should be multiplied by 8 μ_B, where viscosity is in centipoise.

Liquid diffusivities range from 10^{-6} to 10^{-4} cm^2/s for solutes of molecular weight up to about 200 and solvents with viscosity up to 10 cP. Thus, liquid diffusivities are five orders of magnitude smaller than diffusivities for gas mixtures at 1 atm. However, diffusion rates in liquids are not necessarily five orders of magnitude smaller than in gases because, as seen in (3-5), the product of concentration (molar density) and diffusivity determines the rate of diffusion for a given gradient in mole fraction. At 1 atm, the molar density of a liquid is three times that of a gas and, thus, the diffusion rate in liquids is only two orders of magnitude smaller than in gases at 1 atm.

EXAMPLE 3.6 Estimation of Solute Liquid Diffusivity.

Estimate the diffusivity of formic acid (A) in benzene (B) at 25°C and infinite dilution, using the appropriate correlation of Hayduk and Minhas.

Solution

Equation (3-42) applies, with $T = 298$ K

$\mathscr{P}_A = 93.7$ $cm^3\text{-}g^{1/4}/s^{1/2}$-mol $\mathscr{P}_B = 205.3$ $cm^3\text{-}g^{1/4}/s^{1/2}$-mol

$\mu_B = 0.6$ cP at 25°C $\upsilon_B = 96$ cm^3/mol at 80°C

Table 3.5 Parachors for Representative Compounds

	Parachor, cm^3-$g^{1/4}/s^{1/2}$-mol		Parachor, cm^3-$g^{1/4}/s^{1/2}$-mol		Parachor, cm^3-$g^{1/4}/s^{1/2}$-mol
Acetic acid	131.2	Chlorobenzene	244.5	Methyl amine	95.9
Acetone	161.5	Diphenyl	380.0	Methyl formate	138.6
Acetonitrile	122	Ethane	110.8	Naphthalene	312.5
Acetylene	88.6	Ethylene	99.5	*n*-octane	350.3
Aniline	234.4	Ethyl butyrate	295.1	1-pentene	218.2
Benzene	205.3	Ethyl ether	211.7	1-pentyne	207.0
Benzonitrile	258	Ethyl mercaptan	162.9	Phenol	221.3
n-butyric acid	209.1	Formic acid	93.7	*n*-propanol	165.4
Carbon disulfide	143.6	Isobutyl benzene	365.4	Toluene	245.5
Cyclohexane	239.3	Methanol	88.8	Triethyl amine	297.8

Source: Meissner, *Chem. Eng. Prog.*, **45,** 149–153 (1949).

However, for formic acid, $\mathscr{P}_A$ is doubled to 187.4. From (3-41),

$$(D_{AB})_\infty = 1.55 \times 10^{-8}\left[\frac{298^{1.29}(205.3^{0.5}/187.4^{0.42})}{0.6^{0.92}96^{0.23}}\right] = 2.15 \times 10^{-5}\text{cm}^2/\text{s}$$

which is within 6% of the experimental value of 2.28×10^{-5} cm^2/s.

Table 3.6 Structural Contributions for Estimating the Parachor

Carbon–hydrogen:		R—[—CO—]—R′ (ketone)	
C	9.0	R + R′ = 2	51.3
H	15.5	R + R′ = 3	49.0
CH_3	55.5	R + R′ = 4	47.5
CH_2 in —$(CH_2)_n$—		R + R′ = 5	46.3
$n < 12$	40.0	R + R′ = 6	45.3
$n > 12$	40.3	R + R′ = 7	44.1
		—CHO	66
Alkyl groups			
1-Methylethyl	133.3	O (not noted above)	20
1-Methylpropyl	171.9	N (not noted above)	17.5
1-Methylbutyl	211.7	S	49.1
2-Methylpropyl	173.3	P	40.5
1-Ethylpropyl	209.5	F	26.1
1,1-Dimethylethyl	170.4	Cl	55.2
1,1-Dimethylpropyl	207.5	Br	68.0
1,2-Dimethylpropyl	207.9	I	90.3
1,1,2-Trimethylpropyl	243.5	Ethylenic bonds:	
C_6H_5	189.6	Terminal	19.1
		2,3-position	17.7
Special groups:		3,4-position	16.3
—COO—	63.8		
—COOH	73.8	Triple bond	40.6
—OH	29.8		
—NH_2	42.5	Ring closure:	
—O—	20.0	Three-membered	12
—NO_2	74	Four-membered	6.0
—NO_3 (nitrate)	93	Five-membered	3.0
—$CO(NH_2)$	91.7	Six-membered	0.8

Source: Quale [8].

The Stokes–Einstein and Wilke–Chang equations predict an inverse dependence of liquid diffusivity with viscosity, while the Hayduk–Minhas equations predict a somewhat smaller dependence. The consensus is that liquid diffusivity varies inversely with viscosity raised to an exponent closer to 0.5 than to 1.0. The Stokes–Einstein and Wilke–Chang equations also predict that $D_{AB}\mu_B/T$ is a constant over a narrow temperature range. Because μ_B decreases exponentially with temperature, D_{AB} is predicted to increase exponentially with temperature. Over a wide temperature range, it is preferable to express the effect of temperature on D_{AB} by an Arrhenius-type expression,

$$(D_{AB})_\infty = A\exp\left(\frac{-E}{RT}\right) \tag{3-44}$$

where, typically, the activation energy for liquid diffusion, E, is no greater than 6,000 cal/mol.

Equations (3-39), (3-40), and (3-42) apply only to solute A in a dilute solution of solvent B. Unlike binary gas mixtures in which the diffusivity is almost independent of composition, the effect of composition on liquid diffusivity is complex, sometimes showing strong positive or negative deviations from linearity with mole fraction.

Vignes [9] has shown that, except for strongly associated binary mixtures such as chloroform-acetone, which exhibit a rare negative deviation from Raoult's law, infinite-dilution binary diffusivities, $(D)_\infty$, can be combined with mixture activity-coefficient data or correlations thereof to predict liquid binary diffusion coefficients over the entire composition range. The Vignes equations are:

$$D_{AB} = (D_{AB})_\infty^{x_B}(D_{BA})_\infty^{x_A}\left(1 + \frac{\partial \ln \gamma_A}{\partial \ln x_A}\right)_{T,P} \tag{3-45}$$

$$D_{BA} = (D_{BA})_\infty^{x_A}(D_{AB})_\infty^{x_B}\left(1 + \frac{\partial \ln \gamma_B}{\partial \ln x_B}\right)_{T,P} \tag{3-46}$$

EXAMPLE 3.7 Effect of Composition on Liquid Diffusivities.

At 298 K and 1 atm, infinite-dilution diffusion coefficients for the methanol (A)–water (B) system are 1.5×10^{-5} cm^2/s and 1.75×10^{-5} cm^2/s for AB and BA, respectively.

Activity-coefficient data over a range of compositions as estimated by UNIFAC are:

x_A	γ_A	x_B	γ_B
0.5	1.116	0.5	1.201
0.6	1.066	0.4	1.269
0.7	1.034	0.3	1.343
0.8	1.014	0.2	1.424
1.0	1.000	0.0	1.605

Use the Vignes equations to estimate diffusion coefficients over a range of compositions.

Solution

Using a spreadsheet to compute the derivatives in (3-45) and (3-46), which are found to be essentially equal at any composition, and the diffusivities from the same equations, the following results are obtained with $D_{AB} = D_{BA}$ at each composition. The calculations show a minimum diffusivity at a methanol mole fraction of 0.30.

x_A	D_{AB}, cm^2/s	D_{BA}, cm^2/s
0.20	1.10×10^{-5}	1.10×10^{-5}
0.30	1.08×10^{-5}	1.08×10^{-5}
0.40	1.12×10^{-5}	1.12×10^{-5}
0.50	1.18×10^{-5}	1.18×10^{-5}
0.60	1.28×10^{-5}	1.28×10^{-5}
0.70	1.38×10^{-5}	1.38×10^{-5}
0.80	1.50×10^{-5}	1.50×10^{-5}

If the diffusivity is assumed to be linear with the mole fraction, the value at $x_A = 0.50$ is 1.625×10^{-5}, which is almost 40% higher than the predicted value of 1.18×10^{-5}.

§3.2.3 Diffusivities of Electrolytes

For an electrolyte solute, diffusion coefficients of dissolved salts, acids, or bases depend on the ions. However, in the absence of an electric potential, diffusion only of the electrolyte is of interest. The infinite-dilution diffusivity in cm^2/s of a salt in an aqueous solution can be estimated from the Nernst–Haskell equation:

$$(D_{AB})_\infty = \frac{RT[(1/n_+) + (1/n_-)]}{F^2[(1/\lambda_+) + (1/\lambda_-)]} \qquad (3\text{-}47)$$

where n_+ and n_- = valences of the cation and anion; λ_+ and λ_- = limiting ionic conductances in (A/cm^2)(V/cm)(g-equiv/cm^3), with A in amps and V in volts; F = Faraday's constant = 96,500 coulombs/g-equiv; T = temperature, K; and R = gas constant = 8.314 J/mol-K.

Values of λ_+ and λ_- at 25°C are listed in Table 3.7. At other temperatures, these values are multiplied by $T/334\ \mu_B$, where T and μ_B are in K and cP, respectively. As the concentration of the electrolyte increases, the diffusivity at first decreases 10% to 20% and then rises to values at a concentration of 2 N (normal) that approximate the infinite-dilution value. Some representative experimental values from Volume V of the International Critical Tables are given in Table 3.8.

Table 3.7 Limiting Ionic Conductance in Water at 25°C, in (A/cm^2)(V/cm)(g-equiv/cm^3)

Anion	λ_-	Cation	λ_+
OH^-	197.6	H^+	349.8
Cl^-	76.3	Li^+	38.7
Br^-	78.3	Na^+	50.1
I^-	76.8	K^+	73.5
NO_3^-	71.4	NH_4^+	73.4
ClO_4^-	68.0	Ag^+	61.9
HCO_3^-	44.5	Tl^+	74.7
HCO_2^-	54.6	$(\frac{1}{2})Mg^{2+}$	53.1
$CH_3CO_2^-$	40.9	$(\frac{1}{2})Ca^{2+}$	59.5
$ClCH_2CO_2^-$	39.8	$(\frac{1}{2})Sr^{2+}$	50.5
$CNCH_2CO_2^-$	41.8	$(\frac{1}{2})Ba^{2+}$	63.6
$CH_3CH_2CO_2^-$	35.8	$(\frac{1}{2})Cu^{2+}$	54
$CH_3(CH_2)_2CO_2^-$	32.6	$(\frac{1}{2})Zn^{2+}$	53
$C_6H_5CO_2^-$	32.3	$(\frac{1}{3})La^{3+}$	69.5
$HC_2O_4^-$	40.2	$(\frac{1}{3})Co(NH_3)_6^{3+}$	102
$(\frac{1}{2})C_2O_4^{2-}$	74.2		
$(\frac{1}{2})SO_4^{2-}$	80		
$(\frac{1}{3})Fe(CN)_6^{3-}$	101		
$(\frac{1}{4})Fe(CN)_6^{4-}$	111		

Source: Poling, Prausnitz, and O'Connell [2].

Table 3.8 Experimental Diffusivities of Electrolytes in Aqueous Solutions

Solute	Concentration, mol/L	Temperature, °C	Diffusivity, D_{AB}, cm^2/s $\times 10^5$
HCl	0.1	12	2.29
HNO_3	0.05	20	2.62
	0.25	20	2.59
H_2SO_4	0.25	20	1.63
KOH	0.01	18	2.20
	0.1	18	2.15
	1.8	18	2.19
NaOH	0.05	15	1.49
NaCl	0.4	18	1.17
	0.8	18	1.19
	2.0	18	1.23
KCl	0.4	18	1.46
	0.8	18	1.49
	2.0	18	1.58
$MgSO_4$	0.4	10	0.39
$Ca(NO_3)_2$	0.14	14	0.85

EXAMPLE 3.8 Diffusivity of an Electrolyte.

Estimate the diffusivity of KCl in a dilute solution of water at 18.5°C. Compare your result to the experimental value, 1.7×10^{-5} cm^2/s.

Solution

At 18.5°C, $T/334$ $\mu_B = 291.7/[(334)(1.05)] = 0.832$. Using Table 3.7, at 25°C, the limiting ionic conductances are

$$\lambda_+ = 73.5(0.832) = 61.2 \quad \text{and} \quad \lambda_- = 76.3(0.832) = 63.5$$

From (3-47),

$$D_\infty = \frac{(8.314)(291.7)[(1/1) + (1/1)]}{96{,}500^2[(1/61.2) + (1/63.5)]} = 1.62 \times 10^{-5}\text{cm}^2/\text{s}$$

which is 95% of the experimental value.

§3.2.4 Diffusivity of Biological Solutes in Liquids

The Wilke–Chang equation (3-39) is used for solute molecules of liquid molar volumes up to 500 cm^3/mol, which corresponds to molecular weights to almost 600. In biological applications, diffusivities of soluble protein macromolecules having molecular weights greater than 1,000 are of interest. Molecules with molecular weights to 500,000 have diffusivities at 25°C that range from 1×10^{-6} to 1×10^{-9} cm^2/s, which is three orders of magnitude smaller than values of diffusivity for smaller molecules. Data for globular and fibrous protein macromolecules are tabulated by Sorber [10], with some of these diffusivities given in Table 3.9, which includes diffusivities of two viruses and a bacterium. In the absence of data, the equation of Geankoplis [11], patterned after the Stokes–Einstein equation, can be used to estimate protein diffusivities:

$$D_{AB} = \frac{9.4 \times 10^{-15} T}{\mu_B (M_A)^{1/3}} \tag{3-48}$$

where the units are those of (3-39).

Also of interest in biological applications are diffusivities of small, nonelectrolyte molecules in aqueous gels containing up to 10 wt% of molecules such as polysaccharides (agar), which have a tendency to swell. Diffusivities are given by Friedman and Kraemer [12]. In general, the diffusivities of small solute molecules in gels are not less than 50% of the values for the diffusivity of the solute in water.

§3.2.5 Diffusivity in Solids

Diffusion in solids takes place by mechanisms that depend on the diffusing atom, molecule, or ion; the nature of the solid structure, whether it be porous or nonporous, crystalline, or amorphous; and the type of solid material, whether it be metallic, ceramic, polymeric, biological, or cellular. Crystalline materials are further classified according to the type of bonding, as molecular, covalent, ionic, or metallic, with most inorganic solids being ionic. Ceramics can be ionic, covalent, or a combination of the two. Molecular solids have relatively weak forces of attraction among the atoms. In covalent solids, such as quartz silica, two atoms share two or more electrons equally. In ionic solids, such as inorganic salts, one atom loses one or more of its electrons by transfer to other atoms, thus forming ions. In metals, positively charged ions are bonded through a field of electrons that are free to move. Diffusion coefficients in solids cover a range of many orders of magnitude. Despite the complexity of diffusion in solids, Fick's first law can be used if a measured diffusivity is available. However, when the diffusing solute is a gas, its solubility in the solid must be known. If the gas dissociates upon dissolution, the concentration of the dissociated species must be used in Fick's law. The mechanisms of diffusion in solids are complex and difficult to quantify. In the next subsections, examples of diffusion in solids are given,

Table 3.9 Experimental Diffusivities of Large Biological Materials in Aqueous Solutions

	MW or Size	Configuration	T, °C	Diffusivity, D_{AB}, $cm^2/s \times 10^5$
Proteins:				
Alcohol dehydrogenase	79,070	globular	20	0.0623
Aprotinin	6,670	globular	20	0.129
Bovine serum albumin	67,500	globular	25	0.0681
Cytochrome C	11,990	globular	20	0.130
γ–Globulin, human	153,100	globular	20	0.0400
Hemoglobin	62,300	globular	20	0.069
Lysozyme	13,800	globular	20	0.113
Soybean protein	361,800	globular	20	0.0291
Trypsin	23,890	globular	20	0.093
Urease	482,700	globular	25	0.0401
Ribonuclase A	13,690	globular	20	0.107
Collagen	345,000	fibrous	20	0.0069
Fibrinogen, human	339,700	fibrous	20	0.0198
Lipoxidase	97,440	fibrous	20	0.0559
Viruses:				
Tobacco mosaic virus	40,600,000	rod-like	20	0.0046
T4 bacteriophage	90 nm × 200 nm	head and tail	22	0.0049
Bacteria:				
P. aeruginosa	~0.5 μm × 1.0 μm	rod-like, motile	ambient	2.1

together with measured diffusion coefficients that can be used with Fick's first law.

Porous solids

For porous solids, predictions of the diffusivity of gaseous and liquid solute species in the pores can be made. These methods are considered only briefly here, with details deferred to Chapters 14, 15, and 16, where applications are made to membrane separations, adsorption, and leaching. This type of diffusion is also of importance in the analysis and design of reactors using porous solid catalysts. Any of the following four mass-transfer mechanisms or combinations thereof may take place:

1. Molecular diffusion through pores, which present tortuous paths and hinder movement of molecules when their diameter is more than 10% of the pore
2. Knudsen diffusion, which involves collisions of diffusing gaseous molecules with the pore walls when pore diameter and pressure are such that molecular mean free path is large compared to pore diameter
3. Surface diffusion involving the jumping of molecules, adsorbed on the pore walls, from one adsorption site to another based on a surface concentration-driving force
4. Bulk flow through or into the pores

When diffusion occurs only in the fluid in the pores, it is common to use an effective diffusivity, D_{eff}, based on (1) the total cross-sectional area of the porous solid rather than the cross-sectional area of the pore and (2) a straight path, rather than the tortuous pore path. If pore diffusion occurs only by molecular diffusion, Fick's law (3-3) is used with the effective diffusivity replacing the ordinary diffusion coefficient, D_{AB}:

$$D_{\text{eff}} = \frac{D_{\text{AB}}\epsilon}{\tau} \tag{3-49}$$

where ϵ is the fractional solid porosity (typically 0.5) and τ is the pore-path *tortuosity* (typically 2 to 3), which is the ratio of the pore length to the length if the pore were straight. The effective diffusivity is determined by experiment, or predicted from (3-49) based on measurement of the porosity and tortuosity and use of the predictive methods for molecular diffusivity. As an example of the former, Boucher, Brier, and Osburn [13] measured effective diffusivities for the leaching of processed soybean oil (viscosity = 20.1 cP at 120 °F) from 1/16-in.-thick porous clay plates with liquid tetrachloroethylene solvent. The rate of extraction was controlled by diffusion of the soybean oil in the clay plates. The measured D_{eff} was 1.0×10^{-6} cm^2/s. Due to the effects of porosity and tortuosity, this value is one order of magnitude less than the molecular diffusivity, D_{AB}, of oil in the solvent.

Crystalline solids

Diffusion through nonporous crystalline solids depends markedly on the crystal lattice structure. As discussed in Chapter 17, only seven different crystal lattice structures exist. For a cubic lattice (simple, body-centered, and face-centered), the diffusivity is equal in all directions (isotropic). In the six other lattice structures (including hexagonal and tetragonal), the diffusivity, as in wood, can be anisotropic. Many metals, including Ag, Al, Au, Cu, Ni, Pb, and Pt, crystallize into the face-centered cubic lattice structure. Others, including Be, Mg, Ti, and Zn, form anisotropic, hexagonal structures. The mechanisms of diffusion in crystalline solids include:

1. Direct exchange of lattice position, probably by a ring rotation involving three or more atoms or ions
2. Migration by small solutes through interlattice spaces called interstitial sites
3. Migration to a vacant site in the lattice
4. Migration along lattice imperfections (dislocations), or gain boundaries (crystal interfaces)

Diffusion coefficients associated with the first three mechanisms can vary widely and are almost always at least one order of magnitude smaller than diffusion coefficients in low-viscosity liquids. Diffusion by the fourth mechanism can be faster than by the other three. Experimental diffusivity values, taken mainly from Barrer [14], are given in Table 3.10. The diffusivities cover gaseous, ionic, and metallic solutes. The values cover an enormous 26-fold range. Temperature effects can be extremely large.

Metals

Important applications exist for diffusion of gases through metals. To diffuse through a metal, a gas must first dissolve in the metal. As discussed by Barrer [14], all light gases do

Table 3.10 Diffusivities of Solutes in Crystalline Metals and Salts

Metal/Salt	Solute	T, °C	D, cm^2/s
Ag	Au	760	3.6×10^{-10}
	Sb	20	3.5×10^{-21}
	Sb	760	1.4×10^{-9}
Al	Fe	359	6.2×10^{-14}
	Zn	500	2×10^{-9}
	Ag	50	1.2×10^{-9}
Cu	Al	20	1.3×10^{-30}
	Al	850	2.2×10^{-9}
	Au	750	2.1×10^{-11}
Fe	H_2	10	1.66×10^{-9}
	H_2	100	1.24×10^{-7}
	C	800	1.5×10^{-8}
Ni	H_2	85	1.16×10^{-8}
	H_2	165	1.05×10^{-7}
	CO	950	4×10^{-8}
W	U	1727	1.3×10^{-11}
AgCl	Ag^+	150	2.5×10^{-14}
	Ag^+	350	7.1×10^{-8}
	Cl^-	350	3.2×10^{-16}
KBr	H_2	600	5.5×10^{-4}
	Br_2	600	2.64×10^{-4}

not dissolve in all metals. Hydrogen dissolves in Cu, Al, Ti, Ta, Cr, W, Fe, Ni, Pt, and Pd, but not in Au, Zn, Sb, and Rh. Nitrogen dissolves in Zr but not in Cu, Ag, or Au. The noble gases do not dissolve in common metals. When H_2, N_2, and O_2 dissolve in metals, they dissociate and may react to form hydrides, nitrides, and oxides. Molecules such as ammonia, carbon dioxide, carbon monoxide, and sulfur dioxide also dissociate. Example 3.9 illustrates how hydrogen gas can slowly leak through the wall of a small, thin pressure vessel.

EXAMPLE 3.9 Diffusion of Hydrogen in Steel.

Hydrogen at 200 psia and 300°C is stored in a 10-cm-diameter steel pressure vessel of wall thickness 0.125 inch. Solubility of hydrogen in steel, which is proportional to the square root of the hydrogen partial pressure, is 3.8×10^{-6} mol/cm^3 at 14.7 psia and 300°C. The diffusivity of hydrogen in steel at 300°C is 5×10^{-6} cm^2/s. If the inner surface of the vessel wall remains saturated at the hydrogen partial pressure and the hydrogen partial pressure at the outer surface is zero, estimate the time for the pressure in the vessel to decrease to 100 psia because of hydrogen loss.

Solution

Integrating Fick's first law, (3-3), where A is H_2 and B is the metal, assuming a linear concentration gradient, and equating the flux to the loss of hydrogen in the vessel,

$$-\frac{dn_A}{dt} = \frac{D_{AB}A\Delta c_A}{\Delta z} \tag{1}$$

Because $p_A = 0$ outside the vessel, $\Delta c_A = c_A$ = solubility of A at the inside wall surface in mol/cm^3 and $c_A = 3.8 \times 10^{-6}\left(\frac{p_A}{14.7}\right)^{0.5}$, where p_A is the pressure of A inside the vessel in psia. Let p_{A_o} and n_{A_o} be the initial pressure and moles of A in the vessel. Assuming the ideal-gas law and isothermal conditions,

$$n_A = n_{A_o}p_A/p_{A_o} \tag{2}$$

Differentiating (2) with respect to time,

$$\frac{dn_A}{dt} = \frac{n_{A_o}}{p_{A_o}}\frac{dp_A}{dt} \tag{3}$$

Combining (1) and (3),

$$\frac{dp_A}{dt} = -\frac{D_{AB}A(3.8 \times 10^{-6})p_A^{0.5}p_{A_o}}{n_{A_o}\Delta z(14.7)^{0.5}} \tag{4}$$

Integrating and solving for t,

$$t = \frac{2n_{A_o}\Delta z(14.7)^{0.5}}{3.8 \times 10^{-6}D_{AB}Ap_{A_o}}(p_{A_o}^{0.5} - p_A^{0.5})$$

Assuming the ideal-gas law,

$$n_{A_o} = \frac{(200/14.7)[(3.14 \times 10^3)/6]}{82.05(300 + 273)} = 0.1515 \text{ mol}$$

The mean-spherical shell area for mass transfer, A, is

$$A = \frac{3.14}{2}\left[(10)^2 + (10.635)^2\right] = 336 \text{ cm}^2$$

The time for the pressure to drop to 100 psia is

$$t = \frac{2(0.1515)(0.125 \times 2.54)(14.7)^{0.5}}{3.8 \times 10^{-6}(5 \times 10^{-6})(336)(200)}(200^{0.5} - 100^{0.5})$$
$$= 1.2 \times 10^6 \text{ s or } 332 \text{ h}$$

Silica and glass

Another area of interest is diffusion of light gases through silica, whose two elements, Si and O, make up about 60% of the earth's crust. Solid silica exists in three crystalline forms (quartz, tridymite, and cristobalite) and in various amorphous forms, including fused quartz. Table 3.11 includes diffusivities, D, and solubilities as Henry's law constants, H, at 1 atm for helium and hydrogen in fused quartz as calculated from correlations of Swets, Lee, and Frank [15] and Lee [16]. The product of diffusivity and solubility is the permeability, P_M. Thus,

$$P_M = DH \tag{3-50}$$

Unlike metals, where hydrogen usually diffuses as the atom, hydrogen diffuses as a molecule in glass.

For hydrogen and helium, diffusivities increase rapidly with temperature. At ambient temperature they are three orders of magnitude smaller than they are in liquids. At high temperatures they approach those in liquids. Solubilities vary slowly with temperature. Hydrogen is orders of magnitude less soluble in glass than helium. Diffusivities for oxygen are included in Table 3.11 from studies by Williams [17] and Sucov [18]. At 1000°C, the two values differ widely because, as discussed by Kingery, Bowen, and Uhlmann [19], in the former case, transport occurs by molecular diffusion, while in the latter, transport is by slower network diffusion as oxygen jumps from one position in the network to another. The activation energy for the latter is much larger than that for the former (71,000 cal/mol versus 27,000 cal/mol). The choice of glass can be critical in vacuum operations because of this wide range of diffusivity.

Ceramics

Diffusion in ceramics has been the subject of numerous studies, many of which are summarized in Figure 3.4, which

Table 3.11 Diffusivities and Solubilities of Gases in Amorphous Silica at 1 atm

Gas	Temp, °C	Diffusivity, cm^2/s	Solubility mol/cm^3-atm
He	24	2.39×10^{-8}	1.04×10^{-7}
	300	2.26×10^{-6}	1.82×10^{-7}
	500	9.99×10^{-6}	9.9×10^{-8}
	1,000	5.42×10^{-5}	1.34×10^{-7}
H_2	300	6.11×10^{-8}	3.2×10^{-14}
	500	6.49×10^{-7}	2.48×10^{-13}
	1,000	9.26×10^{-6}	2.49×10^{-12}
O_2	1,000	6.25×10^{-9}	(molecular)
	1,000	9.43×10^{-15}	(network)

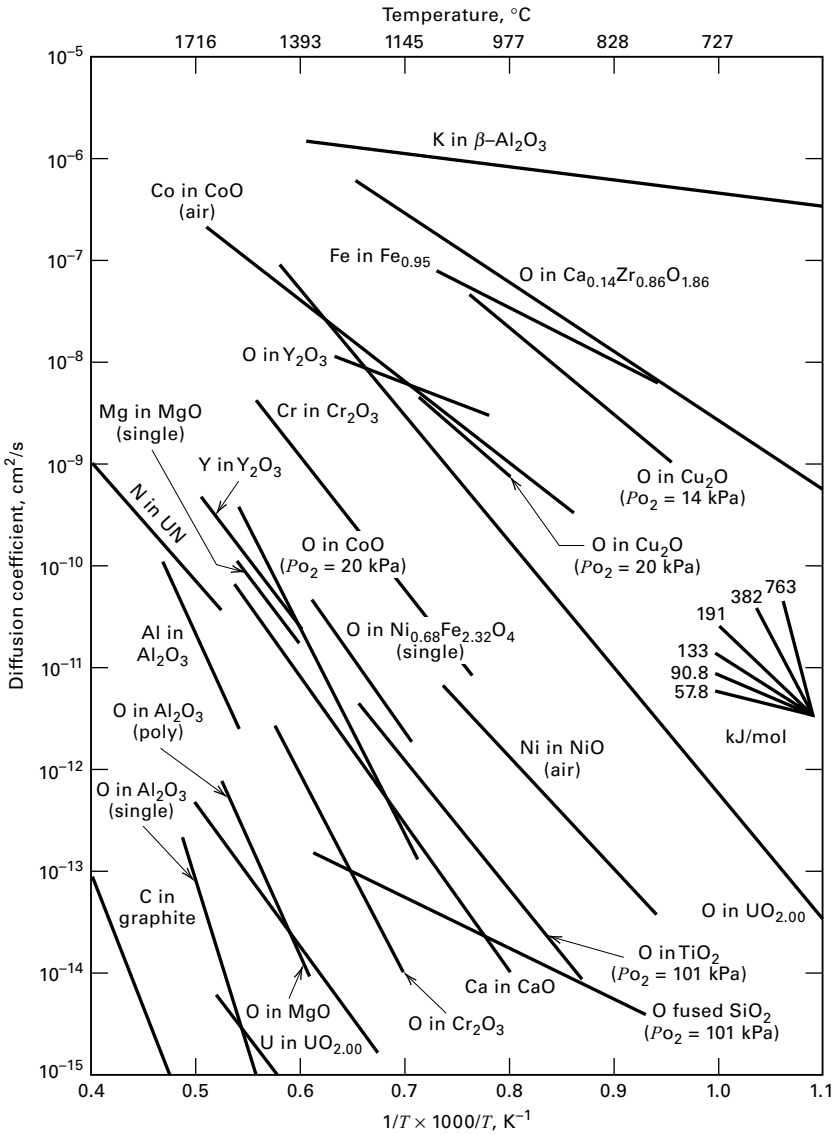

Figure 3.4 Diffusion coefficients for single and polycrystalline ceramics.
[From W.D. Kingery, H.K. Bowen, and D.R. Uhlmann, *Introduction to Ceramics*, 2nd ed., Wiley Interscience, New York (1976) with permission.]

is from Kingery et al. [19], where diffusivity is plotted as a function of the inverse of temperature in the high-temperature range. In this form, the slopes of the curves are proportional to the activation energy for diffusion, E, where

$$D = D_o \exp\left(-\frac{E}{RT}\right) \tag{3-51}$$

An insert in Figure 3.4 relates the slopes of the curves to activation energy. The diffusivity curves cover a ninefold range from 10^{-6} to 10^{-15} cm^2/s, with the largest values corresponding to the diffusion of potassium in β-Al_2O_3 and one of the smallest for the diffusion of carbon in graphite. As discussed in detail by Kingery et al. [19], diffusion in crystalline oxides depends not only on temperature but also on whether the oxide is stoichiometric or not (e.g., FeO and $Fe_{0.95}O$) and on impurities. Diffusion through vacant sites of nonstoichiometric oxides is often classified as metal-deficient or oxygen-deficient. Impurities can hinder diffusion by filling vacant lattice or interstitial sites.

Polymers

Diffusion through nonporous polymers is dependent on the type of polymer, whether it be crystalline or amorphous and, if the latter, glassy or rubbery. Commercial crystalline polymers are about 20% amorphous, and it is through these regions that diffusion occurs. As with the transport of gases through metals, transport through polymer membranes is characterized by the solution-diffusion mechanism of (3-50). Fick's first law, in the following integrated forms, is then applied to compute the mass-transfer flux.

Gas species:

$$N_i = \frac{H_i D_i}{z_2 - z_1}(p_{i_1} - p_{i_2}) = \frac{P_{M_i}}{z_2 - z_1}(p_{i_1} - p_{i_2}) \tag{3-52}$$

where p_i is the partial pressure at a polymer surface.

Table 3.12 Diffusivities of Solutes in Rubbery Polymers

Polymer	Solute	Temperature, K	Diffusivity, cm^2/s
Polyisobutylene	*n*-Butane	298	1.19×10^{-9}
	i-Butane	298	5.3×10^{-10}
	n-Pentane	298	1.08×10^{-9}
	n-Hexadecane	298	6.08×10^{-10}
Hevea rubber	*n*-Butane	303	2.3×10^{-7}
	i-Butane	303	1.52×10^{-7}
	n-Pentane	303	2.3×10^{-7}
	n-Hexadecane	298	7.66×10^{-8}
Polymethylacrylate	Ethyl alcohol	323	2.18×10^{-10}
Polyvinylacetate	*n*-Propyl alcohol	313	1.11×10^{-12}
	n-Propyl chloride	313	1.34×10^{-12}
	Ethyl chloride	343	2.01×10^{-9}
	Ethyl bromide	343	1.11×10^{-9}
Polydimethylsiloxane	*n*-Hexadecane	298	1.6×10^{-6}
1,4-Polybutadiene	*n*-Hexadecane	298	2.21×10^{-7}
Styrene-butadiene rubber	*n*-Hexadecane	298	2.66×10^{-8}

Liquid species:

$$N_i = \frac{K_i D_i}{z_2 - z_1}(c_{i_1} - c_{i_2}) \tag{3-53}$$

where K_i, the equilibrium partition coefficient, is the ratio of the concentration in the polymer to the concentration, c_i, in the liquid at the polymer surface. The product $K_i D_i$ is the liquid permeability.

Diffusivities for light gases in four polymers, given in Table 14.6, range from 1.3×10^{-9} to 1.6×10^{-6} cm^2/s, which is magnitudes less than for diffusion in a gas.

Diffusivity of liquids in rubbery polymers has been studied as a means of determining viscoelastic parameters. In Table 3.12, taken from Ferry [20], diffusivities are given for solutes in seven different rubber polymers at near-ambient conditions. The values cover a sixfold range, with the largest diffusivity being that for *n*-hexadecane in polydimethylsiloxane. The smallest diffusivities correspond to the case in which the temperature approaches the glass-transition temperature, where the polymer becomes glassy in structure. This more rigid structure hinders diffusion. As expected, smaller molecules have higher diffusivities. A study of *n*-hexadecane in styrene-butadiene copolymers at 25°C by Rhee and Ferry [21] shows a large effect on diffusivity of polymer fractional free volume.

Polymers that are 100% crystalline permit little or no diffusion of gases and liquids. The diffusivity of methane at 25°C in polyoxyethylene oxyisophthaloyl decreases from 0.30×10^{-9} to 0.13×10^{-9} cm^2/s when the degree of crystallinity increases from 0 to 40% [22]. A measure of crystallinity is the polymer density. The diffusivity of methane at 25°C in polyethylene decreases from 0.193×10^{-6} to 0.057×10^{-6} cm^2/s when specific gravity increases from 0.914 to 0.964 [22]. Plasticizers cause diffusivity to increase. When polyvinylchloride is plasticized with 40% tricresyl triphosphate, the diffusivity of CO at 27°C increases from 0.23×10^{-8} to 2.9×10^{-8} cm^2/s [22].

EXAMPLE 3.10 Diffusion of Hydrogen through a Membrane.

Hydrogen diffuses through a nonporous polyvinyltrimethylsilane membrane at 25°C. The pressures on the sides of the membrane are 3.5 MPa and 200 kPa. Diffusivity and solubility data are given in Table 14.9. If the hydrogen flux is to be 0.64 $kmol/m^2$-h, how thick in micrometers (μm) should the membrane be?

Solution

Equation (3-52) applies. From Table 14.9,

$$D = 160 \times 10^{-11} m^2/s, \quad H = S = 0.54 \times 10^{-4} mol/m^3\text{-Pa}$$

$$\text{From (3-50), } P_M = DH = (160 \times 10^{-11})(0.64 \times 10^{-4})$$
$$= 86.4 \times 10^{-15} \text{mol/m-s-Pa}$$
$$p_1 = 3.5 \times 10^6 \text{ Pa}, \quad p_2 = 0.2 \times 10^6 \text{ Pa}$$

$$\text{Membrane thickness} = z_2 - z_1 = \Delta z = P_M(p_1 - p_2)/N$$

$$\Delta z = \frac{86.4 \times 10^{-15}(3.5 \times 10^6 - 0.2 \times 10^6)}{[0.64(1000)/3600]}$$
$$= 1.6 \times 10^{-6} m = 1.6\ \mu m$$

Membranes must be thin to achieve practical permeation rates.

Cellular solids and wood

A widely used cellular solid is wood, whose structure is discussed by Gibson and Ashby [23]. Chemically, wood consists of lignin, cellulose, hemicellulose, and minor amounts of

organic chemicals and elements. The latter are extractable, and the former three, which are all polymers, give wood its structure. Green wood also contains up to 25 wt% moisture in the cell walls and cell cavities. Adsorption or desorption of moisture in wood causes anisotropic swelling and shrinkage.

Wood often consists of (1) highly elongated hexagonal or rectangular cells, called tracheids in softwood (coniferous species, e.g., spruce, pine, and fir) and fibers in hardwood (deciduous or broad-leaf species, e.g., oak, birch, and walnut); (2) radial arrays of rectangular-like cells, called rays; and (3) enlarged cells with large pore spaces and thin walls, called sap channels because they conduct fluids up the tree.

Many of the properties of wood are anisotropic. For example, stiffness and strength are 2 to 20 times greater in the axial direction of the tracheids or fibers than in the radial and tangential directions of the trunk. This anisotropy extends to permeability and diffusivity of wood penetrants, such as moisture and preservatives. According to Stamm [24], the permeability of wood to liquids in the axial direction can be up to 10 times greater than in the transverse direction.

Movement of liquids and gases through wood occurs during drying and treatment with preservatives, fire retardants, and other chemicals. It takes place by capillarity, pressure permeability, and diffusion. All three mechanisms of movement of gases and liquids in wood are considered by Stamm [24]. Only diffusion is discussed here.

The simplest form of diffusion is that of a water-soluble solute through wood saturated with water, so no dimensional changes occur. For the diffusion of urea, glycerine, and lactic acid into hardwood, Stamm [24] lists diffusivities in the axial direction that are 50% of ordinary liquid diffusivities. In the radial direction, diffusivities are 10% of the axial values. At 26.7°C, the diffusivity of zinc sulfate in water is 5×10^{-6} cm^2/s. If loblolly pine sapwood is impregnated with zinc sulfate in the radial direction, the diffusivity is 0.18×10^{-6} cm^2/s [24].

The diffusion of water in wood is complex. Water is held in the wood in different ways. It may be physically adsorbed on cell walls in monomolecular layers, condensed in preexisting or transient cell capillaries, or absorbed into cell walls to form a solid solution.

Because of the practical importance of lumber drying rates, most diffusion coefficients are measured under drying conditions in the radial direction across the fibers. Results depend on temperature and specific gravity. Typical results are given by Sherwood [25] and Stamm [24]. For example, for beech with a swollen specific gravity of 0.4, the diffusivity increases from a value of 1×10^{-6} cm^2/s at 10°C to 10×10^{-6} cm^2/s at 60°C.

§3.3 STEADY- AND UNSTEADY-STATE MASS TRANSFER THROUGH STATIONARY MEDIA

Mass transfer occurs in (1) stagnant or stationary media, (2) fluids in laminar flow, and (3) fluids in turbulent flow, each requiring a different calculation procedure. The first is presented in this section, the other two in subsequent sections.

Fourier's law is used to derive equations for the rate of heat transfer by conduction for steady-state and unsteady-state conditions in stationary media consisting of shapes such as slabs, cylinders, and spheres. Analogous equations can be derived for mass transfer using Fick's law.

In one dimension, the molar rate of mass transfer of A in a binary mixture is given by a modification of (3-12), which includes bulk flow and molecular diffusion:

$$n_A = x_A(n_A + n_B) - cD_{AB}A\left(\frac{dx_A}{dz}\right) \tag{3-54}$$

If A is undergoing mass transfer but B is stationary, $n_B = 0$. It is common to assume that c is a constant and x_A is small. The bulk-flow term is then eliminated and (3-54) becomes Fick's first law:

$$n_A = -cD_{AB}A\left(\frac{dx_A}{dz}\right) \tag{3-55}$$

Alternatively, (3-55) can be written in terms of a concentration gradient:

$$n_A = -D_{AB}A\left(\frac{dc_A}{dz}\right) \tag{3-56}$$

This equation is analogous to Fourier's law for the rate of heat conduction, Q:

$$Q = -kA\left(\frac{dT}{dz}\right) \tag{3-57}$$

§3.3.1 Steady-State Diffusion

For steady-state, one-dimensional diffusion with constant D_{AB}, (3-56) can be integrated for various geometries, the results being analogous to heat conduction.

1. Plane wall with a thickness, $z_2 - z_1$:

$$\boxed{n_A = D_{AB}A\left(\frac{c_{A_1} - c_{A_2}}{z_2 - z_2}\right)} \tag{3-58}$$

2. Hollow cylinder of inner radius r_1 and outer radius r_2, with diffusion in the radial direction outward:

$$n_A = 2\pi L\frac{D_{AB}(c_{A_1} - c_{A_2})}{\ln(r_2/r_1)} \tag{3-59}$$

or

$$n_A = D_{AB}A_{LM}\left(\frac{c_{A_1} - c_{A_2}}{r_2 - r_1}\right) \tag{3-60}$$

where

A_{LM} = log mean of the areas $2\pi rL$ at r_1 and r_2
L = length of the hollow cylinder

3. Spherical shell of inner radius r_1 and outer radius r_2, with diffusion in the radial direction outward:

$$n_A = \frac{4\pi r_1 r_2 D_{AB}(c_{A_1} - c_{A_2})}{r_2 - r_1} \tag{3-61}$$

or
$$n_A = D_{AB} A_{GM} \left(\frac{c_{A_1} - c_{A_2}}{r_2 - r_1} \right) \tag{3-62}$$

where A_{GM} = geometric mean of the areas $4\pi r^2$.

When $r_1/r_2 < 2$, the arithmetic mean area is no more than 4% greater than the log mean area. When $r_1/r_2 < 1.33$, the arithmetic mean area is no more than 4% greater than the geometric mean area.

§3.3.2 Unsteady-State Diffusion

Consider one-dimensional molecular diffusion of species A in stationary B through a differential control volume with diffusion in the z-direction only, as shown in Figure 3.5. Assume constant diffusivity and negligible bulk flow. The molar flow rate of species A by diffusion in the z-direction is given by (3-56):

$$n_{A_z} = -D_{AB} A \left(\frac{\partial c_A}{\partial z} \right)_z \tag{3-63}$$

At the plane, $z = z + \Delta z$, the diffusion rate is

$$n_{A_{z+\Delta z}} = -D_{AB} A \left(\frac{\partial c_A}{\partial z} \right)_{z+\Delta z} \tag{3-64}$$

The accumulation of species A in the control volume is

$$A \frac{\partial c_A}{\partial t} \Delta z \tag{3-65}$$

Since rate in – rate out = accumulation,

$$-D_{AB} A \left(\frac{\partial c_A}{\partial z} \right)_z + D_{AB} A \left(\frac{\partial c_A}{\partial z} \right)_{z+\Delta z} = A \left(\frac{\partial c_A}{\partial t} \right) \Delta z \tag{3-66}$$

Rearranging and simplifying,

$$D_{AB} \left[\frac{(\partial c_A/\partial z)_{z+\Delta z} - (\partial c_A/\partial z)_z}{\Delta z} \right] = \frac{\partial c_A}{\partial t} \tag{3-67}$$

In the limit, as $\Delta z \to 0$,

$$\frac{\partial c_A}{\partial t} = D_{AB} \frac{\partial^2 c_A}{\partial z^2} \tag{3-68}$$

Equation (3-68) is Fick's second law for one-dimensional diffusion.

The more general form for three-dimensional rectangular coordinates is

$$\boxed{\frac{\partial c_A}{\partial t} = D_{AB} \left(\frac{\partial^2 c_A}{\partial x^2} + \frac{\partial^2 c_A}{\partial y^2} + \frac{\partial^2 c_A}{\partial z^2} \right)} \tag{3-69}$$

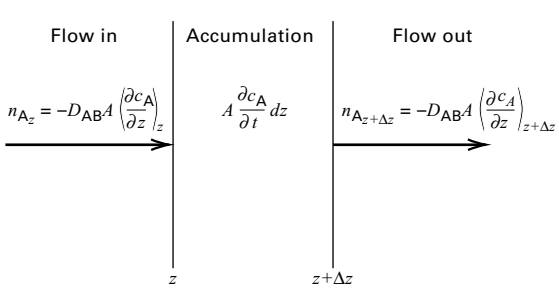

Figure 3.5 Unsteady-state diffusion through a volume $A\,dz$.

For one-dimensional diffusion in the radial direction only for cylindrical and spherical coordinates, Fick's second law becomes, respectively,

$$\frac{\partial c_A}{\partial t} = \frac{D_{AB}}{r} \frac{\partial}{\partial r} \left(r \frac{\partial c_A}{\partial r} \right) \tag{3-70}$$

and
$$\frac{\partial c_A}{\partial t} = \frac{D_{AB}}{r^2} \frac{\partial}{\partial r} \left(r^2 \frac{\partial c_A}{\partial r} \right) \tag{3-71}$$

Equations (3-68) to (3-71) are analogous to Fourier's second law of heat conduction, where c_A is replaced by temperature, T, and diffusivity, D_{AB}, by thermal diffusivity, $\alpha = k/\rho C_P$. The analogous three equations for heat conduction for constant, isotropic properties are, respectively:

$$\frac{\partial T}{\partial t} = \alpha \left(\frac{\partial^2 T}{\partial x^2} + \frac{\partial^2 T}{\partial y^2} + \frac{\partial^2 T}{\partial z^2} \right) \tag{3-72}$$

$$\frac{\partial T}{\partial t} = \frac{\alpha}{r} \frac{\partial}{\partial r} \left(r \frac{\partial T}{\partial r} \right) \tag{3-73}$$

$$\frac{\partial T}{\partial t} = \frac{\alpha}{r^2} \frac{\partial}{\partial r} \left(r^2 \frac{\partial T}{\partial r} \right) \tag{3-74}$$

Analytical solutions to these partial differential equations in either Fick's-law or Fourier's-law form are available for a variety of boundary conditions. They are derived and discussed by Carslaw and Jaeger [26] and Crank [27].

§3.3.3 Diffusion in a Semi-infinite Medium

Consider the semi-infinite medium shown in Figure 3.6, which extends in the z-direction from $z = 0$ to $z = \infty$. The x and y coordinates extend from $-\infty$ to $+\infty$ but are not of interest because diffusion is assumed to take place only in the z-direction. Thus, (3-68) applies to the region $z \geq 0$. At time $t \leq 0$, the concentration is c_{A_o} for $z \geq 0$. At $t = 0$, the surface of the semi-infinite medium at $z = 0$ is instantaneously brought to the concentration $c_{A_s} > c_{A_o}$ and held there for $t > 0$, causing diffusion into the medium to occur. Because the medium is infinite in the z-direction, diffusion cannot extend to $z = \infty$ and, therefore, as $z \to \infty$, $c_A = c_{A_o}$ for all $t \geq 0$. Because (3-68) and its one boundary (initial) condition in time and two boundary conditions in distance are linear in the dependent variable, c_A, an exact solution can be obtained by combination of variables [28] or the Laplace transform method [29]. The result, in terms of fractional concentration change, is

$$\theta = \frac{c_A - c_{A_o}}{c_{A_s} - c_{A_o}} = \operatorname{erfc} \left(\frac{z}{2\sqrt{D_{AB} t}} \right) \tag{3-75}$$

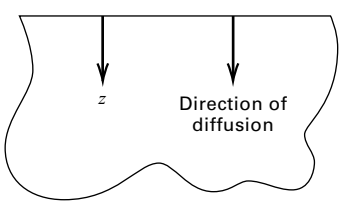

Figure 3.6 One-dimensional diffusion into a semi-infinite medium.

where the complementary error function, erfc, is related to the error function, erf, by

$$\text{erfc}(x) = 1 - \text{erf}(x) = 1 - \frac{2}{\sqrt{\pi}}\int_0^x e^{-\eta^2} d\eta \qquad (3\text{-}76)$$

The error function is included in most spreadsheet programs and handbooks, such as *Handbook of Mathematical Functions* [30]. The variation of erf(x) and erfc(x) is:

x	erf(x)	erfc(x)
0	0.0000	1.0000
0.5	0.5205	0.4795
1.0	0.8427	0.1573
1.5	0.9661	0.0339
2.0	0.9953	0.0047
∞	1.0000	0.0000

Equation (3-75) determines the concentration in the semi-infinite medium as a function of time and distance from the surface, assuming no bulk flow. It applies rigorously to diffusion in solids, and also to stagnant liquids and gases when the medium is dilute in the diffusing solute.

In (3-75), when $(z/2\sqrt{D_{AB}t}) = 2$, the complementary error function is only 0.0047, which represents less than a 1% change in the ratio of the concentration change at $z = z$ to the change at $z = 0$. It is common to call $z = 4\sqrt{D_{AB}t}$ the penetration depth, and to apply (3-75) to media of finite thickness as long as the thickness is greater than the penetration depth.

The instantaneous rate of mass transfer across the surface of the medium at $z = 0$ can be obtained by taking the derivative of (3-75) with respect to distance and substituting it into Fick's first law applied at the surface of the medium. Then, using the Leibnitz rule for differentiating the integral of (3-76), with $x = z/2\sqrt{D_{AB}t}$,

$$\begin{aligned} n_A &= -D_{AB}A\left(\frac{\partial c_A}{\partial z}\right)_{z=0} \\ &= D_{AB}A\left(\frac{c_{A_s} - c_{A_o}}{\sqrt{\pi D_{AB}t}}\right)\exp\left(-\frac{z^2}{4D_{AB}t}\right)\Bigg|_{z=0} \end{aligned} \qquad (3\text{-}77)$$

Thus,
$$n_A|_{z=0} = \sqrt{\frac{D_{AB}}{\pi t}}A(c_{A_s} - c_{A_o}) \qquad (3\text{-}78)$$

The total number of moles of solute, $\mathcal{N}_A$, transferred into the semi-infinite medium is obtained by integrating (3-78) with respect to time:

$$\begin{aligned} \mathcal{N}_A &= \int_o^t n_A|_{z=0}dt = \sqrt{\frac{D_{AB}}{\pi}}A(c_{A_s} - c_{A_o})\int_o^t \frac{dt}{\sqrt{t}} \\ &= 2A(c_{A_s} - c_{A_o})\sqrt{\frac{D_{AB}t}{\pi}} \end{aligned} \qquad (3\text{-}79)$$

EXAMPLE 3.11 Rates of Diffusion in Stagnant Media.

Determine how long it will take for the dimensionless concentration change, $\theta = (c_A - c_{A_o})/(c_{A_s} - c_{A_o})$, to reach 0.01 at a depth $z = 100$ cm in a semi-infinite medium. The medium is initially at a solute concentration c_{A_o}, after the surface concentration at $z = 0$ increases to c_{A_s}, for diffusivities representative of a solute diffusing through a stagnant gas, a stagnant liquid, and a solid.

Solution

For a gas, assume $D_{AB} = 0.1$ cm^2/s. From (3-75) and (3-76),

$$\theta = 0.01 = 1 - \text{erf}\left(\frac{z}{2\sqrt{D_{AB}t}}\right)$$

Therefore,
$$\text{erf}\left(\frac{z}{2\sqrt{D_{AB}t}}\right) = 0.99$$

From tables of the error function,
$$\left(\frac{z}{2\sqrt{D_{AB}t}}\right) = 1.8214$$

Solving,
$$t = \left[\frac{100}{1.8214(2)}\right]^2 \frac{1}{0.10} = 7{,}540\,\text{s} = 2.09\,\text{h}$$

In a similar manner, the times for typical gas, liquid, and solid media are found to be drastically different, as shown below.

Semi-infinite Medium	D_{AB}, cm^2/s	Time for $\theta = 0.01$ at 1 m
Gas	0.10	2.09 h
Liquid	1×10^{-5}	2.39 year
Solid	1×10^{-9}	239 centuries

The results show that molecular diffusion is very slow, especially in liquids and solids. In liquids and gases, the rate of mass transfer can be greatly increased by agitation to induce turbulent motion. For solids, it is best to reduce the size of the solid.

§3.3.4 Medium of Finite Thickness with Sealed Edges

Consider a rectangular, parallelepiped stagnant medium of thickness $2a$ in the z-direction, and either infinitely long dimensions in the y- and x-directions or finite lengths $2b$ and $2c$. Assume that in Figure 3.7a the edges parallel to the z-direction are sealed, so diffusion occurs only in the z-direction, and that initially, the concentration of the solute in the medium is uniform at c_{A_o}. At time $t = 0$, the two unsealed surfaces at $z = \pm a$ are brought to and held at concentration $c_{A_s} > c_{A_o}$. Because of symmetry, $\partial c_A/\partial z = 0$ at $z = 0$. Assume constant D_{AB}. Again (3-68) applies, and an exact solution can be obtained because both (3-68) and the boundary conditions are linear in c_A. The result from Carslaw and Jaeger [26], in terms of the fractional, unaccomplished concentration change, E, is

$$\begin{aligned} E = 1 - \theta = \frac{c_{A_s} - c_A}{c_{A_s} - c_{A_o}} &= \frac{4}{\pi}\sum_{n=0}^{\infty}\frac{(-1)^n}{(2n+1)} \\ &\times \exp\left[-D_{AB}(2n+1)^2\pi^2 t/4a^2\right]\cos\frac{(2n+1)\pi z}{2a} \end{aligned} \qquad (3\text{-}80)$$

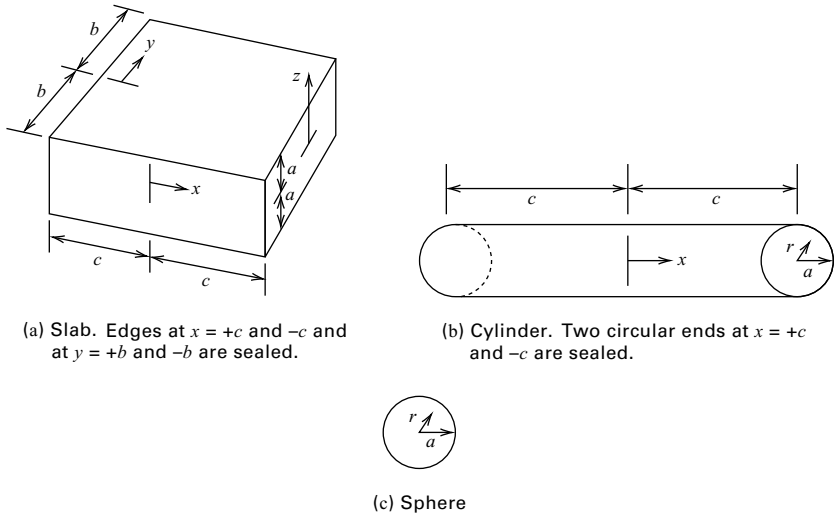

(a) Slab. Edges at $x = +c$ and $-c$ and at $y = +b$ and $-b$ are sealed.

(b) Cylinder. Two circular ends at $x = +c$ and $-c$ are sealed.

(c) Sphere

Figure 3.7 Unsteady-state diffusion in media of finite dimensions.

or, in terms of the complementary error function,

$$E = 1 - \theta = \frac{c_{A_s} - c_A}{c_{A_s} - c_{A_o}} = \sum_{n=0}^{\infty} (-1)^n \times \left[\operatorname{erfc} \frac{(2n+1)a - z}{2\sqrt{D_{AB}t}} + \operatorname{erfc} \frac{(2n+1)a + z}{2\sqrt{D_{AB}t}} \right] \tag{3-81}$$

For large values of $D_{AB}t/a^2$, called the Fourier number for mass transfer, the infinite series solutions of (3-80) and (3-81) converge rapidly, but for small values (e.g., short times), they do not. However, in the latter case, the solution for the semi-infinite medium applies for $D_{AB}t/a^2 < \frac{1}{16}$. A plot of the solution is given in Figure 3.8.

The instantaneous rate of mass transfer across the surface of either unsealed face of the medium (i.e., at $z = \pm a$) is obtained by differentiating (3-80) with respect to z, evaluating the result at $z = a$, and substituting into Fick's first law to give

$$n_A|_{z=a} = \frac{2D_{AB}(c_{A_s} - c_{A_o})A}{a} \times \sum_{n=0}^{\infty} \exp\left[-\frac{D_{AB}(2n+1)^2\pi^2 t}{4a^2} \right] \tag{3-82}$$

The total moles transferred across either unsealed face is determined by integrating (3-82) with respect to time:

$$\mathcal{N}_A = \int_o^t n_A|_{z=a} dt = \frac{8(c_{A_s} - c_{A_o})Aa}{\pi^2} \times \sum_{n=0}^{\infty} \frac{1}{(2n+1)^2} \left\{ 1 - \exp\left[-\frac{D_{AB}(2n+1)^2\pi^2 t}{4a^2} \right] \right\} \tag{3-83}$$

For a slab, the average concentration of the solute $c_{A_{avg}}$, as a function of time, is

$$\frac{c_{A_s} - c_{A_{avg}}}{c_{A_s} - c_{A_o}} = \frac{\int_o^a (1 - \theta) dz}{a} \tag{3-84}$$

Substitution of (3-80) into (3-84), followed by integration, gives

$$E_{avg_{slab}} = (1 - \theta_{ave})_{slab} = \frac{c_{A_s} - c_{A_{avg}}}{c_{A_s} - c_{A_o}} = \frac{8}{\pi^2} \sum_{n=0}^{\infty} \frac{1}{(2n+1)^2} \exp\left[-\frac{D_{AB}(2n+1)^2\pi^2 t}{4a^2} \right] \tag{3-85}$$

This equation is plotted in Figure 3.9. The concentrations are in mass of solute per mass of dry solid or mass of solute/volume. This assumes that during diffusion, the solid does not shrink or expand; thus, the mass of dry solid per unit volume of wet solid remains constant. In drying it is common to express moisture content on a dry-solid basis.

When the edges of the slab in Figure 3.7a are not sealed, the method of Newman [31] can be used with (3-69) to determine concentration changes within the slab. In this method,

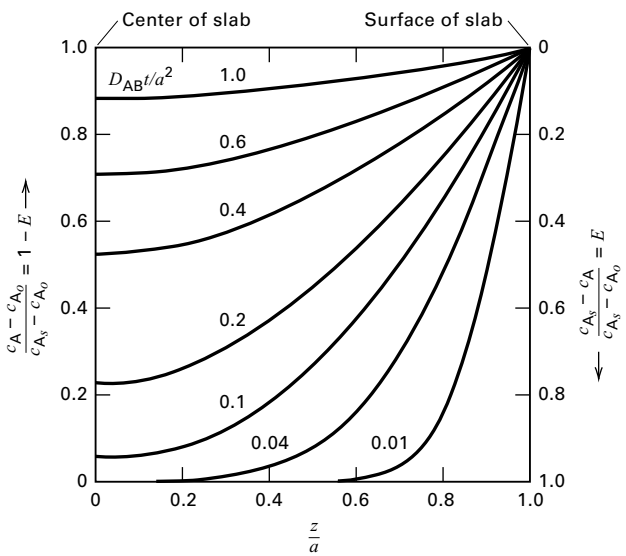

Figure 3.8 Concentration profiles for unsteady-state diffusion in a slab.

Adapted from H.S. Carslaw and J.C. Jaeger, *Conduction of Heat in Solids*, 2nd ed., Oxford University Press, London (1959).]

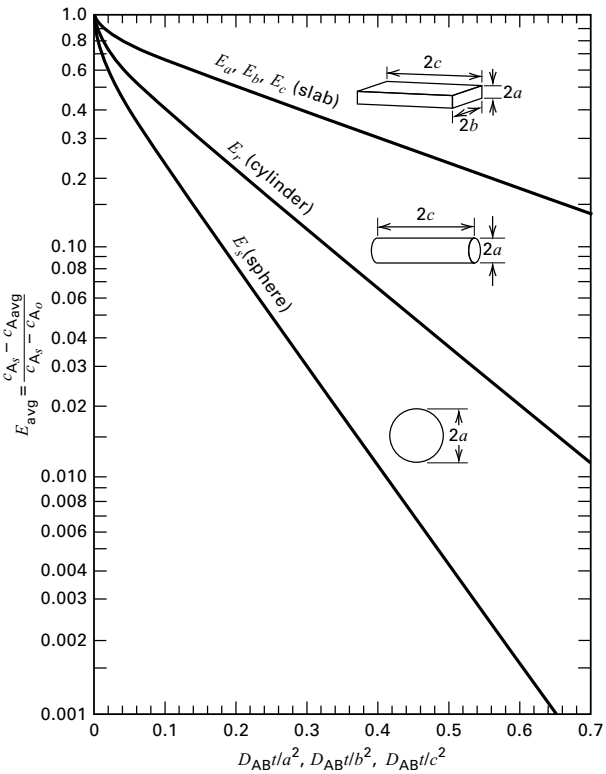

Figure 3.9 Average concentrations for unsteady-state diffusion.

[Adapted from R.E. Treybal, *Mass-Transfer Operations*, 3rd ed., McGraw-Hill, New York (1980).]

E or E_{avg} is given in terms of E values from the solution of (3-68) for each of the coordinate directions by

$$E = E_x E_y E_z \tag{3-86}$$

Corresponding solutions for infinitely long, circular cylinders and spheres are available in Carslaw and Jaeger [26] and are plotted in Figures 3.9 to 3.11. For a short cylinder whose ends are not sealed, E or E_{avg} is given by the method of Newman as

$$E = E_r E_x \tag{3-87}$$

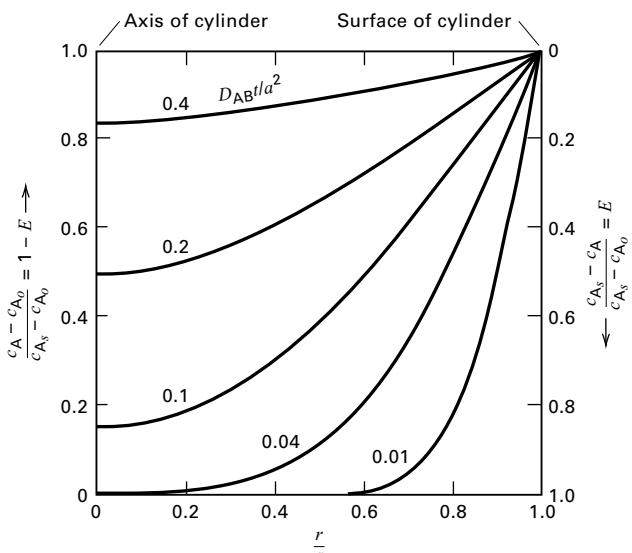

Figure 3.10 Concentration profiles for unsteady-state diffusion in a cylinder.

[Adapted from H.S. Carslaw and J.C. Jaeger, *Conduction of Heat in Solids*, 2nd ed., Oxford University Press, London (1959).]

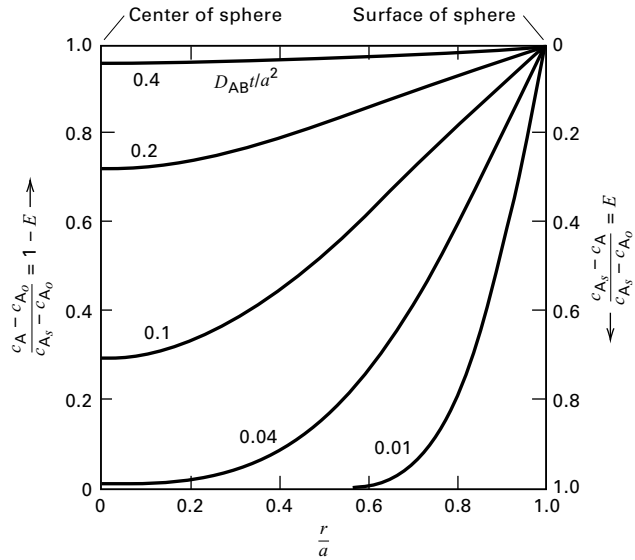

Figure 3.11 Concentration profiles for unsteady-state diffusion in a sphere.

[Adapted from H.S. Carslaw and J.C. Jaeger, *Conduction of Heat in Solids*, 2nd ed., Oxford University Press, London (1959).]

For anisotropic materials, Fick's second law in the form of (3-69) does not hold. Although the general anisotropic case is exceedingly complex, as shown in the following example, its mathematical treatment is relatively simple when the principal axes of diffusivity coincide with the coordinate system.

EXAMPLE 3.12 Diffusion of Moisture from Lumber.

A board of lumber 5 × 10 × 20 cm initially contains 20 wt% moisture. At time zero, all six faces are brought to an equilibrium moisture content of 2 wt%. Diffusivities for moisture at 25°C are 2×10^{-5} cm^2/s in the axial (z) direction along the fibers and 4×10^{-6} cm^2/s in the two directions perpendicular to the fibers. Calculate the time in hours for the average moisture content to drop to 5 wt% at 25°C. At that time, determine the moisture content at the center of the slab. All moisture contents are on a dry basis.

Solution

In this case, the solid is anisotropic, with $D_x = D_y = 4 \times 10^{-6}$ cm^2/s and $D_z = 2 \times 10^{-5}$ cm^2/s, where dimensions $2c$, $2b$, and $2a$ in the x-, y-, and z-directions are 5, 10, and 20 cm, respectively. Fick's second law for an isotropic medium, (3-69), must be rewritten as

$$\frac{\partial c_A}{\partial t} = D_x\left[\frac{\partial^2 c_A}{\partial x^2} + \frac{\partial^2 c_A}{\partial y^2}\right] + D_z \frac{\partial^2 c_A}{\partial z^2} \tag{1}$$

To transform (1) into the form of (3-69) [26], let

$$x_1 = x\sqrt{\frac{D}{D_x}}, \quad y_1 = y\sqrt{\frac{D}{D_x}}, \quad z_1 = z\sqrt{\frac{D}{D_z}} \tag{2}$$

where D is arbitrarily chosen. With these changes, (1) becomes

$$\frac{\partial c_A}{\partial t} = D\left(\frac{\partial^2 c_A}{\partial x_1^2} + \frac{\partial^2 c_A}{\partial y_1^2} + \frac{\partial^2 c_A}{\partial z_1^2}\right) \tag{3}$$

This is the same form as (3-69), and since the boundary conditions do not involve diffusivities, Newman's method applies, using Figure 3.9, where concentration c_A is replaced by weight-percent moisture on a dry basis. From (3-86) and (3-85),

$$E_{\text{ave}_{\text{slab}}} = E_{\text{avg}_x} E_{\text{avg}_y} E_{\text{avg}_z} = \frac{c_{A_{\text{ave}}} - c_{A_s}}{c_{A_o} - c_{A_s}} = \frac{5-2}{20-2} = 0.167$$

Let $D = 1 \times 10^{-5}$ cm^2/s.

z_1 Direction (axial):

$$a_1 = a\left(\frac{D}{D_z}\right)^{1/2} = \frac{20}{2}\left(\frac{1\times10^{-5}}{2\times10^{-5}}\right)^{1/2} = 7.07\,\text{cm}$$

$$\frac{Dt}{a_1^2} = \frac{1\times10^{-5}t}{7.07^2} = 2.0\times10^{-7}t, \text{s}$$

y_1 Direction:

$$b_1 = b\left(\frac{D}{D_y}\right)^{1/2} = \frac{20}{2}\left(\frac{1\times10^{-5}}{4\times10^{-6}}\right)^{1/2} = 7.906\,\text{cm}$$

$$\frac{Dt}{b_1^2} = \frac{1\times10^{-5}t}{7.906^2} = 1.6\times10^{-7}t, \text{s}$$

x_1 Direction:

$$c_1 = c\left(\frac{D}{D_x}\right)^{1/2} = \frac{5}{2}\left(\frac{1\times10^{-5}}{4\times10^{-6}}\right)^{1/2} = 3.953\,\text{cm}$$

$$\frac{Dt}{c_1^2} = \frac{1\times10^{-5}t}{3.953^2} = 6.4\times10^{-7}t, \text{s}$$

Figure 3.9 is used iteratively with assumed values of time in seconds to obtain values of E_{avg} for each of the three coordinates until (3-86) equals 0.167.

t, h	t, s	$E_{\text{avg}_{z_1}}$	$E_{\text{avg}_{y_1}}$	$E_{\text{avg}_{x_1}}$	E_{avg}
100	360,000	0.70	0.73	0.46	0.235
120	432,000	0.67	0.70	0.41	0.193
135	486,000	0.65	0.68	0.37	0.164

Therefore, it takes approximately 136 h.

For 136 h = 490,000 s, Fourier numbers for mass transfer are

$$\frac{Dt}{a_1^2} = \frac{(1\times10^{-5})(490{,}000)}{7.07^2} = 0.0980$$

$$\frac{Dt}{b_1^2} = \frac{(1\times10^{-5})(490{,}000)}{7.906^2} = 0.0784$$

$$\frac{Dt}{c_1^2} = \frac{(1\times10^{-5})(490{,}000)}{3.953^2} = 0.3136$$

From Figure 3.8, at the center of the slab,

$$E_{\text{center}} = E_{z_1}E_{y_1}E_{x_1} = (0.945)(0.956)(0.605) = 0.547$$

$$= \frac{c_{A_s} - c_{A_{\text{center}}}}{c_{A_s} - c_{A_o}} = \frac{2 - c_{A_{\text{center}}}}{2-20} = 0.547$$

Solving, c_A at the center = 11.8 wt% moisture

§3.4 MASS TRANSFER IN LAMINAR FLOW

Many mass-transfer operations involve diffusion in fluids in laminar flow. As with convective heat-transfer in laminar flow, the calculation of such operations is amenable to well-defined theory. This is illustrated in this section by three common applications: (1) a fluid falling as a film down a wall; (2) a fluid flowing slowly along a horizontal, flat plate; and (3) a fluid flowing slowly through a circular tube, where mass transfer occurs, respectively, between a gas and the falling liquid film, from the surface of the flat plate into the flowing fluid, and from the inside surface of the tube into the flowing fluid.

§3.4.1 Falling Laminar, Liquid Film

Consider a thin liquid film containing A and nonvolatile B, falling in laminar flow at steady state down one side of a vertical surface and exposed to pure gas, A, which diffuses into the liquid, as shown in Figure 3.12. The surface is infinitely wide in the x-direction (normal to the page), flow is in the downward y-direction, and mass transfer of A is in the z-direction. Assume that the rate of mass transfer of A into the liquid film is so small that the liquid velocity in the z-direction, u_z, is zero. From fluid mechanics, in the absence of end effects the equation of motion for the liquid film in fully developed laminar flow in the y-direction is

$$\mu\frac{d^2u_y}{dz^2} + \rho g = 0 \tag{3-88}$$

Usually, fully developed flow, where u_y is independent of the distance y, is established quickly. If δ is the film thickness and the boundary conditions are $u_y = 0$ at $z = \delta$ (no slip at the solid surface) and $du_y/dz = 0$ at $z = 0$ (no drag at the gas–liquid interface), (3-88) is readily integrated to give a parabolic velocity profile:

$$u_y = \frac{\rho g\delta^2}{2\mu}\left[1 - \left(\frac{z}{\delta}\right)^2\right] \tag{3-89}$$

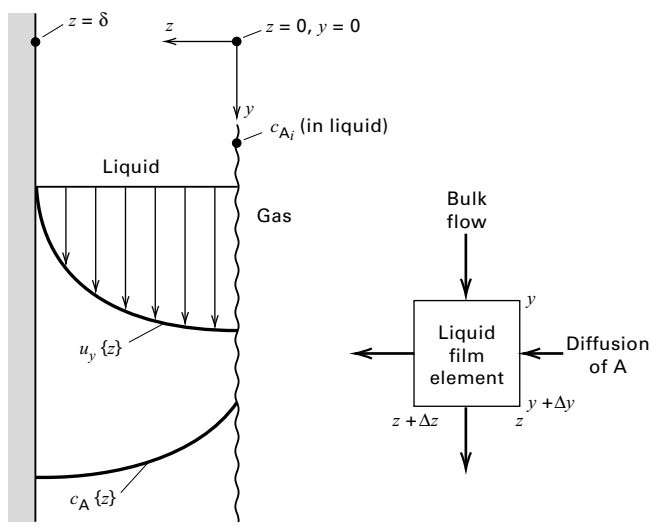

Figure 3.12 Mass transfer from a gas into a falling, laminar liquid film.

The maximum liquid velocity occurs at $z = 0$,

$$(u_y)_{\max} = \frac{\rho g \delta^2}{2\mu} \tag{3-90}$$

The bulk-average velocity in the liquid film is

$$\bar{u}_y = \frac{\int_0^\delta u_y dz}{\delta} = \frac{\rho g \delta^2}{3\mu} \tag{3-91}$$

Thus, with no entrance effects, the film thickness for fully developed flow is independent of location y and is

$$\delta = \left(\frac{3\bar{u}_y \mu}{\rho g}\right)^{1/2} = \left(\frac{3\mu\Gamma}{\rho^2 g}\right)^{1/3} \tag{3-92}$$

where Γ = liquid film flow rate per unit width of film, W. For film flow, the Reynolds number, which is the ratio of the inertial force to the viscous force, is

$$N_{\mathrm{Re}} = \frac{4 r_H \bar{u}_y \rho}{\mu} = \frac{4\delta \bar{u}_y \rho}{\mu} = \frac{4\Gamma}{\mu} \tag{3-93}$$

where r_H = hydraulic radius = (flow cross section)/(wetted perimeter) = $(W\delta)/W = \delta$ and, by continuity, $\Gamma = \bar{u}_y \rho \delta$.

Grimley [32] found that for $N_{\mathrm{Re}} < 8$ to 25, depending on surface tension and viscosity, flow in the film is laminar and the interface between the liquid film and gas is flat. The value of 25 is obtained with water. For 8 to 25 $< N_{\mathrm{Re}} <$ 1,200, the flow is still laminar, but ripples may appear at the interface unless suppressed by the addition of wetting agents.

For a flat interface and a low rate of mass transfer of A, Eqs. (3-88) to (3-93) hold, and the film velocity profile is given by (3-89). Consider a mole balance on A for an incremental volume of liquid film of constant density, as shown in Figure 3.12. Neglect bulk flow in the z-direction and axial diffusion in the y-direction. Thus, mass transfer of A from the gas into the liquid occurs only by molecular diffusion in the z-direction. Then, at steady state, neglecting accumulation or depletion of A in the incremental volume (quasi-steady-state assumption),

$$\begin{aligned} &-D_{\mathrm{AB}}(\Delta y)(\Delta x)\left(\frac{\partial c_{\mathrm{A}}}{\partial z}\right)_z + u_y c_{\mathrm{A}}|_y (\Delta z)(\Delta x) \\ &\quad = -D_{\mathrm{AB}}(\Delta y)(\Delta x)\left(\frac{\partial c_{\mathrm{A}}}{\partial z}\right)_{z+\Delta z} + u_y c_{\mathrm{A}}|_{y+\Delta y}(\Delta z)(\Delta x) \end{aligned} \tag{3-94}$$

Rearranging and simplifying (3-94),

$$\left[\frac{u_y c_{\mathrm{A}}|_{y+\Delta y} - u_y c_{\mathrm{A}}|_y}{\Delta y}\right] = D_{\mathrm{AB}}\left[\frac{(\partial c_{\mathrm{A}}/\partial z)_{z+\Delta z} - (\partial c_{\mathrm{A}}/\partial z)_z}{\Delta z}\right] \tag{3-95}$$

which, in the limit, as $\Delta z \to 0$ and $\Delta y \to 0$, becomes

$$u_y \frac{\partial c_{\mathrm{A}}}{\partial y} = D_{\mathrm{AB}} \frac{\partial^2 c_{\mathrm{A}}}{\partial z^2} \tag{3-96}$$

Substituting the velocity profile of (3-89) into (3-96),

$$\frac{\rho g \delta^2}{2\mu}\left[1 - \left(\frac{z}{\delta}\right)^2\right] \frac{\partial c_{\mathrm{A}}}{\partial y} = D_{\mathrm{AB}} \frac{\partial^2 c_{\mathrm{A}}}{\partial z^2} \tag{3-97}$$

This PDE was solved by Johnstone and Pigford [33] and Olbrich and Wild [34] for the following boundary conditions, where the initial concentration of A in the liquid film is c_{A_o}:

$$\begin{aligned} c_{\mathrm{A}} &= c_{\mathrm{A}_i} \quad \text{at } z = 0 \quad \text{for } y > 0 \\ c_{\mathrm{A}} &= c_{\mathrm{A}_o} \quad \text{at } y = 0 \quad \text{for } 0 < z < \delta \\ \partial c_{\mathrm{A}}/\partial z &= 0 \quad \text{at } z = \delta \quad \text{for } 0 < y < L \end{aligned}$$

where L = height of the vertical surface. The solution of Olbrich and Wild is in the form of an infinite series, giving c_{A} as a function of z and y. Of greater interest, however, is the average concentration of A in the film at the bottom of the wall, where $y = L$, which, by integration, is

$$\bar{c}_{\mathrm{A}_y} = \frac{1}{\bar{u}_y \delta}\int_0^\delta u_y c_{\mathrm{A}_y} dz \tag{3-98}$$

For the condition $y = L$, the result is

$$\begin{aligned} \frac{c_{\mathrm{A}_i} - \bar{c}_{\mathrm{A}_L}}{c_{\mathrm{A}_i} - c_{\mathrm{A}_o}} &= 0.7857 e^{-5.1213\eta} + 0.09726 e^{-39.661\eta} \\ &\quad + 0.036093 e^{-106.25\eta} + \cdots \end{aligned} \tag{3-99}$$

where

$$\eta = \frac{2 D_{\mathrm{AB}} L}{3\delta^2 \bar{u}_y} = \frac{8/3}{N_{\mathrm{Re}} N_{\mathrm{Sc}} (\delta/L)} = \frac{8/3}{(\delta/L) N_{\mathrm{Pe_M}}} \tag{3-100}$$

$$\boxed{\begin{aligned} N_{\mathrm{Sc}} &= \text{Schmidt number} = \frac{\mu}{\rho D_{\mathrm{AB}}} \\ &= \frac{\text{momentum diffusivity, } \mu/\rho}{\text{mass diffusivity, } D_{\mathrm{AB}}} \end{aligned}} \tag{3-101}$$

$$\begin{aligned} N_{\mathrm{Pe_M}} &= N_{\mathrm{Re}} N_{\mathrm{Sc}} = \text{Peclet number for mass transfer} \\ &= \frac{4\delta \bar{u}_y}{D_{\mathrm{AB}}} \end{aligned} \tag{3-102}$$

The Schmidt number is analogous to the Prandtl number, used in heat transfer:

$$\boxed{N_{\mathrm{Pr}} = \frac{C_P \mu}{k} = \frac{(\mu/\rho)}{(k/\rho C_P)} = \frac{\text{momentum diffusivity}}{\text{thermal diffusivity}}}$$

The Peclet number for mass transfer is analogous to the Peclet number for heat transfer:

$$N_{\mathrm{Pe_H}} = N_{\mathrm{Re}} N_{\mathrm{Pr}} = \frac{4\delta \bar{u}_y C_{\mathrm{P}} \rho}{k}$$

Both are ratios of convective to molecular transport.

The total rate of absorption of A from the gas into the liquid film for height L and width W is

$$n_{\mathrm{A}} = \bar{u}_y \delta W (\bar{c}_{\mathrm{A}_L} - c_{\mathrm{A}_o}) \tag{3-103}$$

§3.4.2 Mass-Transfer Coefficients

Mass-transfer problems involving flowing fluids are often solved using *mass-transfer coefficients*, which are analogous to heat-transfer coefficients. For the latter, *Newton's law of*

cooling defines a heat-transfer coefficient, h:

$$Q = hA\Delta T \tag{3-104}$$

where Q = rate of heat transfer, A = area for heat transfer (normal to the direction of heat transfer), and ΔT = temperature-driving force.

For mass transfer, a composition-driving force replaces ΔT. Because composition can be expressed in a number of ways, different mass-transfer coefficients result. If concentration is used, Δc_A is selected as the driving force and

$$\boxed{n_A = k_c A \Delta c_A} \tag{3-105}$$

which defines a mass-transfer coefficient, k_c, in mol/time-area-driving force, for a concentration driving force. Unfortunately, no name is in general use for (3-105).

For the falling laminar film, $\Delta c_A = c_{A_i} - \bar{c}_A$, where $\bar{c}_A$ is the bulk average concentration of A in the film, which varies with vertical location, y, because even though c_{A_i} is independent of y, the average film concentration of A increases with y. A theoretical expression for k_c in terms of diffusivity is formed by equating (3-105) to Fick's first law at the gas–liquid interface:

$$\boxed{k_c A(c_{A_j} - \bar{c}_A) = -D_{AB} A \left(\frac{\partial c_A}{\partial z}\right)_{z=0}} \tag{3-106}$$

Although this is the most widely used approach for defining a mass-transfer coefficient, for a falling film it fails because $(\partial c_A/\partial z)$ at $z = 0$ is not defined. Therefore, another approach is used. For an incremental height,

$$n_A = \bar{u}_y \delta W \, d\bar{c}_A = k_c(c_{A_\perp} - \bar{c}_A) W \, dy \tag{3-107}$$

This defines a local value of k_c, which varies with distance y because $\bar{c}_A$ varies with y. An average value of k_c, over height L, can be defined by separating variables and integrating (3-107):

$$\begin{aligned} k_{c_{avg}} &= \frac{\int_0^L k_c dy}{L} = \frac{\bar{u}_y \delta \int_{c_{A_o}}^{c_{A_L}} [d\bar{c}_A/(c_{A_i} - \bar{c}_A)]}{L} \\ &= \frac{\bar{u}_y \delta}{L} \ln \frac{c_{A_i} - c_{A_o}}{c_{A_i} - \bar{c}_{A_L}} \end{aligned} \tag{3-108}$$

The argument of the natural logarithm in (3-108) is obtained from the reciprocal of (3-99). For values of η in (3-100) greater than 0.1, only the first term in (3-99) is significant (error is less than 0.5%). In that case,

$$k_{c_{avg}} = \frac{\bar{u}_y \delta}{L} \ln \frac{e^{5.1213\eta}}{0.7857} \tag{3-109}$$

Since $\ln e^x = x$,

$$k_{c_{avg}} = \frac{\bar{u}_y \delta}{L}(0.241 + 5.1213\eta) \tag{3-110}$$

In the limit for large η, using (3-100) and (3-102), (3-110) becomes

$$k_{c_{avg}} = 3.414 \frac{D_{AB}}{\delta} \tag{3-111}$$

As suggested by the Nusselt number, $N_{Nu} = h\delta/k$ for heat transfer, where δ is a characteristic length, a Sherwood number for mass transfer is defined for a falling film as

$$\boxed{N_{Sh_{avg}} = \frac{k_{c_{avg}} \delta}{D_{AB}}} \tag{3-112}$$

From (3-111), $N_{Sh_{avg}} = 3.414$, which is the smallest value the Sherwood number can have for a falling liquid film. The average mass-transfer flux of A is

$$N_{A_{avg}} = \frac{n_{A_{avg}}}{A} = k_{c_{avg}}(c_{A_i} - \bar{c}_A)_{mean} \tag{3-113}$$

For $\eta < 0.001$ in (3-100), when the liquid-film flow regime is still laminar without ripples, the time of contact of gas with liquid is short and mass transfer is confined to the vicinity of the interface. Thus, the film acts as if it were infinite in thickness. In this limiting case, the downward velocity of the liquid film in the region of mass transfer is $u_{y_{max}}$, and (3-96) becomes

$$u_{y_{max}} \frac{\partial c_A}{\partial y} = D_{AB} \frac{\partial^2 c_A}{\partial z^2} \tag{3-114}$$

Since from (3-90) and (3-91) $u_{y_{max}} = 3u_y/2$, (3-114) becomes

$$\frac{\partial c_A}{\partial y} = \left(\frac{2D_{AB}}{3\bar{u}_y}\right) \frac{\partial^2 c_A}{\partial z^2} \tag{3-115}$$

where the boundary conditions are

$$\begin{aligned} c_A &= c_{A_o} \text{ for } z > 0 \text{ and } y > 0 \\ c_A &= c_{A_i} \text{ for } z = 0 \text{ and } y > 0 \\ c_A &= c_{A_i} \text{ for large } z \text{ and } y > 0 \end{aligned}$$

Equation (3-115) and the boundary conditions are equivalent to the case of the semi-infinite medium in Figure 3.6. By analogy to (3-68), (3-75), and (3-76), the solution is

$$E = 1 - \theta = \frac{c_{A_i} - c_A}{c_{A_i} - c_{A_o}} = \text{erf}\left(\frac{z}{2\sqrt{2D_{AB}y/3\bar{u}_y}}\right) \tag{3-116}$$

Assuming that the driving force for mass transfer in the film is $c_{A_i} - c_{A_0}$, Fick's first law can be used at the gas–liquid interface to define a mass-transfer coefficient:

$$N_A = -D_{AB} \left.\frac{\partial c_A}{\partial z}\right|_{z=0} = k_c(c_{A_i} - c_{A_o}) \tag{3-117}$$

To obtain the gradient of c_A at $z = 0$ from (3-116), note that the error function is defined as

$$\text{erf } z = \frac{2}{\sqrt{\pi}} \int_0^z e^{-t^2} dt \tag{3-118}$$

Combining (3-118) with (3-116) and applying the Leibnitz differentiation rule,

$$\left.\frac{\partial c_A}{\partial z}\right|_{z=0} = -(c_{A_i} - c_{A_o}) \sqrt{\frac{3\bar{u}_y}{2\pi D_{AB} y}} \tag{3-119}$$

Substituting (3-119) into (3-117) and introducing the Peclet number for mass transfer from (3-102), the local mass-

transfer coefficient as a function of distance down from the top of the wall is obtained:

$$k_c = \sqrt{\frac{3D_{AB}^2 N_{Pe_M}}{8\pi y\delta}} = \sqrt{\frac{3D_{AB}\Gamma}{2\pi y\delta\rho}} \tag{3-120}$$

The average value of k_c over the film height, L, is obtained by integrating (3-120) with respect to y, giving

$$k_{c_{avg}} = \sqrt{\frac{6D_{AB}\Gamma}{\pi\delta\rho L}} = \sqrt{\frac{3D_{AB}^2}{2\pi\delta L}N_{Pe_M}} \tag{3-121}$$

Combining (3-121) with (3-112) and (3-102),

$$N_{Sh_{avg}} = \sqrt{\frac{3\delta}{2\pi L}N_{Pe_M}} = \sqrt{\frac{4}{\pi\eta}} \tag{3-122}$$

where, by (3-108), the proper mean concentration driving force to use with $k_{c_{avg}}$ is the log mean. Thus,

$$\begin{aligned}(c_{A_i} - \bar{c}_A)_{mean} &= (c_{A_i} - \bar{c}_A)_{LM} \\ &= \frac{(c_{A_i} - c_{A_o}) - (c_{A_i} - c_{A_L})}{\ln[(c_{A_i} - c_{A_o})/(c_{A_i} - \bar{c}_{A_L})]}\end{aligned} \tag{3-123}$$

When ripples are present, values of $k_{c_{avg}}$ and $N_{Sh_{avg}}$ are considerably larger than predicted by the above equations.

The above development shows that asymptotic, closed-form solutions are obtained with relative ease for large and small values of η, as defined by (3-100). These limits, in terms of the average Sherwood number, are shown in Figure 3.13. The general solution for intermediate values of η is not available in closed form. Similar limiting solutions for large and small values of dimensionless groups have been obtained for a large variety of transport and kinetic phenomena (Churchill [35]). Often, the two limiting cases can be patched together to provide an estimate of the intermediate solution, if an intermediate value is available from experiment or the general numerical solution. The procedure is discussed by Churchill and Usagi [36]. The general solution of Emmert and Pigford [37] to the falling, laminar liquid film problem is included in Figure 3.13.

EXAMPLE 3.13 Absorption of CO_2 into a Falling Water Film.

Water (B) at 25°C, in contact with CO_2 (A) at 1 atm, flows as a film down a wall 1 m wide and 3 m high at a Reynolds number of 25. Estimate the rate of absorption of CO_2 into water in kmol/s:

$$D_{AB} = 1.96 \times 10^{-5}\,\text{cm}^2/\text{s}; \quad \rho = 1.0\,\text{g/cm}^3;$$
$$\mu_L = 0.89\,\text{cP} = 0.00089\,\text{kg/m-s}$$

Solubility of CO_2 at 1 atm and 25°C $= 3.4 \times 10^{-5}$ mol/cm^3.

Solution

From (3-93), $\quad \Gamma = \dfrac{N_{Re}\mu}{4} = \dfrac{25(0.89)(0.001)}{4} = 0.00556\dfrac{\text{kg}}{\text{m-s}}$

From (3-101),

$$N_{Sc} = \frac{\mu}{\rho D_{AB}} = \frac{(0.89)(0.001)}{(1.0)(1{,}000)(1.96 \times 10^{-5})(10^{-4})} = 454$$

From (3-92),

$$\delta = \left[\frac{3(0.89)(0.001)(0.00556)}{1.0^2(1.000)^2(9.807)}\right]^{1/3} = 1.15 \times 10^{-4}\,\text{m}$$

From (3-90) and (3-91), $\bar{u}_y = (2/3)u_{y_{max}}$. Therefore,

$$\bar{u}_y = \frac{2}{3}\left[\frac{(1.0)(1{,}000)(9.807)(1.15 \times 10^{-4})^2}{2(0.89)(0.001)}\right] = 0.0486\,\text{m/s}$$

From (3-100),

$$\eta = \frac{8/3}{(25)(454)[(1.15 \times 10^{-4})/3]} = 6.13$$

Therefore, (3-111) applies, giving

$$k_{c_{avg}} = \frac{3.41(1.96 \times 10^{-5})(10^{-4})}{1.15 \times 10^{-4}} = 5.81 \times 10^{-5}\,\text{m/s}$$

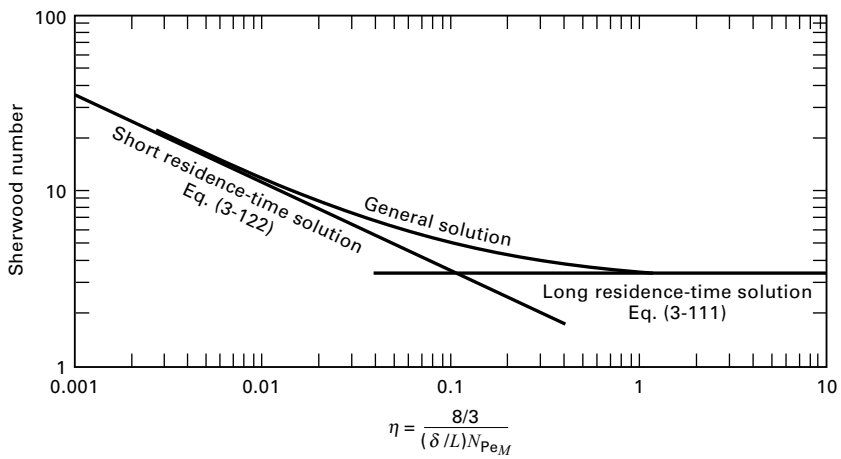

Figure 3.13 Limiting and general solutions for mass transfer to a falling, laminar liquid film.

To obtain the rate of absorption, $\bar{c}_{A_L}$ is determined. From (3-103) and (3-113),

$$n_A = \bar{u}_y \delta W(\bar{c}_{A_L} - c_{A_o}) = k_{c_{avg}} A \frac{(\bar{c}_{A_L} - c_{A_o})}{\ln[(c_{A_i} - c_{A_o})/(c_{A_i} - c_{A_L})]}$$

Thus,
$$\ln\left(\frac{c_{A_i} - c_{A_o}}{c_{A_i} - \bar{c}_{A_L}}\right) = \frac{k_{c_{avg}} A}{\bar{u}_y \delta W}$$

Solving for $\bar{c}_{A_L}$,

$$\bar{c}_{A_L} = c_{A_i} - (c_{A_i} - c_{A_o}) \exp\left(-\frac{k_{c_{avg}} A}{\bar{u}_y \delta W}\right)$$

$$L = 3\,\text{m}, \quad W = 1\,\text{m}, \quad A = WL = (1)(3) = 3\,\text{m}^2$$

$$c_{A_o} = 0, \quad c_{A_i} = 3.4 \times 10^{-5}\,\text{mol/cm}^3 = 3.4 \times 10^{-2}\,\text{kmol/m}^3$$

$$\bar{c}_{A_L} = 3.4 \times 10^{-2}\left\{1 - \exp\left[-\frac{(5.81 \times 10^{-5})(3)}{(0.0486)(1.15 \times 10^{-4})(1)}\right]\right\}$$

$$= 3.4 \times 10^{-2}\,\text{kmol/m}^3$$

Thus, the exiting liquid film is saturated with CO_2, which implies equilibrium at the gas–liquid interface. From (3-103),

$$n_A = 0.0486(1.15 \times 10^{-4})(3.4 \times 10^{-2}) = 1.9 \times 10^{-7}\,\text{kmol/s}$$

§3.4.3 Molecular Diffusion to a Fluid Flowing Across a Flat Plate—The Boundary Layer Concept

Consider the flow of fluid (B) over a thin, horizontal, flat plate, as shown in Figure 3.14. Some possibilities for mass transfer of species A into B are: (1) the plate consists of material A, which is slightly soluble in B; (2) A is in the pores of an inert solid plate from which it evaporates or dissolves into B; and (3) the plate is a dense polymeric membrane through which A can diffuse and pass into fluid B. Let the fluid velocity profile upstream of the plate be uniform at a free-system velocity of u_o. As the fluid passes over the plate, the velocity u_x in the direction x of flow is reduced to zero at the wall, which establishes a velocity profile due to drag. At a certain distance z that is normal to and upward out from the plate surface, the fluid velocity is 99% of u_o. This distance, which increases with increasing distance x from the leading edge of the plate, is defined as the *velocity boundary-layer* thickness, δ. Essentially all flow retardation is assumed to occur in the boundary layer, as first suggested by Prandtl [38]. The buildup of this layer, the velocity profile, and the drag force

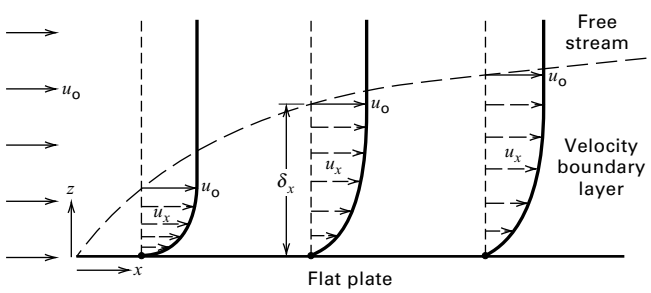

Figure 3.14 Laminar boundary layer for flow across a flat plate.

can be determined for laminar flow by solving the Navier–Stokes equations.

For a Newtonian fluid of constant density and viscosity, with no pressure gradients in the x- or y-directions, these equations for the boundary layer are

$$\frac{\partial u_x}{\partial x} + \frac{\partial u_z}{\partial z} = 0 \tag{3-124}$$

$$u_x \frac{\partial u_x}{\partial x} + u_z \frac{\partial u_x}{\partial z} = \frac{\mu}{\rho}\left(\frac{\partial^2 u_x}{\partial z^2}\right) \tag{3-125}$$

The boundary conditions are

$$u_x = u_o \text{ at } x = 0 \text{ for } z > 0, \quad u_x = 0 \text{ at } z = 0 \text{ for } x > 0$$
$$u_x = u_o \text{ at } z = \infty \text{ for } x > 0, \quad u_z = 0 \text{ at } z = 0 \text{ for } x > 0$$

A solution of (3-124) and (3-125) was first obtained by Blasius [39], as described by Schlichting [40]. The result in terms of a local friction factor, f_x; a local shear stress at the wall, τ_{w_x}; and a local drag coefficient at the wall, C_{D_x}, is

$$\frac{C_{D_x}}{2} = \frac{f_x}{2} = \frac{\tau_{w_x}}{\rho u_o^2} = \frac{0.322}{N_{Re_x}^{0.5}} \tag{3-126}$$

where
$$N_{Re_x} = \frac{x u_o \rho}{\mu} \tag{3-127}$$

The drag is greatest at the leading edge of the plate, where the Reynolds number is smallest. Values of the drag coefficient obtained by integrating (3-126) from $x = 0$ to L are

$$\frac{C_{D_{avg}}}{2} = \frac{f_{avg}}{2} = \frac{0.664}{(N_{Re_L})^{0.5}} \tag{3-128}$$

The thickness of the velocity boundary layer increases with distance along the plate:

$$\frac{\delta}{x} = \frac{4.96}{N_{Re_x}^{0.5}} \tag{3-129}$$

A reasonably accurate expression for a velocity profile was obtained by Pohlhausen [41], who assumed the empirical form of the velocity in the boundary layer to be $u_x = C_1 z + C_2 z^3$.

If the boundary conditions

$$u_x = 0 \text{ at } z = 0,\ u_x = u_o \text{ at } z = \delta,\ \partial u_x/\partial z = 0 \text{ at } z = \delta$$

are applied to evaluate C_1 and C_2, the result is

$$\frac{u_x}{u_o} = 1.5\left(\frac{z}{\delta}\right) - 0.5\left(\frac{z}{\delta}\right)^3 \tag{3-130}$$

This solution is valid only for a laminar boundary layer, which by experiment persists up to $N_{Re_x} = 5 \times 10^5$.

When mass transfer of A from the surface of the plate into the boundary layer occurs, a species continuity equation applies:

$$u_x \frac{\partial c_A}{\partial x} + u_z \frac{\partial c_A}{\partial z} = D_{AB}\left(\frac{\partial^2 c_A}{\partial x^2}\right) \tag{3-131}$$

If mass transfer begins at the leading edge of the plate and the concentration in the fluid at the solid–fluid interface is

maintained constant, the additional boundary conditions are

$$\begin{aligned} c_A &= c_{A_o} \text{ at } x = 0 \quad \text{for } z > 0, \\ c_A &= c_{A_i} \text{ at } z = 0 \quad \text{for } x > 0, \\ \text{and } c_A &= c_{A_o} \text{ at } z = \infty \text{ for } x > 0 \end{aligned}$$

If the rate of mass transfer is low, the velocity profiles are undisturbed. The analogous heat-transfer problem was first solved by Pohlhausen [42] for $N_{Pr} > 0.5$, as described by Schlichting [40]. The analogous result for mass transfer is

$$\frac{N_{Sh_x}}{N_{Re_x} N_{Sc}^{1/3}} = \frac{0.332}{N_{Re_x}^{0.5}} \tag{3-132}$$

where

$$\boxed{N_{Sh_x} = \frac{x k_{c_x}}{D_{AB}}} \tag{3-133}$$

and the driving force for mass transfer is $c_{A_i} - c_{A_o}$.

The concentration boundary layer, where essentially all of the resistance to mass transfer resides, is defined by

$$\frac{c_{A_i} - c_A}{c_{A_i} - c_{A_o}} = 0.99 \tag{3-134}$$

and the ratio of the concentration boundary-layer thickness, δ_c, to the velocity boundary thickness, δ, is

$$\delta_c/\delta = 1/N_{Sc}^{1/3} \tag{3-135}$$

Thus, for a liquid boundary layer where $N_{Sc} > 1$, the concentration boundary layer builds up more slowly than the velocity boundary layer. For a gas boundary layer where $N_{Sc} \approx 1$, the two boundary layers build up at about the same rate. By analogy to (3-130), the concentration profile is

$$\frac{c_{A_i} - c_A}{c_{A_i} - c_{A_o}} = 1.5\left(\frac{z}{\delta_c}\right) - 0.5\left(\frac{z}{\delta_c}\right)^3 \tag{3-136}$$

Equation (3-132) gives the local Sherwood number. If this expression is integrated over the length of the plate, L, the average Sherwood number is found to be

$$N_{Sh_{avg}} = 0.664\, N_{Re_L}^{1/2} N_{Sc}^{1/3} \tag{3-137}$$

where

$$N_{Sh_{avg}} = \frac{L k_{c_{avg}}}{D_{AB}} \tag{3-138}$$

EXAMPLE 3.14 Sublimation of Naphthalene from a Flat Plate.

Air at 100°C, 1 atm, and a free-stream velocity of 5 m/s flows over a 3-m-long, horizontal, thin, flat plate of naphthalene, causing it to sublime. Determine the: (a) length over which a laminar boundary layer persists, (b) rate of mass transfer over that length, and (c) thicknesses of the velocity and concentration boundary layers at the point of transition of the boundary layer to turbulent flow. The physical properties are: vapor pressure of naphthalene = 10 torr; viscosity of air = 0.0215 cP; molar density of air = 0.0327 kmol/m^3; and diffusivity of naphthalene in air = 0.94×10^{-5} m^2/s.

Solution

(a) $N_{Re_x} = 5 \times 10^5$ for transition to turbulent flow. From (3-127),

$$x = L = \frac{\mu N_{Re_x}}{u_o \rho} = \frac{[(0.0215)(0.001)](5 \times 10^5)}{(5)[(0.0327)(29)]} = 2.27 \text{ m}$$

at which transition to turbulent flow begins.

(b) $c_{A_o} = 0$, $c_{A_i} = \dfrac{10(0.0327)}{760} = 4.3 \times 10^{-4}$ kmol/m^3.

From (3-101),

$$N_{Sc} = \frac{\mu}{\rho D_{AB}} = \frac{[(0.0215)(0.001)]}{[(0.0327)(29)](0.94 \times 10^{-5})} = 2.41$$

From (3-137),

$$N_{Sh_{avg}} = 0.664(5 \times 10^5)^{1/2}(2.41)^{1/3} = 630$$

From (3-138),

$$k_{c_{avg}} = \frac{630(0.94 \times 10^{-5})}{2.27} = 2.61 \times 10^{-3} \text{m/s}$$

For a width of 1 m, $A = 2.27$ m^2,

$$\begin{aligned} n_A &= k_{c_{avg}} A (c_{A_i} - c_{A_o}) = 2.61 \times 10^{-3}(2.27)(4.3 \times 10^{-4}) \\ &= 2.55 \times 10^{-6} \text{kmol/s} \end{aligned}$$

(c) From (3-129), at $x = L = 2.27$ m,

$$\delta = \frac{3.46(2.27)}{(5 \times 10^5)^{0.5}} = 0.0111 \text{ m}$$

From (3-135), $\quad \delta_c = \dfrac{0.0111}{(2.41)^{1/3}} = 0.0083$ m

§3.4.4 Molecular Diffusion from the Inside Surface of a Circular Tube to a Flowing Fluid—The Fully Developed Flow Concept

Figure 3.15 shows the development of a laminar velocity boundary layer when a fluid flows from a vessel into a straight, circular tube. At the entrance, *a*, the velocity profile is flat. A velocity boundary layer then begins to build up, as shown at *b*, *c*, and *d* in Figure 3.15. The central core outside the boundary layer has a flat velocity profile where the flow is accelerated over the entrance velocity. Finally, at plane *e*, the boundary layer fills the tube. Now the flow is fully developed. The distance from plane *a* to plane *e* is the entry region.

The entry length L_e is the distance from the entrance to the point at which the centerline velocity is 99% of fully developed flow. From Langhaar [43],

$$L_e/D = 0.0575\, N_{Re} \tag{3-139}$$

For fully developed laminar flow in a tube, by experiment the Reynolds number, $N_{Re} = D\bar{u}_x\rho/\mu$, where $\bar{u}_x$ is the flow-average velocity in the axial direction, x, and D is the inside diameter of the tube, must be less than 2,100. Then the equation of motion in the axial direction is

$$\frac{\mu}{r}\frac{\partial}{\partial r}\left(r\frac{\partial u_x}{\partial r}\right) - \frac{dP}{\partial x} = 0 \tag{3-140}$$

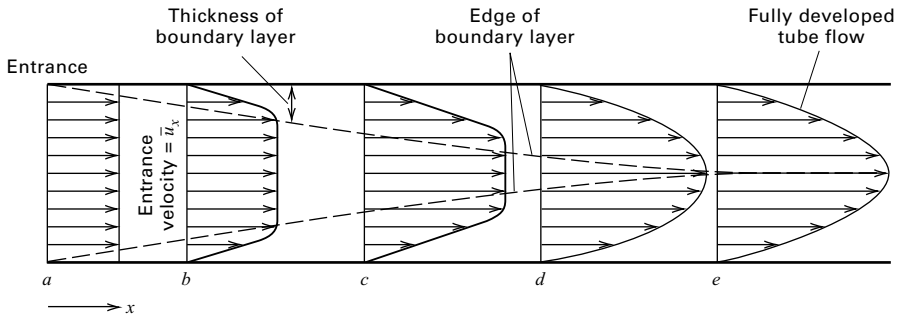

Figure 3.15 Buildup of a laminar velocity boundary layer for flow in a circular tube.

with boundary conditions:

$$r = 0 \text{ (axis of the tube)}, \quad \partial u_x/\partial r = 0$$

and $$r = r_w \text{(tube wall)}, \quad u_x = 0$$

Equation (3-140) was integrated by Hagen in 1839 and Poiseuille in 1841. The resulting equation for the velocity profile, in terms of the flow-average velocity, is

$$u_x = 2\bar{u}_x\left[1 - \left(\frac{r}{r_w}\right)^2\right] \tag{3-141}$$

or, in terms of the maximum velocity at the tube axis,

$$u_x = u_{x_{\max}}\left[1 - \left(\frac{r}{r_w}\right)^2\right] \tag{3-142}$$

According to (3-142), the velocity profile is parabolic.

The shear stress, pressure drop, and Fanning friction factor are obtained from solutions to (3-140):

$$\tau_w = -\mu\left(\frac{\partial u_x}{\partial r}\right)\bigg|_{r=r_w} = \frac{4\mu\bar{u}_x}{r_w} \tag{3-143}$$

$$-\frac{dP}{dx} = \frac{32\mu\bar{u}_x}{D^2} = \frac{2f\rho\bar{u}_x^2}{D} \tag{3-144}$$

with $$f = \frac{16}{N_{\text{Re}}} \tag{3-145}$$

At the upper limit of laminar flow, $N_{\text{Re}} = 2{,}100$, and $L_e/D = 121$, but at $N_{\text{Re}} = 100$, L_e/D is only 5.75. In the entry region, the friction factor is considerably higher than the fully developed flow value given by (3-145). At $x = 0$, f is infinity, but it decreases exponentially with x, approaching the fully developed flow value at L_e. For example, for $N_{\text{Re}} = 1{,}000$, (3-145) gives $f = 0.016$, with $L_e/D = 57.5$. From $x = 0$ to $x/D = 5.35$, the average friction factor from Langhaar is 0.0487, which is three times the fully developed value.

In 1885, Graetz [44] obtained a solution to the problem of convective heat transfer between the wall of a circular tube, at a constant temperature, and a fluid flowing through the tube in fully developed laminar flow. Assuming constant properties and negligible conduction in the axial direction, the energy equation, after substituting (3-141) for u_x, is

$$2\bar{u}_x\left[1 - \left(\frac{r}{r_w}\right)^2\right]\frac{\partial T}{\partial x} = \frac{k}{\rho C_p}\left[\frac{1}{r}\frac{\partial}{\partial r}\left(r\frac{\partial T}{\partial r}\right)\right] \tag{3-146}$$

with boundary conditions:

$$x = 0 \text{ (where heat transfer begins)}, \quad T = T_0, \text{ for all } r$$
$$x > 0, \quad r = r_w, \; T = T_i \text{ and } x > 0, \; r = 0, \; \partial T/\partial r = 0$$

The analogous species continuity equation for mass transfer, neglecting bulk flow in the radial direction and axial diffusion, is

$$2\bar{u}_x\left[1 - \left(\frac{r}{r_w}\right)^2\right]\frac{\partial c_A}{\partial x} = D_{AB}\left[\frac{1}{r}\frac{\partial}{\partial r}\left(r\frac{\partial c_A}{\partial r}\right)\right] \tag{3-147}$$

with analogous boundary conditions.

The Graetz solution of (3-147) for the temperature or concentration profile is an infinite series that can be obtained from (3-146) by separation of variables using the method of Frobenius. A detailed solution is given by Sellars, Tribus, and Klein [45]. The concentration profile yields expressions for the mass-transfer coefficient and the Sherwood number. For large x, the concentration profile is fully developed and the local Sherwood number, N_{Sh_x}, approaches a limiting value of 3.656. When x is small, such that the concentration boundary layer is very thin and confined to a region where the fully developed velocity profile is linear, the local Sherwood number is obtained from the classic Leveque [46] solution, presented by Knudsen and Katz [47]:

$$N_{\text{Sh}_x} = \frac{k_{c_x}D}{D_{AB}} = 1.077\left[\frac{N_{\text{Pe}_M}}{(x/D)}\right]^{1/3} \tag{3-148}$$

where $$N_{\text{Pe}_M} = \frac{D\bar{u}_x}{D_{AB}} \tag{3-149}$$

The limiting solutions, together with the general Graetz solution, are shown in Figure 3.16, where $N_{\text{Sh}_x} = 3.656$ is valid for $N_{\text{Pe}_M}/(x/D) < 4$ and (3-148) is valid for $N_{\text{Pe}_M}/(x/D) > 100$. These solutions can be patched together if a point from the general solution is available at the intersection in a manner like that discussed in §3.4.2.

Where mass transfer occurs, an average Sherwood number is derived by integrating the general expression for the local

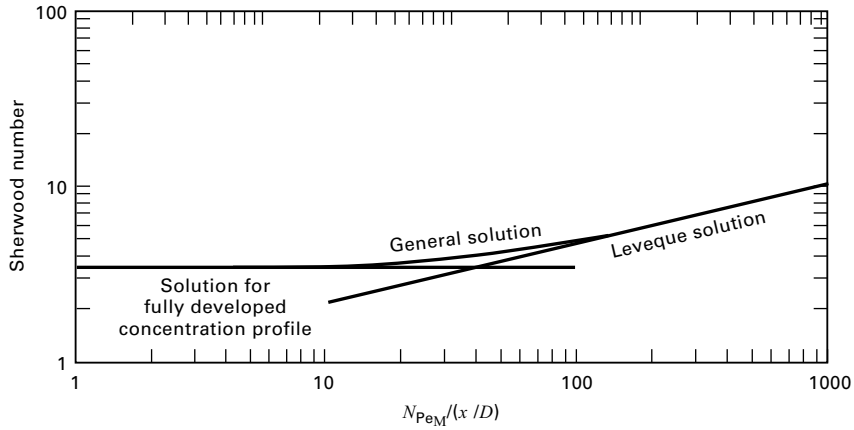

Figure 3.16 Limiting and general solutions for mass transfer to a fluid in laminar flow in a straight, circular tube.

Sherwood number. An empirical representation for that average, proposed by Hausen [48], is

$$N_{Sh_{avg}} = 3.66 + \frac{0.0668[N_{Pe_M}/(x/D)]}{1 + 0.04[N_{Pe_M}/(x/D)]^{2/3}} \qquad (3\text{-}150)$$

which is based on a log-mean concentration driving force.

EXAMPLE 3.15 Mass Transfer of Benzoic Acid into Water Flowing in Laminar Motion Through a Tube.

Linton and Sherwood [49] dissolved tubes of benzoic acid (A) into water (B) flowing in laminar flow through the tubes. Their data agreed with predictions based on the Graetz and Leveque equations. Consider a 5.23-cm-inside-diameter, 32-cm-long tube of benzoic acid, preceded by 400 cm of straight metal pipe wherein a fully developed velocity profile is established. Water enters at 25°C at a velocity corresponding to a Reynolds number of 100. Based on property data at 25°C, estimate the average concentration of benzoic acid leaving the tube before a significant increase in the inside diameter of the benzoic acid tube occurs because of dissolution. The properties are: solubility of benzoic acid in water = 0.0034 g/cm^3; viscosity of water = 0.89 cP = 0.0089 g/cm-s; and diffusivity of benzoic acid in water at infinite dilution = 9.18×10^{-6} cm^2/s.

Solution

$$N_{Sc} = \frac{0.0089}{(1.0)(9.18 \times 10^{-6})} = 970$$

$$N_{Re} = \frac{D\bar{u}_x\rho}{\mu} = 100$$

from which $\bar{u}_x = \dfrac{(100)(0.0089)}{(5.23)(1.0)} = 0.170$ cm/s

From (3-149), $N_{Pe_M} = \dfrac{(5.23)(0.170)}{9.18 \times 10^{-6}} = 9.69 \times 10^4$

$$\frac{x}{D} = \frac{32}{5.23} = 6.12$$

$$\frac{N_{Pe_M}}{(x/D)} = \frac{9.69 \times 10^4}{6.12} = 1.58 \times 10^4$$

From (3-150),

$$N_{Sh_{avg}} = 3.66 + \frac{0.0668(1.58 \times 10^4)}{1 + 0.04(1.58 \times 10^4)^{2/3}} = 44$$

$$k_{c_{avg}} = N_{Sh_{avg}}\left(\frac{D_{AB}}{D}\right) = 44\frac{(9.18 \times 10^{-6})}{5.23} = 7.7 \times 10^{-5}\text{cm/s}$$

Using a log mean driving force,

$$n_A = \bar{u}_x S(\bar{c}_{A_x} - c_{A_o}) = k_{c_{avg}} A \frac{[(c_{A_i} - c_{A_o}) - (c_{A_i} - \bar{c}_{A_x})]}{\ln[(c_{A_i} - c_{A_o})/(c_{A_i} - \bar{c}_{A_x})]}$$

where S is the cross-sectional area for flow. Simplifying,

$$\ln\left(\frac{c_{A_i} - c_{A_o}}{c_{A_i} - \bar{c}_{A_x}}\right) = \frac{k_{c_{avg}} A}{\bar{u}_x S}$$

$$c_{A_o} = 0 \quad \text{and} \quad c_{A_i} = 0.0034\,\text{g/cm}^3$$

$$S = \frac{\pi D^2}{4} = \frac{(3.14)(5.23)^2}{4} = 21.5\,\text{cm}^2 \quad \text{and}$$

$$A = \pi D x = (3.14)(5.23)(32) = 526\,\text{cm}^2$$

$$\ln\left(\frac{0.0034}{0.0034 - \bar{c}_{A_x}}\right) = \frac{(7.7 \times 10^{-5})(526)}{(0.170)(21.5)} = 0.0111$$

$$\bar{c}_{A_x} = 0.0034 - \frac{0.0034}{e^{0.0111}} = 0.000038\,\text{g/cm}^3$$

Thus, the concentration of benzoic acid in the water leaving the cast tube is far from saturation.

§3.5 MASS TRANSFER IN TURBULENT FLOW

The two previous sections described mass transfer in stagnant media (§3.3) and laminar flow (§3.4), where in (3-1), only two mechanisms needed to be considered: molecular diffusion and bulk flow, with the latter often ignored. For both cases, rates of mass transfer can be calculated theoretically using Fick's law of diffusion. In the chemical industry, turbulent flow is more common because it includes eddy diffusion, which results in much higher heat and mass-transfer rates, and thus, requires smaller equipment. Lacking a fundamental theory for eddy diffusion, estimates of mass-transfer rates rely on empirical correlations developed from experimental

Table 3.13 Some Useful Dimensionless Groups

Name	Formula	Meaning	Analogy
	Fluid Mechanics		
Drag Coefficient	$C_D = \dfrac{2F_D}{Au^2\rho}$	$\dfrac{\text{Drag force}}{\text{Projected area} \times \text{Velocity head}}$	
Fanning Friction Factor	$f = \dfrac{\Delta P}{L}\dfrac{D}{2\bar{u}^2\rho}$	$\dfrac{\text{Pipe wall shear stress}}{\text{Velocity head}}$	
Froude Number	$N_{\text{Fr}} = \dfrac{\bar{u}^2}{gL}$	$\dfrac{\text{Inertial force}}{\text{Gravitational force}}$	
Reynolds Number	$N_{\text{Re}} = \dfrac{L\bar{u}\rho}{\mu} = \dfrac{L\bar{u}}{v} = \dfrac{LG}{\mu}$	$\dfrac{\text{Inertial force}}{\text{Viscous force}}$	
Weber Number	$N_{\text{We}} = \dfrac{\bar{u}^2\rho L}{\sigma}$	$\dfrac{\text{Inertial force}}{\text{Surface-tension force}}$	
	Heat Transfer		
j-Factor for Heat Transfer	$j_{\text{H}} = N_{\text{St}_{\text{H}}}(N_{\text{Pr}})^{2/3}$		j_M
Nusselt Number	$N_{\text{Nu}} = \dfrac{hL}{k}$	$\dfrac{\text{Convective heat transfer}}{\text{Conductive heat transfer}}$	N_{Sh}
Peclet Number for Heat Transfer	$N_{\text{Pe}_{\text{H}}} = N_{\text{Re}}N_{\text{Pr}} = \dfrac{L\bar{u}\rho C_p}{k}$	$\dfrac{\text{Bulk transfer of heat}}{\text{Conductive heat transfer}}$	$N_{\text{Pe}_{\text{M}}}$
Prandtl Number	$N_{\text{Pr}} = \dfrac{C_p\mu}{k} = \dfrac{v}{\alpha}$	$\dfrac{\text{Momentum diffusivity}}{\text{Thermal diffusivity}}$	N_{Sc}
Stanton Number for Heat Transfer	$N_{\text{St}_{\text{H}}} = \dfrac{N_{\text{Nu}}}{N_{\text{Re}}N_{\text{Pr}}} = \dfrac{h}{C_pG}$	$\dfrac{\text{Heat transfer}}{\text{Thermal capacity}}$	$N_{\text{St}_{\text{M}}}$
	Mass Transfer		
j-Factor for Mass Transfer (analogous to the *j*-Factor for Heat Transfer)	$j_{\text{M}} = N_{\text{St}_{\text{M}}}(N_{\text{Sc}})^{2/3}$		j_H
Lewis Number	$N_{\text{Le}} = \dfrac{N_{\text{Sc}}}{N_{\text{Pr}}} = \dfrac{k}{\rho C_p D_{\text{AB}}} = \dfrac{\alpha}{D_{\text{AB}}}$	$\dfrac{\text{Thermal diffusivity}}{\text{Mass diffusivity}}$	
Peclet Number for Mass Transfer (analogous to the Peclet Number for Heat Transfer)	$N_{\text{Pe}_{\text{M}}} = N_{\text{Re}}N_{\text{Sc}} = \dfrac{L\bar{u}}{D_{\text{AB}}}$	$\dfrac{\text{Bulk transfer of mass}}{\text{Molecular diffusion}}$	$N_{\text{Pe}_{\text{H}}}$
Schmidt Number (analogous to the Prandtl Number)	$N_{\text{Sc}} = \dfrac{\mu}{\rho D_{\text{AB}}} = \dfrac{v}{D_{\text{AB}}}$	$\dfrac{\text{Momentum diffusivity}}{\text{Mass diffusivity}}$	N_{Pr}
Sherwood Number (analogous to the Nusselt Number)	$N_{\text{Sh}} = \dfrac{k_cL}{D_{\text{AB}}}$	$\dfrac{\text{Convective mass transfer}}{\text{Molecular diffusion}}$	N_{Nu}
Stanton Number for Mass Transfer (analogous to the Stanton Number for Heat Transfer)	$N_{\text{St}_{\text{M}}} = \dfrac{N_{\text{Sh}}}{N_{\text{Re}}N_{\text{Sc}}} = \dfrac{k_c}{\bar{u}\rho}$	$\dfrac{\text{Mass transfer}}{\text{Mass capacity}}$	$N_{\text{St}_{\text{H}}}$

L = characteristic length, G = mass velocity $= \bar{u}\rho$, Subscripts: M = mass transfer H = heat transfer

data. These correlations are comprised of the same dimensionless groups of §3.4 and use analogies with heat and momentum transfer. For reference as this section is presented, the most useful dimensionless groups for fluid mechanics, heat transfer, and mass transfer are listed in Table 3.13. Note that most of the dimensionless groups used in empirical equations for mass transfer are analogous to dimensionless groups used in heat transfer. The Reynolds number from fluid mechanics is used widely in empirical equations of heat and mass transfer.

As shown by a famous dye experiment conducted by Osborne Reynolds [50] in 1883, a fluid in laminar flow moves parallel to the solid boundaries in streamline patterns. Every fluid particle moves with the same velocity along a streamline, and there are no normal-velocity components. For a Newtonian fluid in laminar flow, momentum, heat, and mass transfer are by molecular transport, governed by Newton's law of viscosity, Fourier's law of heat conduction, and Fick's law of molecular diffusion, as described in the previous section.

In turbulent flow, where transport processes are orders of magnitude higher than in laminar flow, streamlines no longer exist, except near a wall, and eddies of fluid, which are large compared to the mean free path of the molecules in the fluid, mix with each other by moving from one region to another in fluctuating motion. This eddy mixing by velocity fluctuations

occurs not only in the direction of flow but also in directions normal to flow, with the former referred to as axial transport but with the latter being of more interest. Momentum, heat, and mass transfer now occur by the two parallel mechanisms given in (3-1): (1) molecular diffusion, which is slow; and (2) turbulent or eddy diffusion, which is rapid except near a solid surface, where the flow velocity accompanying turbulence tends to zero. Superimposed on molecular and eddy diffusion is (3) mass transfer by bulk flow, which may or may not be significant.

In 1877, Boussinesq [51] modified Newton's law of viscosity to include a parallel eddy or turbulent viscosity, μ_t. Analogous expressions were developed for turbulent-flow heat and mass transfer. For flow in the x-direction and transport in the z-direction normal to flow, these expressions are written in flux form (in the absence of bulk flow in the z-direction) as:

$$\tau_{zx} = -(\mu + \mu_t)\frac{du_x}{dz} \tag{3-151}$$

$$q_z = -(k + k_t)\frac{dT}{dz} \tag{3-152}$$

$$N_{A_z} = -(D_{AB} + D_t)\frac{dc_A}{dz} \tag{3-153}$$

where the double subscript zx on the shear stress, τ, stands for x-momentum in the z-direction. The molecular contributions, μ, k, and D_{AB}, are properties of the fluid and depend on chemical composition, temperature, and pressure; the turbulent contributions, μ_t, k_t, and D_t, depend on the mean fluid velocity in the flow direction and on position in the fluid with respect to the solid boundaries.

In 1925, Prandtl [52] developed an expression for μ_t in terms of an eddy mixing length, l, which is a function of position and is a measure of the average distance that an eddy travels before it loses its identity and mingles with other eddies. The mixing length is analogous to the mean free path of gas molecules, which is the average distance a molecule travels before it collides with another molecule. By analogy, the same mixing length is valid for turbulent-flow heat transfer and mass transfer. To use this analogy, (3-151) to (3-153) are rewritten in diffusivity form:

$$\frac{\tau_{zx}}{\rho} = -(\nu + \epsilon_M)\frac{du_x}{dz} \tag{3-154}$$

$$\frac{q_z}{C_p\rho} = -(\alpha + \epsilon_H)\frac{dT}{dz} \tag{3-155}$$

$$N_{A_z} = -(D_{AB} + \epsilon_D)\frac{dc_A}{dz} \tag{3-156}$$

where ϵ_M, ϵ_H, and ϵ_D are momentum, heat, and mass eddy diffusivities, respectively; ν is the momentum diffusivity (kinematic viscosity, μ/ρ); and α is the thermal diffusivity, $k/\rho C_P$. As an approximation, the three eddy diffusivities may be assumed equal. This is valid for ϵ_H and ϵ_D, but data indicate that $\epsilon_M/\epsilon_H = \epsilon_M/\epsilon_D$ is sometimes less than 1.0 and as low as 0.5 for turbulence in a free jet.

§3.5.1 Reynolds Analogy

If (3-154) to (3-156) are applied at a solid boundary, they can be used to determine transport fluxes based on transport coefficients, with driving forces from the wall (or interface), i, at $z = 0$, to the bulk fluid, designated with an overbar, $\bar{}$:

$$\frac{\tau_{zx}}{\bar{u}_x} = -(\nu + \epsilon_M)\frac{d(\rho u_x/\bar{u}_x)}{dz}\bigg|_{z=0} = \frac{f\rho}{2}\bar{u}_x \tag{3-157}$$

$$q_z = -(\alpha + \epsilon_H)\frac{d(\rho C_P T)}{dz}\bigg|_{z=0} = h(T_i - \overline{T}) \tag{3-158}$$

$$N_{A_z} = -(D_{AB} + \epsilon_D)\frac{dc_A}{dz}\bigg|_{z=0} = k_c(c_A - \bar{c}_A) \tag{3-159}$$

To develop useful analogies, it is convenient to use dimensionless velocity, temperature, and solute concentration, defined by

$$\theta = \frac{u_x}{\bar{u}_x} = \frac{T_i - T}{T_i - \overline{T}} = \frac{c_{A_j} - c_A}{c_{A_i} - \bar{c}_A} \tag{3-160}$$

If (3-160) is substituted into (3-157) to (3-159),

$$\begin{aligned}\frac{\partial\theta}{\partial z}\bigg|_{z=0} &= \frac{f\bar{u}_x}{2(\nu + \epsilon_M)} = \frac{h}{\rho C_P(\alpha + \epsilon_H)} \\ &= \frac{k_c}{(D_{AB} + \epsilon_D)}\end{aligned} \tag{3-161}$$

which defines analogies among momentum, heat, and mass transfer. If the three eddy diffusivities are equal and molecular diffusivities are everywhere negligible or equal, i.e., $\nu = \alpha = D_{AB}$, (3-161) simplifies to

$$\frac{f}{2} = \frac{h}{\rho C_P \bar{u}_x} = \frac{k_c}{\bar{u}_x} \tag{3-162}$$

Equation (3-162) defines the Stanton number for heat transfer listed in Table 3.13,

$$N_{St_H} = \frac{h}{\rho C_P \bar{u}_x} = \frac{h}{GC_P} \tag{3-163}$$

where G = mass velocity $= \bar{u}_x\rho$. The Stanton number for mass transfer is

$$\boxed{N_{St_M} = \frac{k_c}{\bar{u}_x} = \frac{k_c\rho}{G}} \tag{3-164}$$

Equation (3-162) is referred to as the *Reynolds analogy*. Its development is significant, but its application for the estimation of heat- and mass-transfer coefficients from measurements of the Fanning friction factor for turbulent flow is valid only when $N_{Pr} = \nu/\alpha = N_{Sc} = \nu/D_{AB} = 1$. Thus, the Reynolds analogy has limited practical value and is rarely used. Reynolds postulated its existence in 1874 [53] and derived it in 1883 [50].

§3.5.2 Chilton–Colburn Analogy

A widely used extension of the Reynolds analogy to Prandtl and Schmidt numbers other than 1 was devised in the 1930s

by Colburn [54] for heat transfer and by Chilton and Colburn [55] for mass transfer. Using experimental data, they corrected the Reynolds analogy for differences in dimensionless velocity, temperature, and concentration distributions by incorporating the Prandtl number, N_{Pr}, and the Schmidt number, N_{Sc}, into (3-162) to define empirically the following three *j-factors* included in Table 3.13.

$$\boxed{\begin{aligned} j_M \equiv \frac{f}{2} = j_H &\equiv \frac{h}{GC_P}(N_{Pr})^{2/3} \\ &= j_D \equiv \frac{k_c \rho}{G}(N_{Sc})^{2/3} \end{aligned}} \tag{3-165}$$

Equation (3-165) is the *Chilton–Colburn analogy* or the Colburn analogy for estimating transport coefficients for turbulent flow. For $N_{Pr} = N_{Sc} = 1$, (3-165) equals (3-162).

From experimental studies, the *j*-factors depend on the geometric configuration and the Reynolds number, N_{Re}. Based on decades of experimental transport data, the following representative *j*-factor correlations for turbulent transport to or from smooth surfaces have evolved. Additional correlations are presented in later chapters. These correlations are reasonably accurate for N_{Pr} and N_{Sc} in the range 0.5 to 10.

1. Flow through a straight, circular tube of inside diameter D:

$$j_M = j_H = j_D = 0.023(N_{Re})^{-0.2} \tag{3-166}$$

for $10{,}000 < N_{Re} = DG/\mu < 1{,}000{,}000$

2. Average transport coefficients for flow across a flat plate of length L:

$$j_M = j_H = j_D = 0.037(N_{Re})^{-0.2} \tag{3-167}$$

for $5 \times 10^5 < N_{Re} = Lu_o/\mu < 5 \times 10^8$

3. Average transport coefficients for flow normal to a long, circular cylinder of diameter D, where the drag coefficient includes both form drag and skin friction, but only the skin friction contribution applies to the analogy:

$$(j_M)_{\text{skin friction}} = j_H = j_D = 0.193(N_{Re})^{-0.382} \tag{3-168}$$

for $4{,}000 < N_{Re} < 40{,}000$

$$(j_M)_{\text{skin friction}} = j_H = j_D = 0.0266(N_{Re})^{-0.195} \tag{3-169}$$

for $40{,}000 < N_{Re} < 250{,}000$

$$\text{with} \qquad N_{Re} = \frac{DG}{\mu}$$

4. Average transport coefficients for flow past a single sphere of diameter D:

$$\begin{aligned} (j_M)_{\text{skin friction}} &= j_H = j_D = 0.37(N_{Re})^{-0.4} \\ \text{for} \quad 20 < N_{Re} &= \frac{DG}{\mu} < 100{,}000 \end{aligned} \tag{3-170}$$

5. Average transport coefficients for flow through beds packed with spherical particles of uniform size D_P:

$$\begin{aligned} j_H = j_D &= 1.17(N_{Re})^{-0.415} \\ \text{for} \quad 10 < N_{Re} &= \frac{D_P G}{\mu} < 2{,}500 \end{aligned} \tag{3-171}$$

The above correlations are plotted in Figure 3.17, where the curves are not widely separated but do not coincide because of necessary differences in Reynolds number definitions. When using the correlations in the presence of appreciable temperature and/or composition differences, Chilton and Colburn recommend that N_{Pr} and N_{Sc} be evaluated at the average conditions from the surface to the bulk stream.

§3.5.3 Other Analogies

New theories have led to improvements of the Reynolds analogy to give expressions for the Fanning friction factor and Stanton numbers for heat and mass transfer that are less empirical than the Chilton–Colburn analogy. The first major improvement was by Prandtl [56] in 1910, who divided the flow into two regions: (1) a thin laminar-flow *sublayer* of thickness δ next to the wall boundary, where only molecular transport occurs; and (2) a turbulent region dominated by eddy transport, with $\epsilon_M = \epsilon_H = \epsilon_D$.

Further improvements to the Reynolds analogy were made by von Karman, Martinelli, and Deissler, as discussed in

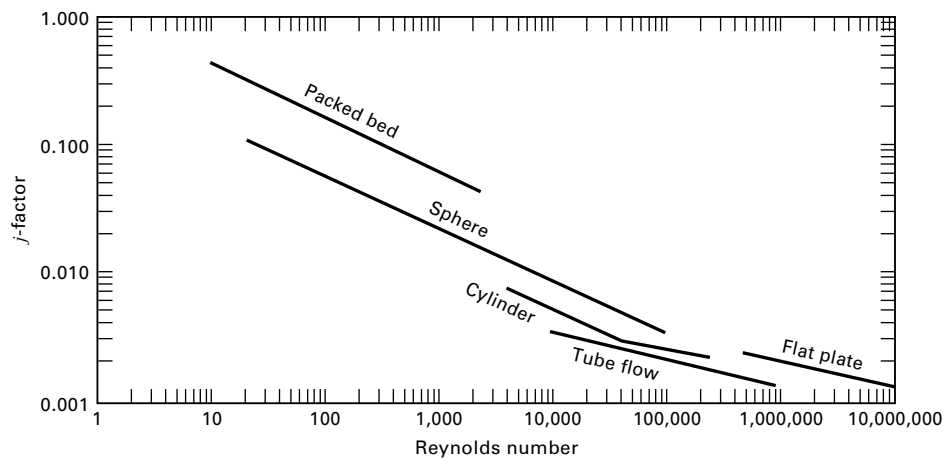

Figure 3.17 Chilton–Colburn *j*-factor correlations.

detail by Knudsen and Katz [47]. The first two investigators inserted a buffer zone between the laminar sublayer and turbulent core. Deissler gradually reduced the eddy diffusivities as the wall was approached. Other advances were made by van Driest [64], who used a modified form of the Prandtl mixing length; Reichardt [65], who eliminated the zone concept by allowing the eddy diffusivities to decrease continuously from a maximum to zero at the wall; and Friend and Metzner [57], who obtained improved accuracy at Prandtl and Schmidt numbers to 3,000. Their results for flow through a circular tube are

$$N_{\mathrm{St_H}} = \frac{f/2}{1.20 + 11.8\sqrt{f/2}(N_{\mathrm{Pr}} - 1)(N_{\mathrm{Pr}})^{-1/3}} \tag{3-172}$$

$$N_{\mathrm{St_M}} = \frac{f/2}{1.20 + 11.8\sqrt{f/2}(N_{\mathrm{Sc}} - 1)(N_{\mathrm{Sc}})^{-1/3}} \tag{3-173}$$

where the Fanning friction factor can be estimated over Reynolds numbers from 10,000 to 10,000,000 using the empirical correlation of Drew, Koo, and McAdams [66],

$$f = 0.00140 + 0.125(N_{\mathrm{Re}})^{-0.32} \tag{3-174}$$

which fits the experimental data of Nikuradse [67] and is preferred over (3-165) with (3-166), which is valid only to N_{Re} = 1,000,000. For two- and three-dimensional turbulent-flow problems, some success has been achieved with the κ (kinetic energy of turbulence)–ϵ (rate of dissipation) model of Launder and Spalding [68], which is widely used in computational fluid dynamics (CFD) computer programs.

§3.5.4 Theoretical Analogy of Churchill and Zajic

An alternative to (3-154) to (3-156) for developing equations for turbulent flow is to start with *time-averaged* equations of Newton, Fourier, and Fick. For example, consider a form of Newton's law of viscosity for molecular and turbulent transport of momentum in parallel, where, in a turbulent-flow field in the axial x-direction, instantaneous velocity components u_x and u_z are

$$u_x = \bar{u}_x + u'_x$$
$$u_z = u'_z$$

The ''overbarred'' component is the time-averaged (mean) local velocity, and the primed component is the local fluctuating velocity that denotes instantaneous deviation from the local mean value. The mean velocity in the perpendicular z-direction is zero. The mean local velocity in the x-direction over a long period Θ of time θ is given by

$$\bar{u}_x = \frac{1}{\Theta}\int_0^{\Theta} u_x d\theta = \frac{1}{\Theta}\int_0^{\Theta} (\bar{u}_x + u'_x) d\theta \tag{3-175}$$

Time-averaged fluctuating components u'_x and u'_z are zero.

The local instantaneous rate of momentum transfer by turbulence in the z-direction of x-direction turbulent momentum per unit area at constant density is

$$\rho u'_z(\bar{u}_x + u'_x) \tag{3-176}$$

The time-average of this turbulent momentum transfer is equal to the turbulent component of the shear stress, τ_{zx_t},

$$\begin{aligned}\tau_{zx_t} &= \frac{\rho}{\Theta}\int_0^{\Theta} u'_z(\bar{u}_x + u'_x) d\theta \\ &= \frac{\rho}{\Theta}\left[\int_0^{\Theta} u'_z(\bar{u}_x) d\theta + \int_0^{\Theta} u'_z(u'_x) d\theta\right]\end{aligned} \tag{3-177}$$

Because the time-average of the first term is zero, (3-177) reduces to

$$\tau_{zx_t} = \rho(\overline{u'_z u'_x}) \tag{3-178}$$

which is referred to as a Reynolds stress. Combining (3-178) with the molecular component of momentum transfer gives the following turbulent-flow form of Newton's law of viscosity, where the second term on the right-hand side accounts for turbulence,

$$\tau_{zx} = -\mu\frac{du_x}{dz} + \rho(\overline{u'_z u'_x}) \tag{3-179}$$

If (3-179) is compared to (3-151), it is seen that an alternative approach to turbulence is to develop a correlating equation for the Reynolds stress, $(\overline{u'_z u'_x})$ first introduced by Churchill and Chan [73], rather than an expression for turbulent viscosity μ_t. This stress is a complex function of position and rate of flow and has been correlated for fully developed turbulent flow in a straight, circular tube by Heng, Chan, and Churchill [69]. In generalized form, with tube radius a and $y = (a - z)$ representing the distance from the inside wall to the center of the tube, their equation is

$$\begin{aligned}(\overline{u'_z u'_x})^{++} = \Bigg(&\left[0.7\left(\frac{y^+}{10}\right)^3\right]^{-8/7} + \left|\exp\left\{\frac{-1}{0.436y^+}\right\}\right. \\ &\left. - \frac{1}{0.436a^+}\left(1 + \frac{6.95y^+}{a^+}\right)\right|^{-8/7}\Bigg)^{-7/8}\end{aligned} \tag{3-180}$$

where

$$\begin{aligned}(\overline{u'_z u'_x})^{++} &= -\rho\overline{u'_z u'_x}/\tau \\ a^+ &= a(\tau_w\rho)^{1/2}/\mu \\ y^+ &= y(\tau_w\rho)^{1/2}/\mu\end{aligned}$$

Equation (3-180) is an accurate representation of turbulent flow because it is based on experimental data and numerical simulations described by Churchill and Zajic [70] and Churchill [71]. From (3-142) and (3-143), the shear stress at the wall, τ_w, is related to the Fanning friction factor by

$$f = \frac{2\tau_w}{\rho\bar{u}_x^2} \tag{3-181}$$

where $\bar{u}_x$ is the flow-average velocity in the axial direction. Combining (3-179) with (3-181) and performing the required integrations, both numerically and analytically, leads to the following implicit equation for the Fanning friction factor as a function of the Reynolds number, $N_{\mathrm{Re}} = 2a\bar{u}_x\rho/\mu$:

Table 3.14 Comparison of Fanning Friction Factors for Fully Developed Turbulent Flow in a Smooth, Straight, Circular Tube

N_{Re}	f, Drew et al. (3-174)	f, Chilton–Colburn (3-166)	f, Churchill–Zajic (3-182)
10,000	0.007960	0.007291	0.008087
100,000	0.004540	0.004600	0.004559
1,000,000	0.002903	0.002902	0.002998
10,000,000	0.002119	0.001831	0.002119
100,000,000	0.001744	0.001155	0.001573

$$\left(\frac{2}{f}\right)^{1/2} = 3.2 - 227\frac{\left(\frac{2}{f}\right)^{1/2}}{\frac{N_{Re}}{2}} + 2500\left[\frac{\left(\frac{2}{f}\right)^{1/2}}{\frac{N_{Re}}{2}}\right]^2 + \frac{1}{0.436}\ln\left[\frac{\frac{N_{Re}}{2}}{\left(\frac{2}{f}\right)^{1/2}}\right] \tag{3-182}$$

This equation is in agreement with experimental data over a Reynolds number range of 4,000–3,000,000 and can be used up to a Reynolds number of 100,000,000. Table 3.14 presents a comparison of the Churchill–Zajic equation, (3-182), with (3-174) of Drew et al. and (3-166) of Chilton and Colburn. Equation (3-174) gives satisfactory agreement for Reynolds numbers from 10,000 to 10,000,000, while (3-166) is useful only for Reynolds numbers from 100,000 to 1,000,000.

Churchill and Zajic [70] show that if the equation for the conservation of energy is time-averaged, a turbulent-flow form of Fourier's law of conduction can be obtained with the fluctuation term $(\overline{u_z' T'})$. Similar time-averaging leads to a turbulent-flow form of Fick's law with $(\overline{u_z' c_A'})$. To extend (3-180) and (3-182) to obtain an expression for the Nusselt number for turbulent-flow convective heat transfer in a straight, circular tube, Churchill and Zajic employ an analogy that is free of empiricism but not exact. The result for Prandtl numbers greater than 1 is

$$N_{Nu} = \frac{1}{\left(\frac{N_{Pr_t}}{N_{Pr}}\right)\frac{1}{N_{Nu_1}} + \left[1 - \left(\frac{N_{Pr_t}}{N_{Pr}}\right)^{2/3}\right]\frac{1}{N_{Nu_\infty}}} \tag{3-183}$$

where, from Yu, Ozoe, and Churchill [72],

$$N_{Pr_t} = \text{turbulent Prandtl number} = 0.85 + \frac{0.015}{N_{Pr}} \tag{3-184}$$

which replaces $(\overline{u_z' T'})$, as introduced by Churchill [74],

$$\begin{aligned} N_{Nu_1} &= \text{Nusselt number for} (N_{Pr} = N_{Pr_t}) \\ &= \frac{N_{Re}\left(\frac{f}{2}\right)}{1 + 145\left(\frac{2}{f}\right)^{-5/4}} \end{aligned} \tag{3-185}$$

$$\begin{aligned} N_{Nu_\infty} &= \text{Nusselt number for} (N_{Pr} = \infty) \\ &= 0.07343\left(\frac{N_{Pr}}{N_{Pr_t}}\right)^{1/3} N_{Re}\left(\frac{f}{2}\right)^{1/2} \end{aligned} \tag{3-186}$$

The accuracy of (3-183) is due to (3-185) and (3-186), which are known from theoretical considerations. Although (3-184) is somewhat uncertain, its effect on (3-183) is negligible.

A comparison is made in Table 3.15 of the Churchill et al. correlation (3-183) with that of Friend and Metzner (3-172) and that of Chilton and Colburn (3-166), where, from Table 3.13, $N_{Nu} = N_{St} N_{Re} N_{Pr}$.

In Table 3.15, at a Prandtl number of 1, which is typical of low-viscosity liquids and close to that of most gases, the Chilton–Colburn correlation is within 10% of the Churchill–Zajic equation for Reynolds numbers up to 1,000,000. Beyond that, serious deviations occur (25% at N_{Re} = 10,000,000

Table 3.15 Comparison of Nusselt Numbers for Fully Developed Turbulent Flow in a Smooth, Straight, Circular Tube

Prandtl number, $N_{Pr} = 1$			
N_{Re}	N_{Nu}, Friend–Metzner (3-172)	N_{Nu}, Chilton–Colburn (3-166)	N_{Nu}, Churchill–Zajic (3-183)
10,000	33.2	36.5	37.8
100,000	189	230	232
1,000,000	1210	1450	1580
10,000,000	8830	9160	11400
100,000,000	72700	57800	86000
Prandt number, $N_{Pr} = 1000$			
N_{Re}	N_{Nu}, Friend–Metzner (3-172)	N_{Nu}, Chilton–Colburn (3-166)	N_{Nu}, Churchill–Zajic (3-183)
10,000	527	365	491
100,000	3960	2300	3680
1,000,000	31500	14500	29800
10,000,000	267800	91600	249000
100,000,000	2420000	578000	2140000

and almost 50% at $N_{Re} = 100{,}000{,}000$). Deviations of the Friend–Metzner correlation vary from 15% to 30% over the entire range of Reynolds numbers. At all Reynolds numbers, the Churchill–Zajic equation predicts higher Nusselt numbers and, therefore, higher heat-transfer coefficients.

At a Prandtl number of 1,000, which is typical of high-viscosity liquids, the Friend–Metzner correlation is in fairly close agreement with the Churchill–Zajic equation. The Chilton–Colburn correlation deviates over the entire range of Reynolds numbers, predicting values ranging from 74 to 27% of those from the Churchill–Zajic equation as the Reynolds number increases. The Chilton–Colburn correlation should not be used at high Prandtl numbers for heat transfer or at high Schmidt numbers for mass transfer.

The Churchill–Zajic equation for predicting the Nusselt number provides a power dependence on the Reynolds number. This is in contrast to the typically cited constant exponent of 0.8 for the Chilton–Colburn correlation. For the Churchill–Zajic equation, at $N_{Pr} = 1$, the exponent increases with Reynolds number from 0.79 to 0.88; at a Prandtl number of 1,000, the exponent increases from 0.87 to 0.93.

Extension of the Churchill–Zajic equation to low Prandtl numbers typical of molten metals, and to other geometries is discussed by Churchill [71], who also considers the effect of boundary conditions (e.g., constant wall temperature and uniform heat flux) at low-to-moderate Prandtl numbers.

For calculation of convective mass-transfer coefficients, k_c, for turbulent flow of gases and liquids in straight, smooth, circular tubes, it is recommended that the Churchill–Zajic equation be employed by applying the analogy between heat and mass transfer. Thus, as illustrated in the following example, in (3-183) to (3-186), using Table 3.13, the Sherwood number is substituted for the Nusselt number, and the Schmidt number is substituted for the Prandtl number.

EXAMPLE 3.16 Analogies for Turbulent Transport.

Linton and Sherwood [49] conducted experiments on the dissolving of tubes of cinnamic acid (A) into water (B) flowing turbulently through the tubes. In one run, with a 5.23-cm-i.d. tube, $N_{Re} = 35{,}800$, and $N_{Sc} = 1{,}450$, they measured a Stanton number for mass transfer, N_{St_M}, of 0.0000351. Compare this experimental value with predictions by the Reynolds, Chilton–Colburn, and Friend–Metzner analogies and the Churchill–Zajic equation.

Solution

From either (3-174) or (3-182), the Fanning friction factor is 0.00576.

Reynolds analogy. From (3-162), $N_{St_M} = f/2 = 0.00576/2 = 0.00288$, which, as expected, is in very poor agreement with the experimental value because the effect of the large Schmidt number is ignored.

Chilton–Colburn analogy. From (3-165),

$$N_{St_M} = \left(\frac{f}{2}\right)/(N_{Sc})^{2/3} = \left(\frac{0.00576}{2}\right)/(1450)^{2/3} = 0.0000225,$$

which is 64% of the experimental value.

Friend–Metzner analogy: From (3-173), $N_{St_M} = 0.0000350$, which is almost identical to the experimental value.

Churchill–Zajic equation. Using mass-transfer analogs,

$$(3\text{-}184)\text{gives } N_{Sc_t} = 0.850,\ (3\text{-}185)\text{ gives } N_{Sh_1} = 94,$$
$$(3\text{-}186)\text{gives } N_{Sh_\infty} = 1686, \text{and } (3\text{-}183)\text{ gives } N_{Sh} = 1680$$

From Table 3.13,

$$N_{St_M} = \frac{N_{Sh}}{N_{Re}N_{Sc}} = \frac{1680}{(35800)(1450)} = 0.0000324,$$

which is an acceptable 92% of the experimental value.

§3.6 MODELS FOR MASS TRANSFER IN FLUIDS WITH A FLUID–FLUID INTERFACE

The three previous sections considered mass transfer mainly between solids and fluids, where the interface was a smooth, solid surface. Applications occur in adsorption, drying, leaching, and membrane separations. Of importance in other separation operations is mass transfer across a fluid–fluid interface. Such interfaces exist in absorption, distillation, extraction, and stripping, where, in contrast to fluid–solid interfaces, turbulence may persist to the interface. The following theoretical models have been developed to describe such phenomena in fluids with a fluid-to-fluid interface. There are many equations in this section and the following section, but few applications. However, use of these equations to design equipment is found in many examples in: Chapter 6 on absorption and stripping; Chapter 7 on distillation; and Chapter 8 on liquid–liquid extraction.

§3.6.1 Film Theory

A model for turbulent mass transfer to or from a fluid-phase boundary was suggested in 1904 by Nernst [58], who postulated that the resistance to mass transfer in a given turbulent fluid phase is in a thin, relatively stagnant region at the interface, called a film. This is similar to the laminar sublayer that forms when a fluid flows in the turbulent regime parallel to a flat plate. It is shown schematically in Figure 3.18a for a gas–liquid interface, where the gas is component A, which diffuses into non-volatile liquid B. Thus, a process of absorption of A into liquid B takes place, without vaporization of B, and there is no resistance to mass transfer of A in the gas phase, because it is pure A. At the interface, phase equilibrium is assumed, so the concentration of A at the interface, c_{A_i}, is related to the partial pressure of A at the interface, p_A, by a solubility relation like Henry's law, $c_{A_i} = H_A p_A$. In the liquid film of thickness δ, molecular diffusion occurs with a driving force of $c_{A_i} - c_{A_b}$, where c_{A_b} is the bulk-average concentration of A in the liquid. Since the film is assumed to be very thin, all of the diffusing A is assumed to pass through the film and into the bulk liquid. Accordingly, integration of Fick's first law, (3-3a), gives

$$J_A = \frac{D_{AB}}{\delta}(c_{A_i} - c_{A_b}) = \frac{cD_{AB}}{\delta}(x_{A_i} - x_{A_b}) \qquad (3\text{-}187)$$

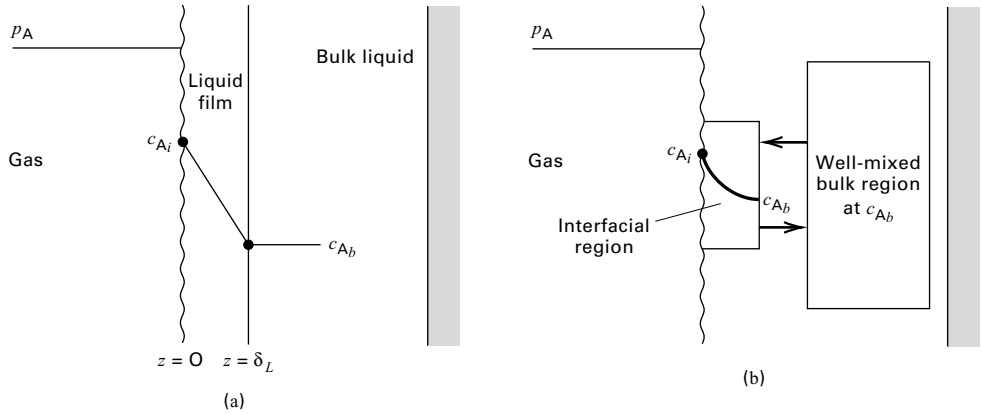

Figure 3.18 Theories for mass transfer from a fluid–fluid interface into a liquid: (a) film theory; (b) penetration and surface-renewal theories.

If the liquid phase is dilute in A, the bulk-flow effect can be neglected so that (3-187) applies to the total flux, and the concentration gradient is linear, as in Figure 3.18a.

$$N_A = \frac{D_{AB}}{\delta}(c_{A_i} - c_{A_b}) = \frac{cD_{AB}}{\delta}(x_{A_i} - c_{A_b}) \tag{3-188}$$

If the bulk-flow effect is not negligible, then, from (3-31),

$$N_A = \frac{cD_{AB}}{\delta}\ln\left[\frac{1 - x_{A_b}}{1 - x_{A_i}}\right] = \frac{cD_{AB}}{\delta(1 - x_A)_{LM}}(x_{A_i} - x_{A_b}) \tag{3-189}$$

where

$$(1 - x_A)_{LM} = \frac{x_{A_i} - x_{A_b}}{\ln[(1 - x_{A_b})/(1 - x_{A_i})]} = (x_B)_{LM} \tag{3-190}$$

In practice, the ratios D_{AB}/δ in (3-188) and $D_{AB}/[\delta\ (1 - x_A)_{LM}]$ in (3-189) are replaced by empirical mass-transfer coefficients k_c and k_c', respectively, because the film thickness, δ, which depends on the flow conditions, is unknown. The subscript, c, on the mass-transfer coefficient refers to a concentration driving force, and the prime superscript denotes that k_c includes both diffusion mechanisms and the bulk-flow effect.

The film theory, which is easy to understand and apply, is often criticized because it predicts that the rate of mass transfer is proportional to molecular diffusivity. This dependency is at odds with experimental data, which indicate a dependency of D^n, where n ranges from 0.5 to 0.75. However, if D_{AB}/δ is replaced with k_c, which is then estimated from the Chilton–Colburn analogy (3-165), k_c is proportional to $D_{AB}^{2/3}$, which is in better agreement with experimental data. In effect, δ is not a constant but depends on D_{AB} (or N_{Sc}). Regardless of whether the criticism is valid, the film theory continues to be widely used in design of mass-transfer separation equipment.

EXAMPLE 3.17 Mass-Transfer Flux in a Packed Absorption Tower.

SO_2 is absorbed from air into water in a packed absorption tower. At a location in the tower, the mass-transfer flux is 0.0270 kmol SO_2/m^2-h, and the liquid-phase mole fractions are 0.0025 and 0.0003, respectively, at the two-phase interface and in the bulk liquid. If the diffusivity of SO_2 in water is 1.7×10^{-5} cm^2/s, determine the mass-transfer coefficient, k_c, and the corresponding film thickness, neglecting the bulk flow effect.

Solution

$$N_{SO_2} = \frac{0.027(1{,}000)}{(3{,}600)(100)^2} = 7.5 \times 10^{-7}\,\frac{\text{mol}}{\text{cm}^2\text{-s}}$$

For dilute conditions, the concentration of water is

$$c = \frac{1}{18.02} = 5.55 \times 10^{-2}\ \text{mol/cm}^3$$

From (3-188),

$$k_c = \frac{D_{AB}}{\delta} = \frac{N_A}{c(x_{A_i} - x_{A_b})} = \frac{7.5 \times 10^{-7}}{5.55 \times 10^{-2}(0.0025 - 0.0003)} = 6.14 \times 10^{-3}\ \text{cm/s}$$

Therefore, $$\delta = \frac{D_{AB}}{k_c} = \frac{1.7 \times 10^{-5}}{6.14 \times 10^{-3}} = 0.0028\ \text{cm}$$

which is small and typical of turbulent-flow processes.

§3.6.2 Penetration Theory

A more realistic mass-transfer model is provided by Higbie's penetration theory [59], shown schematically in Figure 3.18b. The stagnant-film concept is replaced by Boussinesq eddies that: (1) move from the bulk liquid to the interface; (2) stay at the interface for a short, fixed period of time during which they remain static, allowing molecular diffusion to take place in a direction normal to the interface; and (3) leave the interface to mix with the bulk stream. When an eddy moves to the interface, it replaces a static eddy. Thus, eddies are alternately static and moving. Turbulence extends to the interface.

In the penetration theory, unsteady-state diffusion takes place at the interface during the time the eddy is static. This process is governed by Fick's second law, (3-68), with boundary conditions

$$c_A = c_{A_b} \quad \text{at} \quad t = 0 \quad \text{for} \quad 0 \le z \le \infty;$$
$$c_A = c_{A_i} \quad \text{at} \quad z = 0 \quad \text{for} \quad t > 0; \quad \text{and}$$
$$c_A = c_{A_b} \quad \text{at} \quad z = \infty \quad \text{for} \quad t > 0$$

These are the same boundary conditions as in unsteady-state diffusion in a semi-infinite medium. The solution is a rearrangement of (3-75):

$$\frac{c_{A_i} - c_A}{c_{A_i} - c_{A_b}} = \text{erf}\left(\frac{z}{2\sqrt{D_{AB} t_c}}\right) \tag{3-191}$$

where t_c = "contact time" of the static eddy at the interface during one cycle. The corresponding average mass-transfer flux of A in the absence of bulk flow is given by the following form of (3-79):

$$N_A = 2\sqrt{\frac{D_{AB}}{\pi t_c}(c_{A_i} - c_{A_b})} \tag{3-192}$$

or

$$N_A = k_c(c_{A_i} - c_{A_b}) \tag{3-193}$$

Thus, the penetration theory gives

$$k_c = 2\sqrt{\frac{D_{AB}}{\pi t_c}} \tag{3-194}$$

which predicts that k_c is proportional to the square root of the diffusivity, which is at the lower limit of experimental data.

Penetration theory is most useful for bubble, droplet, or random-packing interfaces. For bubbles, the contact time, t_c, of the liquid surrounding the bubble is approximated by the ratio of bubble diameter to its rise velocity. An air bubble of 0.4-cm diameter rises through water at a velocity of about 20 cm/s, making the estimated contact time $0.4/20 = 0.02$ s. For a liquid spray, where no circulation of liquid occurs inside the droplets, contact time is the total time it takes the droplets to fall through the gas. For a packed tower, where the liquid flows as a film over random packing, mixing is assumed to occur each time the liquid film passes from one piece of packing to another. Resulting contact times are about 1 s. In the absence of any estimate for contact time, the mass-transfer coefficient is sometimes correlated by an empirical expression consistent with the 0.5 exponent on D_{AB}, as in (3-194), with the contact time replaced by a function of geometry and the liquid velocity, density, and viscosity.

EXAMPLE 3.18 Contact Time for Penetration Theory.

For the conditions of Example 3.17, estimate the contact time for Higbie's penetration theory.

Solution

From Example 3.17, $k_c = 6.14 \times 10^{-3}$ cm/s and $D_{AB} = 1.7 \times 10^{-5}$ cm^2/s. From a rearrangement of (3-194),

$$t_c = \frac{4D_{AB}}{\pi k_c^2} = \frac{4(1.7 \times 10^{-5})}{3.14(6.14 \times 10^{-3})^2} = 0.57 \text{ s}$$

§3.6.3 Surface-Renewal Theory

The penetration theory is inadequate because the assumption of a constant contact time for all eddies that reach the surface is not reasonable, especially for stirred tanks, contactors with random packings, and bubble and spray columns where bubbles and droplets cover a range of sizes. In 1951, Danckwerts [60] suggested an improvement to the penetration theory that involves the replacement of constant eddy contact time with the assumption of a residence-time distribution, wherein the probability of an eddy at the surface being replaced by a fresh eddy is independent of the age of the surface eddy.

Following Levenspiel's [61] treatment of residence-time distribution, let $F(t)$ be the fraction of eddies with a contact time of less than t. For $t = 0$, $F\{t\} = 0$, and $F\{t\}$ approaches 1 as t goes to infinity. A plot of $F\{t\}$ versus t, as shown in Figure 3.19, is a residence-time or age distribution. If $F\{t\}$ is differentiated with respect to t,

$$\phi\{t\} = dF\{t\}/dt \tag{3-195}$$

where $\phi\{t\}dt$ = the probability that a given surface eddy will have a residence time t. The sum of probabilities is

$$\int_0^\infty \phi\{t\}dt = 1 \tag{3-196}$$

Typical plots of $F\{t\}$ and $\phi\{t\}$ are shown in Figure 3.19, where $\phi\{t\}$ is similar to a normal probability curve.

For steady-state flow into and out of a well-mixed vessel, Levenspiel shows that

$$F\{t\} = 1 - e^{-t/\bar{t}} \tag{3-197}$$

where $\bar{t}$ is the average residence time. This function forms the basis, in reaction engineering, of the ideal model of a continuous, stirred-tank reactor (CSTR). Danckwerts selected the same model for his surface-renewal theory, using the corresponding $\phi\{t\}$ function:

$$\phi\{t\} = se^{-st} \tag{3-198}$$

where

$$s = 1/\bar{t} \tag{3-199}$$

is the fractional rate of surface renewal. As shown in Example 3.19 below, plots of (3-197) and (3-198) are much different from those in Figure 3.19.

The instantaneous mass-transfer rate for an eddy of age t is given by (3-192) for penetration theory in flux form as

$$N_{A_t} = \sqrt{\frac{D_{AB}}{\pi t}}(c_{A_i} - c_{A_b}) \tag{3-200}$$

The integrated average rate is

$$(N_A)_{avg} = \int_0^\infty \phi\{t\} N_{A_t} dt \tag{3-201}$$

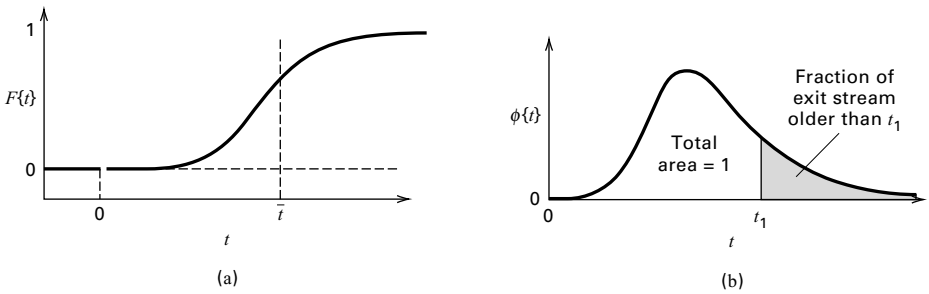

Figure 3.19 Residence-time distribution plots: (a) typical F curve; (b) typical age distribution.
[Adapted from O. Levenspiel, *Chemical Reaction Engineering*, 2nd ed., John Wiley & Sons, New York (1972).]

Combining (3-198), (3-200), and (3-201) and integrating:

$$(N_A)_{avg} = \sqrt{D_{AB}s}(c_{A_i} - c_{A_b}) \tag{3-202}$$

Thus,

$$k_c = \sqrt{D_{AB}s} \tag{3-203}$$

The surface-renewal theory predicts the same dependency of the mass-transfer coefficient on diffusivity as the penetration theory. Unfortunately, s, the fractional rate of surface renewal, is as elusive a parameter as the constant contact time, t_c.

EXAMPLE 3.19 Application of Surface-Renewal Theory.

For the conditions of Example 3.17, estimate the fractional rate of surface renewal, s, for Danckwert's theory and determine the residence time and probability distributions.

Solution

From Example 3.17,

$$k_c = 6.14 \times 10^{-3}\text{cm/s} \quad \text{and} \quad D_{AB} = 1.7 \times 10^{-5}\text{cm}^2\text{/s}$$

From (3-203),

$$s = \frac{k_c^2}{D_{AB}} = \frac{(6.14 \times 10^{-3})^2}{1.7 \times 10^{-5}} = 2.22\ \text{s}^{-1}$$

Thus, the average residence time of an eddy at the surface is $1/2.22 = 0.45$ s.

From (3-198),

$$\phi\{t\} = 2.22e^{-2.22t} \tag{1}$$

From (3-197), the residence-time distribution is

$$F(t) = 1 - e^{-t/0.45} \tag{2}$$

where t is in seconds. Equations (1) and (2) are shown in Figure 3.20. These curves differ from the curves of Figure 3.19.

§3.6.4 Film-Penetration Theory

Toor and Marchello [62] combined features of the film, penetration, and surface-renewal theories into a film-penetration model, which predicts that the mass-transfer coefficient, k_c, varies from $\sqrt{D_{AB}}$ to D_{AB}, with the resistance to mass transfer residing in a film of fixed thickness δ. Eddies move to and from the bulk fluid and this film. Age distributions for time spent in the film are of the Higbie or Danckwerts type. Fick's second law, (3-68), applies, but the boundary conditions are now

$$\begin{aligned} &c_A = c_{A_b} \quad \text{at} \quad t = 0 \quad \text{for} \quad 0 \le z \le \infty; \\ &c_A = c_{A_i} \quad \text{at} \quad z = 0 \quad \text{for} \quad t > 0; \quad \text{and} \\ &c_A = c_{A_b} \quad \text{at} \quad z = \delta \quad \text{for} \quad t > 0 \end{aligned}$$

They obtained the following infinite series solutions using Laplace transforms. For small values of time, t,

$$N_{A_{avg}} = k_c(c_{A_i} - c_{A_b}) = (c_{A_i} - c_{A_b})(sD_{AB})^{1/2} \times \left[1 + 2\sum_{n=1}^{\infty}\exp\left(-2n\delta\sqrt{\frac{s}{D_{AB}}}\right)\right] \tag{3-204}$$

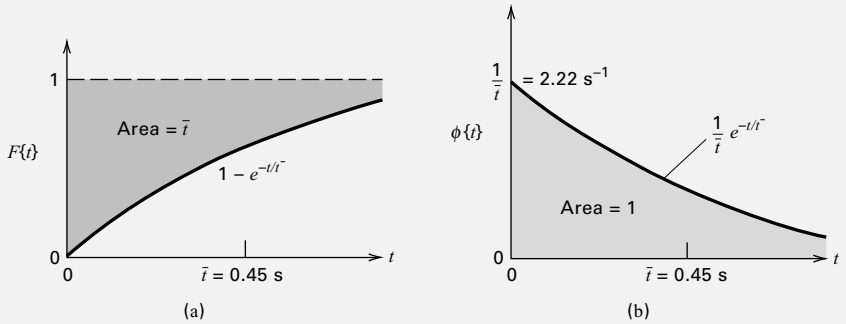

Figure 3.20 Age distribution curves for Example 3.19: (a) F curve; (b) $\phi\{t\}$ curve.

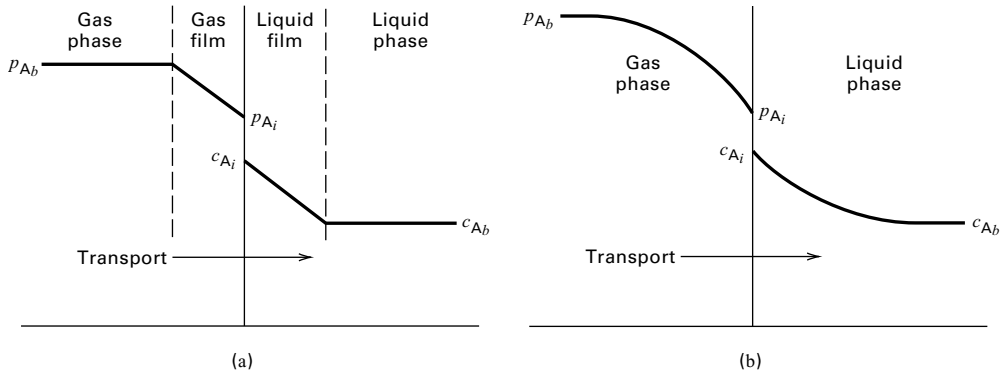

Figure 3.21 Concentration gradients for two-resistance theory: (a) film theory; (b) more realistic gradients.

converges rapidly. For large values of t, the following converges rapidly:

$$N_{A_{avg}} = k_c(c_{A_i} - c_{A_b}) = (c_{A_i} - c_{A_b})\left(\frac{D_{AB}}{\delta}\right) \times \left[1 + 2\sum_{n=0}^{\infty} \frac{1}{1 + n^2\pi^2 \dfrac{D_{AB}}{s\delta^2}}\right] \quad (3\text{-}205)$$

In the limit for a high rate of surface renewal, $s\delta^2/D_{AB}$, (3-204) reduces to the surface-renewal theory, (3-202). For low rates of renewal, (3-205) reduces to the film theory, (3-188). In between, k_c is proportional to D_{AB}^n, where n is 0.5–1.0. Application of the film-penetration theory is difficult because of lack of data for δ and s, but the predicted effect of molecular diffusivity brackets experimental data.

§3.7 TWO-FILM THEORY AND OVERALL MASS-TRANSFER COEFFICIENTS

Gas–liquid and liquid–liquid separation processes involve two fluid phases in contact and require consideration of mass-transfer resistances in both phases. In 1923, Whitman [63] suggested an extension of the film theory to two films in series. Each film presents a resistance to mass transfer, but concentrations in the two fluids at the interface are assumed to be in phase equilibrium. That is, there is no additional interfacial resistance to mass transfer.

The assumption of phase equilibrium at the interface, while widely used, may not be valid when gradients of interfacial tension are established during mass transfer. These gradients give rise to interfacial turbulence, resulting, most often, in considerably increased mass-transfer coefficients. This phenomenon, the *Marangoni effect*, is discussed in detail by Bird, Stewart, and Lightfoot [28], who cite additional references. The effect occurs at vapor–liquid and liquid–liquid interfaces, with the latter having received the most attention. By adding surfactants, which concentrate at the interface, the Marangoni effect is reduced because of interface stabilization, even to the extent that an interfacial mass-transfer resistance (which causes the mass-transfer coefficient to be reduced) results. Unless otherwise indicated, the Marangoni effect will be ignored here, and phase equilibrium will always be assumed at the phase interface.

§3.7.1 Gas (Vapor)–Liquid Case

Consider steady-state mass transfer of A from a gas, across an interface, and into a liquid. It is postulated, as shown in Figure 3.21a, that a thin gas film exists on one side of the interface and a thin liquid film exists on the other side, with diffusion controlling in each film. However, this postulation is not necessary, because instead of writing

$$N_A = \frac{(D_{AB})_G}{\delta_G}(c_{A_b} - c_{A_i})_G = \frac{(D_{AB})_L}{\delta_L}(c_{A_i} - c_{A_b})_L \quad (3\text{-}206)$$

the rate of mass transfer can be expressed in terms of mass-transfer coefficients determined from any suitable theory, with the concentration gradients visualized more realistically as in Figure 3.21b. Any number of different mass-transfer coefficients and driving forces can be used. For the gas phase, under dilute or equimolar counterdiffusion (EMD) conditions, the mass-transfer rate in terms of partial pressures is:

$$\boxed{N_A = k_p(p_{A_b} - p_{A_i})} \quad (3\text{-}207)$$

where k_p is a gas-phase mass-transfer coefficient based on a partial-pressure driving force.

For the liquid phase, with molar concentrations:

$$\boxed{N_A = k_c(c_{A_i} - c_{A_b})} \quad (3\text{-}208)$$

At the interface, c_{A_i} and p_{A_i} are in equilibrium. Applying a version of Henry's law different from that in Table 2.3,[1]

$$c_{A_i} = H_A p_{A_i} \quad (3\text{-}209)$$

Equations (3-207) to (3-209) are commonly used combinations for vapor–liquid mass transfer. Computations of mass-transfer rates are made from a knowledge of bulk concentrations c_{A_b} and p_{A_b}. To obtain an expression for N_A in terms of an overall driving force for mass transfer that includes both

[1]Different forms of Henry's law are found in the literature. They include

$$p_A = H_A x_A, \quad p_A = \frac{c_A}{H_A}, \quad \text{and} \quad y_A = H_A x_A$$

When a Henry's law constant, H_A, is given without citing the defining equation, the equation can be determined from the units of the constant. For example, if the constant has the units of atm or atm/mole fraction, Henry's law is given by $p_A = H_A x_A$. If the units are mol/L-mmHg, Henry's law is $p_A = c_A/H_A$.

fluid phases, (3-207) to (3-209) are combined to eliminate the interfacial concentrations, c_{A_i} and p_{A_i}. Solving (3-207) for p_{A_i}:

$$p_{A_i} = p_{A_b} - \frac{N_A}{k_p} \tag{3-210}$$

Solving (3-208) for c_{A_i}:

$$c_{A_i} = c_{A_b} + \frac{N_A}{k_c} \tag{3-211}$$

Combining (3-211) with (3-209) to eliminate c_{A_i} and combining the result with (3-210) to eliminate p_{A_i} gives

$$\boxed{N_A = \frac{p_{A_b} H_A - c_{A_b}}{(H_A/k_p) + (1/k_c)}} \tag{3-212}$$

Overall Mass-Transfer Coefficients. It is customary to define: (1) a fictitious liquid-phase concentration $c_A^* = p_{A_b} H_A$, which is a fictitious liquid concentration of A in equilibrium with the partial pressure of A in the bulk gas; and (2) an overall mass-transfer coefficient, K_L. Now (3-212) is

$$\boxed{N_A = K_L(c_A^* - c_{A_b}) = \frac{(c_A^* - c_{A_b})}{(H_A/k_p) + (1/k_c)}} \tag{3-213}$$

where K_L is the *overall mass-transfer coefficient* based on the liquid phase and defined by

$$\boxed{\frac{1}{K_L} = \frac{H_A}{k_p} + \frac{1}{k_c}} \tag{3-214}$$

The corresponding overall driving force for mass transfer is also based on the liquid phase, given by $(c_A^* - c_{A_b})$. The quantities H_A/k_p and $1/k_c$ are measures of gas and liquid mass-transfer resistances. When $1/k_c \gg H_A/k_p$, the resistance of the gas phase is negligible and the rate of mass transfer is controlled by the liquid phase, with (3-213) simplifying to

$$N_A = k_c(c_A^* - c_{A_b}) \tag{3-215}$$

so that $K_L \approx k_c$. Because resistance in the gas phase is negligible, the gas-phase driving force becomes $(p_{A_b} - p_{A_i}) \approx 0$, so $p_{A_b} \approx p_{A_i}$.

Alternatively, (3-207) to (3-209) combine to define an overall mass-transfer coefficient, K_G, based on the gas phase:

$$N_A = \frac{p_{A_b} - c_{A_b}/H_A}{(1/k_p) + (1/H_A k_c)} \tag{3-216}$$

In this case, it is customary to define: (1) a fictitious gas-phase partial pressure $p_A^* = c_{A_b}/H_A$, which is the partial pressure of A that would be in equilibrium with the concentration of A in the bulk liquid; and (2) an overall mass-transfer coefficient for the gas phase, K_G, based on a partial-pressure driving force. Thus, (3-216) becomes

$$N_A = K_G(p_{A_b} - p_A^*) = \frac{(p_{A_b} - p_A^*)}{(1/k_p) + (1/H_A k_c)} \tag{3-217}$$

where

$$\boxed{\frac{1}{K_G} = \frac{1}{k_p} + \frac{1}{H_A k_c}} \tag{3-218}$$

Now the resistances are $1/k_p$ and $1/H_A k_c$. If $1/k_p \gg 1/H_A k_c$,

$$N_A = k_p(p_{A_b} - p_A^*) \tag{3-219}$$

so $K_G \approx k_p$. Since the resistance in the liquid phase is then negligible, the liquid-phase driving force becomes $(c_{A_i} - c_{A_b}) \approx 0$, so $c_{A_i} \approx c_{A_b}$.

The choice between (3-213) or (3-217) is arbitrary, but is usually made on the basis of which phase has the largest mass-transfer resistance; if the liquid, use (3-213); if the gas, use (3-217); if neither is dominant, either equation is suitable.

Another common combination for vapor–liquid mass transfer uses mole-fraction driving forces, which define another set of mass-transfer coefficients k_y and k_x:

$$N_A = k_y(y_{A_b} - y_{A_i}) = k_x(x_{A_i} - x_{A_b}) \tag{3-220}$$

Now equilibrium at the interface can be expressed in terms of a K-value for vapor–liquid equilibrium, instead of as a Henry's law constant. Thus,

$$K_A = y_{A_i}/x_{A_i} \tag{3-221}$$

Combining (3-220) and (3-221) to eliminate y_{A_i} and x_{A_i},

$$N_A = \frac{y_{A_b} - x_{A_b}}{(1/K_A k_y) + (1/k_x)} \tag{3-222}$$

Alternatively, fictitious concentrations and overall mass-transfer coefficients can be used with mole-fraction driving forces. Thus, $x_A^* = y_{A_b}/K_A$ and $y_A^* = K_A x_{A_b}$. If the two values of K_A are equal,

$$N_A = K_x(x_A^* - x_{A_b}) = \frac{x_A^* - x_{A_b}}{(1/K_A k_y) + (1/k_x)} \tag{3-223}$$

and

$$N_A = K_y(y_{A_b} - y_A^*) = \frac{y_{A_b} - y_A^*}{(1/k_y) + (K_A/k_x)} \tag{3-224}$$

where K_x and K_y are overall mass-transfer coefficients based on mole-fraction driving forces with

$$\frac{1}{K_x} = \frac{1}{K_A k_y} + \frac{1}{k_x} \tag{3-225}$$

and

$$\frac{1}{K_y} = \frac{1}{k_y} + \frac{K_A}{k_x} \tag{3-226}$$

When using handbook or literature correlations to estimate mass-transfer coefficients, it is important to determine which coefficient (k_p, k_c, k_y, or k_x) is correlated, because often it is not stated. This can be done by checking the units or the form of the Sherwood or Stanton numbers. Coefficients correlated by the Chilton–Colburn analogy are k_c for either the liquid or the gas phase. The various coefficients are related by the following expressions, which are summarized in Table 3.16.

Table 3.16 Relationships among Mass-Transfer Coefficients

Equimolar Counterdiffusion (EMD):

Gases: $N_A = k_y \Delta y_A = k_c \Delta c_A = k_p \Delta p_A$

$k_y = k_c \dfrac{P}{RT} = k_p P$ if ideal gas

Liquids: $N_A = k_x \Delta x_A = k_c \Delta c_A$

$k_x = k_c c$, where c = total molar concentration (A + B)

Unimolecular Diffusion (UMD) with bulk flow:

Gases: Same equations as for EMD with k replaced by $k' = \dfrac{k}{(y_B)_{LM}}$

Liquids: Same equations as for EMD with k replaced by $k' = \dfrac{k}{(X_B)_{LM}}$

When working with concentration units, it is convenient to use:

$k_G(\Delta c_G) = k_c(\Delta c)$ for the gas phase

$k_L(\Delta c_L) = k_c(\Delta c)$ for the liquid phase

Liquid phase:

$$\boxed{k_x = k_c c = k_c\left(\frac{\rho_L}{M}\right)} \tag{3-227}$$

Ideal-gas phase:

$$\boxed{k_y = k_p P = (k_c)_g \frac{P}{RT} = (k_c)_g c = (k_c)_g \left(\frac{\rho_G}{M}\right)} \tag{3-228}$$

Typical units are

	SI	AE
k_c	m/s	ft/h
k_p	kmol/s-m^2-kPa	lbmol/h-ft^2-atm
k_y, k_x	kmol/s-m^2	lbmol/h-ft^2

When unimolecular diffusion (UMD) occurs under nondilute conditions, bulk flow must be included. For binary mixtures, this is done by defining modified mass-transfer coefficients, designated with a prime as follows:

For the liquid phase, using k_c or k_x,

$$k' = \frac{k}{(1 - x_A)_{LM}} = \frac{k}{(x_B)_{LM}} \tag{3-229}$$

For the gas phase, using k_p, k_y, or k_c,

$$k' = \frac{k}{(1 - y_A)_{LM}} = \frac{k}{(y_B)_{LM}} \tag{3-230}$$

Expressions for k' are convenient when the mass-transfer rate is controlled mainly by one of the two resistances. Literature mass-transfer coefficient data are generally correlated in terms of k rather than k'. Mass-transfer coefficients estimated from the Chilton–Colburn analogy [e.g. equations (3-166) to (3-171)] are k_c, not k'_c.

§3.7.2 Liquid–Liquid Case

For mass transfer across two liquid phases, equilibrium is again assumed at the interface. Denoting the two phases by $L^{(1)}$ and $L^{(2)}$, (3-223) and (3-224) become

$$N_A = K_x^{(2)}(x_A^{(2)*} - x_A^{(2)}) = \frac{x_A^{(2)*} - x_{A_b}^{(2)}}{(1/K_{D_A}k_x^{(1)}) + (1/k_x^{(2)})} \tag{3-231}$$

and

$$N_A = K_x^{(1)}(x_{A_b}^{(1)} - x_A^{(1)*}) = \frac{x_{A_b}^{(1)} - x_A^{(1)*}}{(1/k_x^{(1)}) + (K_{D_A}/k_x^{(2)})} \tag{3-232}$$

where

$$K_{D_A} = \frac{x_{A_i}^{(1)}}{x_{A_i}^{(2)}} \tag{3-233}$$

§3.7.3 Case of Large Driving Forces for Mass Transfer

Previously, phase equilibria ratios such as H_A, K_A, and K_{D_A} have been assumed constant across the two phases. When large driving forces exist, however, the ratios may not be constant. This commonly occurs when one or both phases are not dilute with respect to the solute, A, in which case, expressions for the mass-transfer flux must be revised. For mole-fraction driving forces, from (3-220) and (3-224),

$$N_A = k_y(y_{A_b} - y_{A_i}) = K_y(y_{A_b} - y_A^*) \tag{3-234}$$

Thus,

$$\frac{1}{K_y} = \frac{y_{A_b} - y_A^*}{k_y(y_{A_b} - y_{A_i})} \tag{3-235}$$

or

$$\frac{1}{K_y} = \frac{(y_{A_b} - y_{A_i}) + (y_{A_i} - y_A^*)}{k_y(y_{A_b} - y_{A_i})} = \frac{1}{k_y} + \frac{1}{k_y}\left(\frac{y_{A_i} - y_A^*}{y_{A_b} - y_{A_i}}\right) \tag{3-236}$$

From (3-220),

$$\frac{k_x}{k_y} = \frac{(y_{A_b} - y_{A_i})}{(x_{A_i} - x_{A_b})} \tag{3-237}$$

Combining (3-234) and (3-237),

$$\frac{1}{K_y} = \frac{1}{k_y} + \frac{1}{k_x}\left(\frac{y_{A_i} - y_A^*}{x_{A_i} - x_{A_b}}\right) \tag{3-238}$$

Similarly

$$\frac{1}{K_x} = \frac{1}{k_x} + \frac{1}{k_y}\left(\frac{x_A^* - x_{A_i}}{y_{A_b} - y_{A_i}}\right) \tag{3-239}$$

Figure 3.22 shows a curved equilibrium line with values of $y_{A_b}, y_{A_i}, y_A^*, x_A^*, x_{A_i}$, and x_{A_b}. Because the line is curved, the vapor–liquid equilibrium ratio, $K_A = y_A/x_A$, is not constant. As shown, the slope of the curve and thus, K_A, decrease with

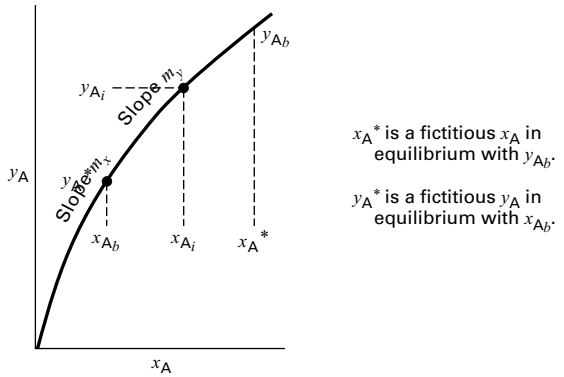

Figure 3.22 Curved equilibrium line.

increasing concentration of A. Denoting two slopes of the equilibrium curve by

$$m_x = \left(\frac{y_{A_i} - y_A^*}{x_{A_i} - x_{A_b}}\right) \tag{3-240}$$

and

$$m_y = \left(\frac{y_{A_b} - y_{A_i}}{x_A^* - x_{A_i}}\right) \tag{3-241}$$

then substituting (3-240) and (3-241) into (3-238) and (3-239), respectively,

$$\frac{1}{K_y} = \frac{1}{k_y} + \frac{m_x}{k_x} \tag{3-242}$$

and

$$\frac{1}{K_x} = \frac{1}{k_x} + \frac{1}{m_y k_y} \tag{3-243}$$

EXAMPLE 3.20 Absorption of SO_2 into Water.

Sulfur dioxide (A) is absorbed into water in a packed column, where bulk conditions are 50°C, 2 atm, $y_{A_b} = 0.085$, and $x_{A_b} = 0.001$. Equilibrium data for SO_2 between air and water at 50°C are

p_{SO_2}, atm	c_{SO_2}, lbmol/ft^3
0.0382	0.00193
0.0606	0.00290
0.1092	0.00483
0.1700	0.00676

Experimental values of the mass-transfer coefficients are:

$$\textit{Liquid phase}: k_c = 0.18 \text{ m/h}$$

$$\textit{Gas phase}: k_p = 0.040 \frac{\text{kmol}}{\text{h-m}^2\text{-}k\text{Pa}}$$

For mole-fraction driving forces, compute the mass-transfer flux: (a) assuming an average Henry's law constant and a negligible bulk-flow effect; (b) utilizing the actual curved equilibrium line and assuming a negligible bulk-flow effect; (c) utilizing the actual curved equilibrium line and taking into account the bulk-flow effect. In addition, (d) determine the magnitude of the two resistances and the values of the mole fractions at the interface that result from part (c).

Solution

Equilibrium data are converted to mole fractions by assuming Dalton's law, $y_A = p_A/P$, for the gas and $x_A = c_A/c$ for the liquid. The concentration of liquid is close to that of water, 3.43 lbmol/ft^3 or 55.0 kmol/m^3. Thus, the mole fractions at equilibrium are:

y_{SO_2}	x_{SO_2}
0.0191	0.000563
0.0303	0.000846
0.0546	0.001408
0.0850	0.001971

These data are fitted with average and maximum absolute deviations of 0.91% and 1.16%, respectively, by the equation

$$y_{SO_2} = 29.74 x_{SO_2} + 6{,}733 x_{SO_2}^2 \tag{1}$$

Differentiating, the slope of the equilibrium curve is

$$m = \frac{dy}{dx} = 29.74 + 13{,}466 x_{SO_2} \tag{2}$$

The given mass-transfer coefficients are converted to k_x and k_y by (3-227) and (3-228):

$$k_x = k_c c = 0.18(55.0) = 9.9 \frac{\text{kmol}}{\text{h-m}^2}$$

$$k_y = k_p P = 0.040(2)(101.3) = 8.1 \frac{\text{kmol}}{\text{h-m}^2}$$

(a) From (1) for $x_{A_b} = 0.001$, $y_A^* = 29.74(0.001) + 6{,}733(0.001)^2 = 0.0365$. From (1) for $y_{A_b} = 0.085$, solving the quadratic equation yields $x_A^* = 0.001975$.

The average slope in this range is

$$m = \frac{0.085 - 0.0365}{0.001975 - 0.001} = 49.7$$

Examination of (3-242) and (3-243) shows that the liquid-phase resistance is controlling because the term in k_x is much larger than the term in k_y. Therefore, from (3-243), using $m = m_x$,

$$\frac{1}{K_x} = \frac{1}{9.9} + \frac{1}{49.7(8.1)} = 0.1010 + 0.0025 = 0.1035$$

or $K_x = 9.66 \frac{\text{kmol}}{\text{h-m}^2}$

From (3-223),

$$N_A = 9.66(0.001975 - 0.001) = 0.00942 \frac{\text{kmol}}{\text{h-m}^2}$$

(b) From part (a), the gas-phase resistance is almost negligible. Therefore, $y_{A_i} \approx y_{A_b}$ and $x_{A_i} \approx x_A^*$.

From (3-241), the slope m_y is taken at the point $y_{A_b} = 0.085$ and $x_A^* = 0.001975$ on the equilibrium line.

By (2), $m_y = 29.74 + 13{,}466(0.001975) = 56.3$. From (3-243),

$$K_x = \frac{1}{(1/9.9) + [1/(56.3)(8.1)]} = 9.69 \frac{\text{kmol}}{\text{h-m}^2}$$

giving $N_A = 0.00945$ kmol/h-m^2. This is a small change from part (a).

(c) Correcting for bulk flow, from the results of parts (a) and (b),

$$y_{A_b} = 0.085,\ y_{A_i} = 0.085,\ x_{A_i} = 0.1975,\ x_{A_b} = 0.001,$$
$$(y_B)_{LM} = 1.0 - 0.085 = 0.915, \text{ and } (x_B)_{LM} \approx 0.9986$$

From (3-229),

$$k'_x = \frac{9.9}{0.9986} = 9.9\frac{\text{kmol}}{\text{h-m}^2} \text{ and } k'_y = \frac{8.1}{0.915} = 8.85\frac{\text{kmol}}{\text{h-m}^2}$$

From (3-243),

$$K_x = \frac{1}{(1/9.9) + [1/56.3(8.85)]} = 9.71\frac{\text{kmol}}{\text{h-m}^2}$$

From (3-223),

$$N_A = 9.7(0.001975 - 0.001) = 0.00947\frac{\text{kmol}}{\text{h-m}^2}$$

which is only a very slight change from parts (a) and (b), where the bulk-flow effect was ignored. The effect is very small because it is important only in the gas, whereas the liquid resistance is controlling.

(d) The relative magnitude of the mass-transfer resistances is

$$\frac{1/m_y k'_y}{1/k'_x} = \frac{1/(56.3)(8.85)}{1/9.9} = 0.02$$

Thus, the gas-phase resistance is only 2% of the liquid-phase resistance. The interface vapor mole fraction can be obtained from (3-223), after accounting for the bulk-flow effect:

$$y_{A_i} = y_{A_b} - \frac{N_A}{k'_y} = 0.085 - \frac{0.00947}{8.85} = 0.084$$

Similarly, $$x_{A_i} = \frac{N_A}{k'_x} + x_{A_b} = \frac{0.00947}{9.9} + 0.001 = 0.00196$$

§3.8 MOLECULAR MASS TRANSFER IN TERMS OF OTHER DRIVING FORCES

Thus far in this chapter, only a concentration driving force (in terms of concentrations, mole fractions, or partial pressures) has been considered, and only one or two species were transferred. Molecular mass transfer of a species such as a charged biological component may be driven by other forces besides its concentration gradient. These include gradients in *temperature*, which induces thermal diffusion via the Soret effect; *pressure*, which drives ultracentrifugation; *electrical potential*, which governs electrokinetic phenomena (dielectrophoresis and magnetophoresis) in ionic systems like permselective membranes; and *concentration gradients* of other species in systems containing three or more components. Three postulates of nonequilibrium thermodynamics may be used to relate such driving forces to frictional motion of a species in the Maxwell–Stefan equations [28, 75, 76]. Maxwell, and later Stefan, used kinetic theory in the mid- to late-19th century to determine diffusion rates based on momentum transfer between molecules. At the same time, Graham and Fick described ordinary diffusion based on binary mixture experiments. These three postulates and applications to bioseparations are presented in this section. Application of the Maxwell–Stefan equations to rate-based models for multicomponent absorption, stripping, and distillation is developed in Chapter 12.

§3.8.1 The Three Postulates of Nonequilibrium Thermodynamics

This brief introduction summarizes a more detailed synopsis found in [28].

First postulate

The first (*quasi-equilibrium*) postulate states that equilibrium thermodynamic relations apply to systems not in equilibrium, provided departures from local equilibrium (gradients) are sufficiently small. This postulate and the second law of thermodynamics allow the diffusional driving force per unit volume of solution, represented by $cRT\mathbf{d}_i$ and which moves species i relative to a solution containing n components, to be written as

$$cRT\mathbf{d}_i \equiv c_i \nabla_{T,P}\mu_i + \left(c_i\overline{V}_i - \omega_i\right)\nabla P - \rho_i\left(\mathbf{g}_i - \sum_{k=1}^{n}\omega_k\mathbf{g}_k\right) \tag{3-244}$$

$$\sum_{i=1}^{n}\mathbf{d}_i = 0 \tag{3-245}$$

where $\mathbf{d}_i$ are driving forces for molecular mass transport, c_i is molar concentration, μ_i is chemical potential, ω_i is mass fraction, $\mathbf{g}_i$ are total body forces (e.g., gravitational or electrical potential) per unit mass, $\overline{V}_i$ is partial molar volume, and ρ_i is mass concentration, all of which are specific to species i. Each driving force is given by a negative spatial gradient in potential, which is the work required to move species i relative to the solution volume. In order from left to right, the three collections of terms on the RHS of (3-244) represent driving forces for *concentration diffusion*, *pressure diffusion*, and *forced diffusion*. The term $c_i\overline{V}_i$ in (3-244) corresponds to the volume fraction of species i, ϕ_i.

Second postulate

The second (*linearity*) postulate allows forces on species in (3-244) to be related to a vector mass flux, $\mathbf{j}_i$. It states that all fluxes in the system may be written as linear relations involving all the forces. For mass flux, the *thermal-diffusion* driving force, $-\beta_{i0}\nabla \ln T$, is added to the previous three forces to give

$$\mathbf{j}_i = -\beta_{i0}\nabla \ln T - \rho_i \sum_{j=1}^{n}\frac{\beta_{ij}}{\rho_i\rho_j}cRT\mathbf{d}_j \tag{3-246}$$

$$\beta_{ij} + \sum_{\substack{k=1\\k\neq j}}^{n}\beta_{ik} = 0 \tag{3-247}$$

where β_{i0} and β_{ij} are phenomenological coefficients (i.e., transport properties). The vector mass flux, $\mathbf{j}_i = \rho_i(\mathbf{v}_i - \mathbf{v})$, is the arithmetic average of velocities of all molecules of

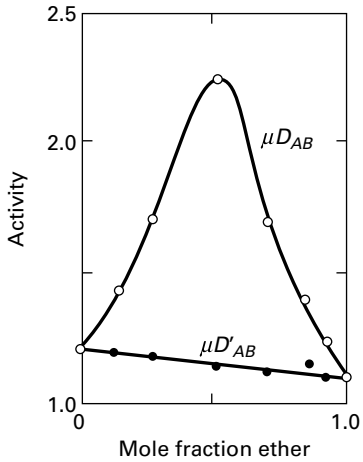

Figure 3.23 Effect of activity on the product of viscosity and diffusivity for liquid mixtures of chloroform and diethyl ether [R.E. Powell, W.E. Roseveare, and H. Eyring, *Ind. Eng. Chem.*, **33**, 430–435 (1941)].

species i in a tiny volume element ($\mathbf{v}_i$) relative to a mass-averaged value of the velocities of all such components in the mixture, $\mathbf{v} = \sum \omega_i \mathbf{v}_i$. It is related to molar flux, $\mathbf{J}_i$, in (3-251).

Third postulate

According to the third postulate, *Onsager's reciprocal relations*—developed using statistical mechanics and supported by data—the matrix of the β_{ij} coefficients in the flux-force relation (3-246) are symmetric ($\beta_{ij} = \beta_{ji}$) in the absence of magnetic fields. These coefficients may be rewritten as multicomponent mass diffusivities D'_{ij}

$$D'_{ij} = \frac{x_i x_j}{\beta_{ij}} cRT \left(= D'_{ji}\right) \tag{3-248}$$

which exhibit less composition dependency than the transport properties, β_{ij}, and reduce to the more familiar binary diffusivity of Fick's Law, D_{AB}, for ideal binary solutions, as shown in Figure 3.23, and illustrated in Example 3.21.

§3.8.2 Maxwell–Stefan Equations

To show the effects of forces on molecular motion of species i, (3-248) is substituted into (3-246), which is solved for the driving forces, $\mathbf{d}_i$, and set equal to (3-244). Using $\mathbf{j}_i = \rho_i(\mathbf{v}_i - \mathbf{v})$, discussed above, a set of $n - 1$ independent rate expressions, called the *Maxwell–Stefan equations*, is obtained:

$$\sum_{j=1}^{n} \frac{x_i x_j}{D'_{ij}} \left(\mathbf{v}_i - \mathbf{v}_j\right) = \frac{1}{cRT} \left[c_i \nabla_{T,P} \mu_i + (\phi_i - \omega_i) \nabla P - \rho_i \left(\mathbf{g}_i - \sum_{k=1}^{n} \omega_k \mathbf{g}_k \right) \right] - \sum_{j=1}^{n} \frac{x_i x_j}{D'_{ij}} \left(\frac{\beta_{i0}}{\rho_i} - \frac{\beta_{j0}}{\rho_j} \right) \nabla \ln T \tag{3-249}$$

The set of rate expressions given by (3-249) shows molecular mass transport of species i driven by gradients in pressure, temperature, and concentration of species i for $j \neq i$ in systems containing three or more components, as well as driven by body forces that induce gradients in potential. The total driving force for species i due to potential gradients collected on the LHS of (3-249) is equal to the sum on the RHS of the cumulative *friction force* exerted on species i—$\zeta_{i,j} x_j (x_i - x_j)$—by every species j in a mixture, where frictional coefficient ζ_{ij} is given by x_i / D'_{ij} in (3-249). The friction exerted by j on i is proportional to the mole fraction of j in the mixture and to the difference in average molecular velocity between species j and i.

Body forces in (3-249) may arise from gravitational acceleration, $\mathbf{g}$; electrostatic potential gradients, $\nabla\varphi$, or mechanically restraining matrices (e.g., permselective membranes and friction between species i and its surroundings), denoted by δ_{im}. These can be written as

$$\mathbf{g}_i = \mathbf{g} - \left(\frac{z_i \Im}{M_i} \right) \nabla\varphi + \delta_{im} \frac{1}{\rho_m} \nabla P \tag{3-250}$$

where z_i is elementary charge and Faraday's constant, $\Im$, = 96,490 absolute coulombs per gram-equivalent.

Chemical versus physical potentials

Potential can be defined as the reversible work required to move an entity relative to other elements in its surroundings. The change in potential per unit distance provides the force that drives local velocity of a species relative to its environment in (3-249). For molecules, potential due to gravity in (3-250)—an external force that affects the whole system—is insignificant relative to chemical potential in (3-249), an internal force that results in motion within the system but not in the system as whole. Gravity produces a driving force downward at height z, resulting from a potential difference due to the work performed to attain the height, $-mg\Delta z$, divided by the height, Δz, which reduces to mg. For gold (a dense molecule), this driving force = (0.197 kg/mol) (10 m/s^2) $\cong$ 2 N/mol. Gravitational potential of gold across the distance of a centimeter is therefore 2×10^{-2} N/mol.

Chemical potential can be defined as the reversible work needed to separate one mole of species i from a large amount of a mixture. Its magnitude increases logarithmically with the species activity, or $\Delta\mu = -RT\Delta \ln(\gamma_i x_i)$. Gold, in an ideal solution ($\gamma_i = 1$) and for ambient conditions at $x_i = 1/\mathrm{e} = 0.368$, experiences a driving force times distance due to a chemical potential of $-(8.314$ J/mol–K)(298 K) $\times$ ln (0.37) = 2,460 J/mol. The predominance of chemical potential leads to an approximate linear simplification of (3-249)—which neglects potentials due to pressure, temperature, and external body forces—that is applicable in many practical situations, as illustrated later in Example 3.25. Situations in which the other potentials are significant are also considered. For instance, Example 3.21 below shows that ultracentrifugation provides a large centripetal (''center-seeking'') force to induce molecular momentum, ∇P, sufficient to move species i in the positive direction, if its mass fraction is greater than its volume fraction (i.e., if component i is denser than its surroundings).

Driving forces for species velocities

Effects of driving forces on species velocity are illustrated in the following seven examples reduced from [28], [75], [76], and [77]. These examples show how to apply (3-249) and (3-250), together with species equations of continuity, the equation of motion, and accompanying auxiliary (bootstrap) relations such as (3-245) and (3-248). The auxiliary expressions are needed to provide the molecular velocity of the selected reference frame because the velocities in (3-249) are relative values. The first example considers concentration-driving forces in binary systems. Measured data for D'_{ij}, which requires simultaneous measurement of γ_i as a function of x_i, are rare. Instead, the multicomponent diffusivity values may be estimated from phenomenological Fick's law diffusivities.

EXAMPLE 3.21 Maxwell–Stefan Equations Related to Fick's Law.

Consider a binary system containing species A and B that is isotropic in all but concentration [75]. Show the correspondence between D_{AB} and D'_{AB} by relating (3-249) to the diffusive molar flux of species A relative to the molar-average velocity of a mixture, $\mathbf{J}_A$, which may be written in terms of the mass-average velocity, $\mathbf{j}_A$:

$$\mathbf{J_A} = -cD_{AB}\nabla x_A = c_A(\mathbf{v}_A - \mathbf{v}_M) = \mathbf{j}_A\frac{cx_Ax_B}{\rho\omega_A\omega_B} \tag{3-251}$$

where $\mathbf{v}_M = x_A\mathbf{v}_A + x_B\mathbf{v}_B$ is the molar-average velocity of a mixture.

Solution

In a binary system, $x_B = 1 - x_A$, and the LHS of (3-249) may be written as

$$\frac{x_Ax_B}{D'_{AB}}(\mathbf{v}_B - \mathbf{v}_A) = \frac{x_A}{D'_{AB}}(x_B\mathbf{v}_B + x_A\mathbf{v}_A - \mathbf{v}_A) = -\frac{x_A}{D'_{AB}}\frac{\mathbf{J}_A}{c_A} \tag{3-252}$$

which relates the friction force to the molar flux. Substituting $\nabla\mu_i = RT\nabla\ln(a_i)$ into the RHS of (3-249), setting it equal to (3-252), and rearranging, gives

$$\mathbf{J}_A = -cD'_{AB}\left\{x_A\nabla\ln a_A + \frac{1}{cRT}[(\phi_A - \omega_A)\nabla P - \rho\omega_A\omega_B(\mathbf{g}_A - \mathbf{g}_B)] + k_T\nabla\ln T\right\} \tag{3-253}$$

$$k_T = \frac{\beta_{A0}}{\rho D'_{AB}}\frac{x_Ax_B}{\omega_A\omega_B} = \alpha_T x_Ax_B = \sigma_T x_Ax_BT \tag{3-254}$$

Equation (3-253) describes binary diffusion in gases or liquids. It is a specialized form of the *generalized Fick equations*. Equation (3-254) relates the *thermal diffusion ratio*, k_T, to the *thermal diffusion factor*, α_T, and the *Soret coefficient*, σ_T. For liquids, σ_T is preferred. For gases, α_T is nearly independent of composition.

Table 3.17 shows concentration- and temperature-dependent k_T values for several binary gas and liquid pairs. Species A moves to the colder region when the value of k_T is positive. This usually corresponds to species A having a larger molecular weight (M_A) or diameter. The sign of k_T may change with temperature.

In this example, the effects of pressure, thermal diffusion, and body force terms in (3-253) may be neglected. Then from the properties of logarithms,

$$x_A\nabla\ln a_A = \nabla x_A + x_A\nabla\ln\gamma_A = \nabla x_A\left(1 + \frac{\partial\ln\gamma_A}{\partial\ln x_A}\right) \tag{3-255}$$

By substituting (3-255) into (3-253) and comparing with (3-251), it is found that

$$D_{AB} = \left(1 + \frac{\partial\ln\gamma_A}{\partial\ln x_A}\right)D'_{AB} \tag{3-256}$$

The activity-based diffusion coefficient D'_{AB} is less concentration-dependent than D_{AB} but requires accurate activity data, so it is used less widely. Multicomponent mixtures of low-density gases have $\gamma_i = 1$ and $\mathbf{d}_i = \nabla x_i$ for concentration diffusion and $D_{AB} = D'_{AB}$ from kinetic theory.

Table 3.17 Experimental Thermal Diffusion Ratios for Low-Density Gas and Liquid Mixtures

Species A-B	T(K)	x_A	$k_T\{x_A,T\}$
Gas			
Ne-He	330	0.80	0.0531
		0.40	0.1004
N_2-H_2	264	0.706	0.0548
		0.225	0.0663
D_2-H_2	327	0.90	0.1045
		0.50	0.0432
		0.10	0.0166
Liquid			
$C_2H_2Cl_4$-n-C_6H_{14}	298	0.5	1.08
$C_2H_4Br_2$-$C_2H_4Cl_2$	298	0.5	0.225
$C_2H_2Cl_4$-CCl_4	298	0.5	0.060
CBr_4-CCl_4	298	0.09	0.129
CCl_4-CH_3OH	313	0.5	1.23
CH_3OH-H_2O	313	0.5	−0.137
Cyclo-C_6H_{12}-C_6H_6	313	0.5	0.100

Data from Bird et al. [28].

EXAMPLE 3.22 Diffusion via a Thermal Gradient (thermal diffusion).

Consider two bulbs connected by a narrow, insulated tube that are filled with a binary mixture of ideal gases [28]. (Examples of binary mixtures are given in Table 3.17.) Maintaining the two bulbs at constant temperatures T_2 and T_1, respectively, typically enriches the larger species at the cold end for a positive value of k_T. Derive an expression for $(x_{A2} - x_{A1})$, the mole-fraction difference between the two bulbs, as a function of k_T, T_2, and T_1 at steady state, neglecting convection currents in the connecting tube.

Solution

There is no net motion of either component at steady state, so $\mathbf{J}_A = 0$. Use (3-253) for the ideal gases ($\gamma_A = 1$), setting the connecting tube on the z-axis, neglecting pressure and body forces, and applying the properties of logarithms to obtain

$$\frac{dx_A}{dz} = -\frac{k_T}{T}\frac{dT}{dz} \tag{3-257}$$

The integral of (3-257) may be evaluated by neglecting composition effects on k_T for small differences in mole fraction and using a value of k_T at a mean temperature, T_m, to yield

$$x_{A2} - x_{A1} = -k_T\{T_m\}\ln\frac{T_2}{T_1} \tag{3-258}$$

where the mean temperature at which to evaluate k_T is

$$T_m = \frac{T_1 T_2}{T_2 - T_1}\ln\frac{T_2}{T_1} \tag{3-259}$$

Substituting values of k_T from Table 3.17 into (3-258) suggests that a very large temperature gradient is required to obtain more than a small composition difference. During World War II, uranium isotopes were separated in cascades of Clausius–Dickel columns based on thermal diffusion between sets of vertical heated and cooled walls. The separation supplemented thermal diffusion with free convection to allow species A, enriched at the cooled wall, to descend and species B, enriched at the heated wall, to ascend. Energy expenditures were enormous.

EXAMPLE 3.23 Diffusion via a Pressure Gradient (pressure diffusion).

Components A and B in a small cylindrical tube of length L, held at radial position $R_o \gg L$ inside an ultracentrifuge, are rotated at constant angular velocity Ω [28]. The species experience a change in molecular momentum, ∇p, due to centripetal (''center-seeking'') acceleration $\mathbf{g}_\Omega = \Omega^2 r$ given by the equation of motion,

$$\frac{dp}{dr} = \rho g_\Omega = \rho\Omega^2 r = \rho\frac{v_\theta^2}{r} \tag{3-260}$$

where $v_\theta = \delta_\theta \Omega r$ is the linear velocity. Derive expressions for (1) the migration velocity, v_{migr}, of dilute A in B (e.g., protein in H_2O) in terms of relative molecular weight, and for (2) the distribution of the two components at steady state in terms of their partial molar volumes, $\bar{V}_i$, i = A, B, and the pressure gradient, neglecting changes in $\bar{V}_i$ and γ_i over the range of conditions in the centrifuge tube.

Solution

The radial motion of species A is obtained by substituting (3-255) into the radial component of the binary Maxwell–Stefan equation in (3-253) for an isothermal tube free of external body forces to give

$$\mathbf{J}_A = -cD'_{AB}\left[\left(1 + \frac{\partial \ln\gamma_A}{\partial \ln x_A}\right)\frac{dx_A}{dr} + \frac{1}{cRT}(\phi_A - \omega_A)\frac{dP}{dr}\right] \tag{3-261}$$

where the pressure gradient of the migration term in (3-261) remains relatively constant in the tube since $L \ll R_o$. Molecular-weight dependence in this term in the limit of a dilute solution of protein (A) in H_2O (B) arises in the volume and mass fractions, respectively,

$$\varphi_A = c_A\bar{V}_A = x_A c\bar{V}_A \approx x_A\frac{\bar{V}_A}{\bar{V}_B} = x_A\frac{M_A}{M_B}\frac{\hat{V}_A}{\hat{V}_B} \tag{3-262}$$

$$\omega_A = \frac{\rho_A}{\rho} = \frac{c_A M_A}{cM} = x_A\frac{M_A}{x_A M_A + x_B M_B} \approx x_A\frac{M_A}{M_B} \tag{3-263}$$

where $\hat{V}_i = \bar{V}_i/M_i$ is the partial specific volume of species i, which is 1 mL/g for H_2O and ~0.75 mL/g for a globular protein (see Table 3.18). A pseudo-binary Fickian diffusivity given by (3-256) to be substituted into (3-261) may be estimated using Stokes law:

$$D_{AB} = \frac{\kappa T}{6\pi\mu_B R_A f_A} \tag{3-264}$$

where R_A is the radius of a sphere whose volume equals that of the protein, and protein nonsphericity is accounted for by a hydrodynamic shape factor, f_A. Substituting (3-256), (3-260), (3-262), and (3-263) into (3-261) gives

$$\mathbf{J}_A = -cD_{AB}\frac{dx_A}{dr} + c_A\left\{-\frac{D'_{AB}}{cRT}\left[\frac{M_A}{M_B}\left(\frac{\hat{V}_A}{\hat{V}_B} - 1\right)\right]\rho\Omega^2 r\right\} \tag{3-265}$$

where the term inside the curly brackets on the RHS of (3-265) corresponds to the *migration velocity*, v_{migr}, in the $+r$ direction driven by centripetal force in proportion to the relative molecular weight, M_A/M_B. The ratio of v_{migr} to centripetal force in (3-265) is the sedimentation coefficient, s, which is typically expressed in Svedberg (S) units (1 S = 10^{-13} sec), named after the inventor of the ultracentrifuge. Protein molecular-weight values obtained by photoelectric scanning detection of v_{migr} to determine s in pure water (w) at 20° (i.e., $s_{20,w}$) are summarized in Table 3.18. Equation (3-265) is the basis for analyzing transient behavior, steady polarization, and preparative application of ultracentrifugation.

Concentration and pressure gradients balance at steady state ($\mathbf{J}_A = 0$), and with constant $\bar{V}_i$ and γ_i in the tube and $x_A \sim x_B$ locally, writing (3-253) for species A gives

$$0 = \frac{dx_A}{dr} + \frac{M_A x_A}{RT}\left(\frac{\bar{V}_A}{M_A} - \frac{1}{\rho}\right)\frac{dp}{dr} \tag{3-266}$$

Multiplying (3-266) by $(\bar{V}_B/x_A)dr$, and substituting a constant centripetal force ($r \approx R_o$) from (3-260), gives

$$\bar{V}_B\frac{dx_A}{x_A} = \bar{V}_B\frac{g_\Omega}{RT}\left(\rho\bar{V}_A - M_A\right)dr \tag{3-267}$$

Writing an equation analogous to (3-267) for species B, and subtracting it from (3-267), gives

$$\bar{V}_B\frac{dx_A}{x_A} - \bar{V}_A\frac{dx_B}{x_B} = \frac{g_\Omega}{RT}\left(M_A\bar{V}_B - M_B\bar{V}_A\right)dr \tag{3-268}$$

Integrating (3-268) from $x_i\{r = 0\} = x_{i0}$ *to* $x_i\{r\}$ for i = A,B, using $r = 0$ at the distal tube end, gives

$$\bar{V}_B\ln\frac{x_A}{x_{A0}} - \bar{V}_A\ln\frac{x_B}{x_{B0}} = \frac{g_\Omega}{RT}\left(M_B\bar{V}_A - M_A\bar{V}_B\right)r \tag{3-269}$$

Table 3.18 Protein Molecular Weights Determined by Ultracentrifugation

Protein	M	$s_{20,w}$ (S)	$\bar{V}_2$ (cm^3g^{-1})
Ribonuclease (bovine)	12,400	1.85	0.728
Lysozyme (chicken)	14,100	1.91	0.688
Serum albumin (bovine)	66,500	4.31	0.734
Hemoglobin	68,000	4.31	0.749
Tropomysin	93,000	2.6	0.71
Fibrinogen (human)	330,000	7.6	0.706
Myosin (rod)	570,000	6.43	0.728
Bushy stunt virus	10,700,000	132	0.74
Tobacco mosaic virus	40,000,000	192	0.73

Data from Cantor and Schimmel [78].

Using the properties of logarithms and taking the exponential of both sides of (3-269) yields the *steady-state species distribution* in terms of the partial molar volumes:

$$\left(\frac{x_A}{x_{A0}}\right)^{\overline{V}_B}\left(\frac{x_{B0}}{x_B}\right)^{\overline{V}_A} = \exp\left[\frac{g_\Omega r}{RT}\left(M_B\overline{V}_A - M_A\overline{V}_B\right)\right] \tag{3-270}$$

The result in (3-269) is independent of transport coefficients and may thus be obtained in an alternative approach using equilibrium thermodynamics.

$$D_{SW} = 2\left(\frac{D'_{M^+W}D'_{X^-W}}{D'_{M^+W}+D'_{X^-W}}\right)\left(1+\frac{\partial \ln \gamma_S}{\partial \ln x_S}\right) \tag{3-278}$$

$$\gamma_S = \gamma_{M^+}\gamma_{X^-} \tag{3-279}$$

where γ_S is the mean activity coefficient given by $a_S = a_M + a_{X-} = x_s^2[(\gamma_M + g_{X^-})^{1/2}]^2 = x_s^2[(\gamma_S)^{1/2}]^2$. Equation (3-278) shows that while fast diffusion of small counterions creates a potential gradient that speeds large ions, the overall diffusivity of the salt pair is dominated by the slower ions (e.g., proteins).

EXAMPLE 3.24 Diffusion in a Ternary System via Gradients in Concentration and Electrostatic Potential.

A 1-1 electrolyte M^+X^- (e.g., NaCl) diffuses in a constriction between two well-mixed reservoirs at different concentrations containing electrodes that exhibit a potential difference, $\Delta\varphi$, measured by a potentiometer under current-free conditions [75]. Derive an expression for salt flux in the system.

Solution

Any pressure difference between the two reservoirs is negligible relative to the reference pressure, $cRT \sim 1{,}350$ atm, at ambient conditions. Electroneutrality, in the absence of current flow through the potentiometer, requires that

$$x_{M^+} = x_{X^-} = x_S = 1 - x_W \tag{3-271}$$

$$N_{M^+} = N_{X^-} = N_S \tag{3-272}$$

Substituting (3-271) into (3-249) and rearranging yields the $n-1$ Maxwell–Stefan relations:

$$\frac{1}{cD'_{M^+W}}(x_W N_{M^+} - x_{M^+}N_W) = -x_{M^+}\nabla_{T,P}a_{M^+} + \frac{\rho_{M^+}}{cRT}\left(\mathbf{g}_{M^+} - \sum_{k=1}^{n}\omega_k\mathbf{g}_\mathbf{k}\right) \tag{3-273}$$

$$\frac{1}{cD'_{X^-W}}(x_W N_{X^-} - x_{X^-}N_W) = -x_{X^-}\nabla_{T,P}a_{X^-} + \frac{\rho_{X^-}}{cRT}\left(\mathbf{g}_{X^-} - \sum_{k=1}^{n}\omega_k\mathbf{g}_\mathbf{k}\right) \tag{3-274}$$

No ion-ion diffusivity appears because $\mathbf{v}_{M^+} - \mathbf{v}_{X^-} = 0$ in the absence of current. Substituting (3-250), (3-271), and (3-272) into (3-273) and (3-274) and rearranging yields

$$\frac{1}{cD'_{M^+W}}(x_W N_S - x_S N_W) = -\frac{\partial \ln a_{M^+}}{\partial \ln x_S}\nabla x_S - \frac{x_S}{RT}\Im\nabla\varphi \tag{3-275}$$

$$\frac{1}{cD'_{X^-W}}(x_W N_S - x_S N_W) = -\frac{\partial \ln a_{X^-}}{\partial \ln x_S}\nabla x_S + \frac{x_S}{RT}\Im\nabla\varphi \tag{3-276}$$

Adding (3-275) and (3-276) eliminates the electrostatic potential, to give

$$N_S = -\left(\frac{1}{cD'_{M^+W}} + \frac{1}{cD'_{X^-W}}\right)^{-1}\frac{\partial \ln (a_{M^+}a_{X^-})}{\partial \ln x_S}\nabla x_S + x_S(N_S + N_W) \tag{3-277}$$

which has the form of Fick's law after a concentration-based diffusivity is defined:

EXAMPLE 3.25 Film Mass Transfer.

Species velocity in (3-249) is due to (1) bulk motion; (2) gradient of a potential $\Delta\psi_i = \psi_{i\delta} - \psi_{io}$ of species i across distance δ (which moves species i relative to the mixture); and (3) friction between species and surroundings [77]. Develop an approximate expression for film mass transfer using linearized potential gradients.

Solution

The driving force that results from the potential gradient, $-d\psi_i/dz$, is approximated by the difference in potential across a film of thickness δ, $-\Delta\psi_i/\delta$. Linearizing the chemical potential difference by

$$\Delta\mu_i = RT\Delta\ln(\gamma_i x_i) \approx RT\frac{x_{i\delta} - x_{io}}{(x_{i\delta} + x_{io})/2} = RT\frac{\Delta x_i}{\bar{x}_i} \tag{3-280}$$

provides a tractable approximation that has reasonable accuracy over a wide range of compositions [77].

Friction from hydrodynamic drag of fluid (1) of viscosity μ_1 on a spherical particle (2) of diameter d_2 is proportional to their relative difference in velocity, $\mathbf{v}$, viz.,

$$-\frac{d\mu_2}{dz} = 3N_A\pi\mu_1(\mathbf{v}_2 - \mathbf{v}_1)d_2 \tag{3-281}$$

where N_A (Avogadro's number) represents particles per mole. A large force is produced when the drag is summed over a mole of particles.

Rearranging (3-281) yields an expression for the Maxwell–Stefan diffusivity in terms of hydrodynamic drag:

$$-\frac{d}{dz}\left(\frac{\mu_2}{RT}\right) = \frac{\mathbf{v}_2 - \mathbf{v}_1}{D'_{12}} \tag{3-282}$$

$$D'_{12} = \frac{RT}{N_A 3\pi\eta_1 d_2} \tag{3-283}$$

Substituting (3-280) into (3-282) and rearranging, after linearizing the derivative across a film of thickness δ, yields the mass transport coefficient, k_{12},

$$\frac{\Delta x_2}{\bar{x}_2} = \frac{\bar{\mathbf{v}}_1 - \bar{\mathbf{v}}_2}{k_{12}} \tag{3-284}$$

$$k_{12} = \frac{D'_{12}}{\delta} \tag{3-285}$$

where k_{ij} is $\sim 10^{-1}$ m/s for gases and 10^{-4} m/s for liquids. These values decrease by approximately a factor of 10 for gases and liquids in porous media.

In a general case that includes any number of components, friction between components j and i per mole of i is proportional to the difference between the mean velocities of j and i, respectively.

Taking friction proportional to the local concentration of j decreases the composition dependence of k_{ij}, viz.,

$$\bar{x}_j \frac{\bar{\mathbf{v}}_j - \bar{\mathbf{v}}_i}{k_{ij}} \tag{3-286}$$

Because assigning a local concentration to a component like a solid membrane component, m, is difficult, a membrane coefficient, k_i, may be introduced instead:

$$\frac{\bar{x}_m}{k_{im}} = \frac{1}{k_i} \tag{3-287}$$

§3.8.3 Maxwell–Stefan Difference Equation

Linearization allows application of a difference form of the Maxwell–Stefan equation, which is obtained by setting the negative driving force on species i equal to the friction on species i, viz. [77]:

$$\frac{\Delta x_i}{\bar{x}_i} + \ldots = \sum_j \bar{x}_j \frac{\bar{\mathbf{v}}_j - \bar{\mathbf{v}}_i}{k_{ij}} \tag{3-288}$$

where the ellipsis . . . allows addition of relevant linearized potentials in addition to the chemical potential. The accuracy of (3-288) is adequate for many engineering calculations. This is illustrated by determining molar solute flux of dilute and nondilute solute during binary stripping, and by estimating concentration polarization and permeate flux in tangential-flow filtration.

Dilute stripping

Consider stripping a trace gas (1) $(\bar{x}_2 \approx 1)$ from a liquid through a gas film into an ambient atmosphere. The atmosphere is taken at a reference velocity ($\mathbf{v}_2 = 0$). Application of (3-288) yields

$$k_{12} \frac{\Delta x_1}{\bar{x}_1} = -\bar{\mathbf{v}}_1 \tag{3-289}$$

or

$$N_1 = c\bar{\mathbf{v}}_1 \bar{x}_1 = -ck_{12}\Delta x_1 \tag{3-290}$$

The result in (3-290), obtained from the Maxwell–Stefan difference equation, is consistent with (3-35) for dilute ($x_2 \sim 1$) solutions, which was obtained from Fick's law.

Nondilute stripping

For this situation, $\bar{x}_1 = 0.5 = \bar{x}_2$, and drift occurs in the gas film. From (3-288),

$$k_{12} \frac{\Delta x_1}{\bar{x}_1} = -0.5 \cdot \bar{\mathbf{v}}_1 \tag{3-291}$$

for which

$$N_1 = c\bar{\mathbf{v}}_1 \bar{x}_1 = -2ck_{12}\Delta x_1 \tag{3-292}$$

The latter result is easily obtained using (3-288) without requiring a drift-correction, as Fick's law would have.

Concentration polarization in tangential flow filtration

Now consider the flux of water (2) through a semipermeable membrane that completely retains a dissolved salt (1) at dilute concentration ($x_2 \approx 1$), as discussed in [77]. Set the velocity of the salt equal to a stationary value in the frame of reference ($\mathbf{v}_1 = 0$). The average salt concentration in a film of thickness δ adjacent to the membrane is

$$\bar{x}_1 = x_{1o} + \frac{x_{1\delta} - x_{1o}}{2} = x_{1o} + \frac{\Delta x_1}{2} \tag{3-293}$$

Using (3-288) gives

$$k_{12} \frac{\Delta x_1}{\bar{x}_1} = \bar{\mathbf{v}}_2 \tag{3-294}$$

Combining (3-293) and (3-294) gives the increase in salt concentration in the film relative to its value in the bulk:

$$\frac{\Delta x_1}{x_{1o}} = \frac{2\dfrac{\bar{\mathbf{v}}_2}{k_{12}}}{2 - \dfrac{\bar{\mathbf{v}}_2}{k_{12}}} \tag{3-295}$$

EXAMPLE 3.26 Flux in Tangential-Flow Filtration.

Relate flux of permeate, j, in tangential-flow filtration to local wall concentration of a completely retained solute, i, using the Maxwell–Stefan difference equation.

Solution

Local permeate flux is given by $N_j = \bar{c}_j \bar{\mathbf{v}}_j$. An expression for local water velocity is obtained by solving (3-295) for $\bar{\mathbf{v}}_j$:

$$\bar{\mathbf{v}}_j = k_{ij} \frac{\Delta x_i}{\Delta x_i/2 + x_{i,b}} \approx k_{ij} \ln \frac{x_{i,w}}{x_{i,b}} \tag{3-296}$$

where subscripts b and w represent bulk feed and wall, respectively. In a film, $k_{ij} = D_{ij}/\delta$. Local permeate flux is then

$$N_j = c_j \frac{D_{ij}}{\delta} \ln \frac{x_{i,w}}{x_{i,b}} \tag{3-297}$$

The result is consistent with the classical stagnant-film model in (14-108), which was obtained using Fick's law.

EXAMPLE 3.27 Maxwell–Stefan Difference Equations Related to Fick's Law.

For a binary system containing species A and B, show how D_{AB} relates to D'_{AB} in the Maxwell–Stefan difference equation by relating (3-288) with the diffusive flux of species A relative to the molar-average velocity of a mixture in (3-3a),

$$J_{\mathrm{A}_z} = -D_{\mathrm{AB}} \frac{dc_{\mathrm{A}}}{dz} = c_{\mathrm{A}}(\mathbf{v}_{\mathrm{A}} - \mathbf{v}_M) \tag{3-298}$$

where $\mathbf{v}_M = x_{\mathrm{A}}\mathbf{v}_{\mathrm{A}} + x_{\mathrm{B}}\mathbf{v}_{\mathrm{B}}$ is the molar-average velocity of a mixture.

Solution

For a binary system, (3-288) becomes

$$\frac{1}{x_{\mathrm{A}}} \frac{dx_{\mathrm{A}}}{dz} = \bar{x}_{\mathrm{B}} \frac{\bar{\mathbf{v}}_{\mathrm{B}} - \bar{\mathbf{v}}_{\mathrm{A}}}{D'_{\mathrm{AB}}} = \frac{\bar{\mathbf{x}}_{\mathrm{B}}\bar{\mathbf{v}}_{\mathrm{B}} + \bar{\mathbf{x}}_{\mathrm{A}}\bar{\mathbf{v}}_{\mathrm{A}} - \bar{\mathbf{v}}_{\mathrm{A}}}{D'_{\mathrm{AB}}} = -\frac{\bar{\mathbf{v}}_{\mathrm{A}} - \mathbf{v}_M}{\mathbf{D}'_{\mathrm{AB}}} \tag{3-299}$$

Comparing (3-298) and (3-299) shows that for the Maxwell–Stefan difference equation

$$D'_{\mathrm{AB}} = D_{AB} \tag{3-300}$$

The result in (3-300) is consistent with kinetic theory for multicomponent mixtures of low-density gases, for which $\gamma_i = 1$ and $\mathbf{d}_i = \nabla x_i$ for concentration diffusion.

This abbreviated introduction to the Maxwell–Stefan relations has shown how this kinetic formulation yields diffusive flux of species proportional to its concentration gradient like Fick's law for binary mixtures, *and* provides a basis for examining molecular motion in separations based on additional driving forces such as temperature, pressure, and body forces. For multicomponent mixtures that are typical of bioseparations, the relations also quantitatively identify how the flux of each species affects the transport of any one species. This approach yields concentration gradients of each species in terms of the fluxes of the other species, which often requires expensive computational inversion. Fick's law may be generalized to obtain single-species flux in terms of concentration gradients for all species, but the resulting Fickian multicomponent diffusion coefficients are conjugates of the binary diffusion coefficients. The linearized Maxwell–Stefan difference equation allows straightforward analysis of driving forces due to concentration-, pressure-, body force-, and temperature-driving forces in complex separations like bioproduct purification, with accuracy adequate for many applications.

SUMMARY

1. Mass transfer is the net movement of a species in a mixture from one region to a region of different concentration, often between two phases across an interface. Mass transfer occurs by molecular diffusion, eddy diffusion, and bulk flow. Molecular diffusion occurs by a number of different driving forces, including concentration (ordinary), pressure, temperature, and external force fields.
2. Fick's first law for steady-state diffusion states that the mass-transfer flux by ordinary molecular diffusion is equal to the product of the diffusion coefficient (diffusivity) and the concentration gradient.
3. Two limiting cases of mass transfer in a binary mixture are equimolar counterdiffusion (EMD) and unimolecular diffusion (UMD). The former is also a good approximation for distillation. The latter includes bulk-flow effects.
4. When data are unavailable, diffusivities (diffusion coefficients) in gases and liquids can be estimated. Diffusivities in solids, including porous solids, crystalline solids, metals, glass, ceramics, polymers, and cellular solids, are best measured. For some solids, e.g., wood, diffusivity is anisotropic.
5. Diffusivities vary by orders of magnitude. Typical values are 0.10, 1×10^{-5}, and 1×10^{-9} $\mathrm{cm^2/s}$ for ordinary molecular diffusion of solutes in a gas, liquid, and solid, respectively.
6. Fick's second law for unsteady-state diffusion is readily applied to semi-infinite and finite stagnant media, including anisotropic materials.
7. Molecular diffusion under laminar-flow conditions is determined from Fick's first and second laws, provided velocity profiles are available. Common cases include falling liquid-film flow, boundary-layer flow on a flat plate, and fully developed flow in a straight, circular tube. Results are often expressed in terms of a mass-transfer coefficient embedded in a dimensionless group called the Sherwood number. The mass-transfer flux is given by the product of the mass-transfer coefficient and a concentration-driving force.
8. Mass transfer in turbulent flow can be predicted by analogy to heat transfer. The Chilton–Colburn analogy utilizes empirical *j*-factor correlations with a Stanton number for mass transfer. A more accurate equation by Churchill and Zajic should be used for flow in tubes, particularly at high Reynolds numbers.
9. Models are available for mass transfer near a two-fluid interface. These include film theory, penetration theory, surface-renewal theory, and the film-penetration theory. These predict mass-transfer coefficients proportional to the diffusivity raised to an exponent that varies from 0.5 to 1.0. Most experimental data provide exponents ranging from 0.5 to 0.75.
10. Whitman's two-film theory is widely used to predict the mass-transfer flux from one fluid, across an interface, and into another fluid, assuming equilibrium at the interface. One resistance is often controlling. The theory defines an overall mass-transfer coefficient determined from the separate coefficients for each of the phases and the equilibrium relationship at the interface.
11. The Maxwell–Stefan relations express molecular motion of species in multicomponent mixtures in terms of potential gradients due to composition, pressure, temperature, and body forces such as gravitational, centripetal, and electrostatic forces. This formulation is useful to characterize driving forces in addition to chemical potential, that act on charged biomolecules in typical bioseparations.

REFERENCES

1. Taylor, R., and R. Krishna, *Multicomponent Mass Transfer*, John Wiley & Sons, New York (1993).

2. Poling, B.E., J.M. Prausnitz, and J.P. O'Connell, *The Properties of Liquids and Gases*, 5th ed., McGraw-Hill, New York (2001).

3. Fuller, E.N., P.D. Schettler, and J.C. Giddings, *Ind. Eng. Chem.*, **58**(5), 18–27 (1966).

4. Takahashi, S., *J. Chem. Eng. Jpn.*, **7**, 417–420 (1974).

5. Slattery, J.C., M.S. thesis, University of Wisconsin, Madison (1955).

6. Wilke, C.R., and P. Chang, *AIChE J.*, **1**, 264–270 (1955).

7. Hayduk, W., and B.S. Minhas, *Can. J. Chem. Eng.*, **60**, 295–299 (1982).

8. Quayle, O.R., *Chem. Rev.*, **53**, 439–589 (1953).

9. Vignes, A., *Ind. Eng. Chem. Fundam.*, **5**, 189–199 (1966).

10. Sorber, H.A., *Handbook of Biochemistry, Selected Data for Molecular Biology*, 2nd ed., Chemical Rubber Co., Cleveland, OH (1970).

11. Geankoplis, C.J., *Transport Processes and Separation Process Principles*, 4th ed., Prentice-Hall, Upper Saddle River, NJ (2003).

12. Friedman, L., and E.O. Kraemer, *J. Am. Chem. Soc.*, **52**, 1298–1314, (1930).

13. Boucher, D.F., J.C. Brier, and J.O. Osburn, *Trans. AIChE*, **38**, 967–993 (1942).

14. Barrer, R.M., *Diffusion in and through Solids*, Oxford University Press, London (1951).

15. Swets, D.E., R.W., Lee, and R.C Frank, *J. Chem. Phys.*, **34**, 17–22 (1961).

16. Lee, R.W., *J. Chem, Phys.*, **38**, 448–455 (1963).

17. Williams, E.L., *J. Am. Ceram. Soc.*, **48**, 190–194 (1965).

18. Sucov, E.W, *J. Am. Ceram. Soc.*, **46**, 14–20 (1963).

19. Kingery, W.D., H.K. Bowen, and D.R. Uhlmann, *Introduction to Ceramics*, 2nd ed., John Wiley & Sons, New York (1976).

20. Ferry, J.D., *Viscoelastic Properties of Polymers*, John Wiley & Sons, New York (1980).

21. Rhee, C.K., and J.D. Ferry, *J. Appl. Polym. Sci.*, **21**, 467–476 (1977).

22. Brandrup, J., and E.H. Immergut, Eds., *Polymer Handbook*, 3rd ed., John Wiley & Sons, New York (1989).

23. Gibson, L.J., and M.F. Ashby, *Cellular Solids, Structure and Properties*, Pergamon Press, Elmsford, NY (1988).

24. Stamm, A.J., *Wood and Cellulose Science*, Ronald Press, New York (1964).

25. Sherwood, T.K., *Ind. Eng. Chem.*, **21**, 12–16 (1929).

26. Carslaw, H.S., and J.C. Jaeger, *Heat Conduction in Solids*, 2nd ed., Oxford University Press, London (1959).

27. Crank, J., *The Mathematics of Diffusion*, Oxford University Press, London (1956).

28. Bird, R.B., W.E. Stewart, and E.N. Lightfoot, *Transport Phenomena*, 2nd ed., John Wiley & Sons, New York (2002).

29. Churchill, R.V., *Operational Mathematics*, 2nd ed., McGraw-Hill, New York (1958).

30. Abramowitz, M., and I. A. Stegun, Eds., *Handbook of Mathematical Functions*, National Bureau of Standards, Applied Mathematics Series 55, Washington, DC (1964).

31. Newman, A.B., *Trans. AIChE*, **27**, 310–333 (1931).

32. Grimley, S.S., *Trans. Inst. Chem. Eng.* (London), **23**, 228–235 (1948).

33. Johnstone, H.F., and R.L. Pigford, *Trans. AIChE*, **38**, 25–51 (1942).

34. Olbrich, W.E., and J.D. Wild, *Chem. Eng. Sci.*, **24**, 25–32 (1969).

35. Churchill, S.W., *The Interpretation and Use of Rate Data: The Rate Concept*, McGraw-Hill, New York (1974).

36. Churchill, S.W., and R. Usagi, *AIChE J.*, **18**, 1121–1128 (1972).

37. Emmert, R.E., and R.L. Pigford, *Chem. Eng. Prog.*, **50**, 87–93 (1954).

38. Prandtl, L., *Proc. 3rd Int. Math. Congress*, Heidelberg (1904); reprinted in *NACA Tech. Memo 452* (1928).

39. Blasius, H., *Z. Math Phys.*, **56**, 1–37 (1908) reprinted in *NACA Tech. Memo 1256* (1950).

40. Schlichting, H., *Boundary Layer Theory*, 4th ed., McGraw-Hill, New York (1960).

41. Pohlhausen, E., *Z. Angew. Math Mech.*, **1**, 252 (1921).

42. Pohlhausen, E., *Z. Angew. Math Mech.*, **1**, 115–121 (1921).

43. Langhaar, H.L., *Trans. ASME*, **64**, A–55 (1942).

44. Graetz, L., *Ann. d. Physik*, **25**, 337–357 (1885).

45. Sellars, J.R., M. Tribus, and J.S. Klein, *Trans. ASME*, **78**, 441–448 (1956).

46. Leveque, J., *Ann. Mines*, [12], **13**, 201, 305, 381 (1928).

47. Knudsen, J.G., and D.L. Katz, *Fluid Dynamics and Heat Transfer*, McGraw-Hill, New York (1958).

48. Hausen, H., *Verfahrenstechnik Beih. z. Ver. Deut. Ing.*, **4**, 91 (1943).

49. Linton, W.H., Jr., and T.K. Sherwood, *Chem. Eng. Prog.*, **46**, 258–264 (1950).

50. Reynolds, O., *Trans. Roy. Soc. (London)*, **174A**, 935–982 (1883).

51. Boussinesq, J., *Mem. Pre. Par. Div. Sav.*, XXIII, Paris (1877).

52. Prandtl, L., *Z. Angew, Math Mech.*, **5**, 136 (1925); reprinted in *NACA Tech. Memo 1231* (1949).

53. Reynolds, O., *Proc. Manchester Lit. Phil. Soc.*, **14**, 7 (1874).

54. Colburn, A.P., *Trans. AIChE*, **29**, 174–210 (1933).

55. Chilton, T.H., and A.P. Colburn, *Ind. Eng. Chem.*, **26**, 1183–1187 (1934).

56. Prandtl, L., *Physik. Z.*, **11**, 1072 (1910).

57. Friend, W.L., and A.B. Metzner, *AIChE J.*, **4**, 393–402 (1958).

58. Nernst, W., *Z. Phys. Chem.*, **47**, 52 (1904).

59. Higbie, R., *Trans. AIChE*, **31**, 365–389 (1935).

60. Danckwerts, P.V., *Ind. Eng. Chem.*, **43**, 1460–1467 (1951).

61. Levenspiel, O., *Chemical Reaction Engineering*, 3rd ed., John Wiley & Sons, New York (1999).

62. Toor, H.L., and J.M. Marchello, *AIChE J.*, **4**, 97–101 (1958).

63. Whitman, W.G., *Chem. Met. Eng.*, **29**, 146–148 (1923).

64. van Driest, E.R., *J. Aero Sci.*, 1007–1011, 1036 (1956).

65. Reichardt, H., Fundamentals of Turbulent Heat Transfer, NACA Report TM-1408 (1957).

66. Drew, T.B., E.C. Koo, and W.H. McAdams, *Trans. Am. Inst. Chem. Engrs.*, **28**, 56 (1933).

67. Nikuradse, J., *VDI-Forschungsheft*, p. 361 (1933).

68. Launder, B.E., and D.B. Spalding, *Lectures in Mathematical Models of Turbulence*, Academic Press, New York (1972).

69. Heng, L., C. Chan, and S.W. Churchill, *Chem. Eng. J.*, **71**, 163 (1998).

70. Churchill, S.W., and S.C. Zajic, *AIChE J.*, **48**, 927–940 (2002).

71. Churchill, S.W., "Turbulent Flow and Convection: The Prediction of Turbulent Flow and Convection in a Round Tube," in J.P. Hartnett and T.F. Irvine, Jr., Ser. Eds., *Advances in Heat Transfer*, Academic Press, New York, Vol. 34, pp. 255–361 (2001).

72. Yu, B., H. Ozoe, and S.W. Churchill, *Chem. Eng. Sci.*, **56**, 1781 (2001).

73. Churchill, S.W., and C. Chan, *Ind. Eng. Chem. Res.*, **34**, 1332 (1995).

74. Churchill, S.W., *AIChE J.*, **43**, 1125 (1997).

75. Lightfoot, E.N., *Transport Phenomena and Living Systems*, John Wiley & Sons, New York (1974).

76. Taylor, R., and R. Krishna, *Multicomponent Mass Transfer*, John Wiley & Sons, New York (1993).

77. Wesselingh, J.A., and R. Krishna, *Mass Transfer in Multicomponent Mixtures*, Delft University Press, Delft (2000).

78. Cantor, C.R., and P.R. Schimmel, *Biophysical Chemistry Part II. Techniques for the study of biological structure and function*, W.H. Freeman and Co., New York (1980).

STUDY QUESTIONS

3.1. What is meant by diffusion?

3.2. Molecular diffusion occurs by any of what four driving forces or potentials? Which one is the most common?

3.3. What is the bulk-flow effect in mass transfer?

3.4. How does Fick's law of diffusion compare to Fourier's law of heat conduction?

3.5. What is the difference between equimolar counterdiffusion (EMD) and unimolecular diffusion (UMD)?

3.6. What is the difference between a mutual diffusion coefficient and a self-diffusion coefficient?

3.7. At low pressures, what are the effects of temperature and pressure on the molecular diffusivity of a species in a binary gas mixture?

3.8. What is the order of magnitude of the molecular diffusivity in cm^2/s for a species in a liquid mixture? By how many orders of magnitude is diffusion in a liquid slower or faster than diffusion in a gas?

3.9. By what mechanisms does diffusion occur in porous solids?

3.10. What is the effective diffusivity?

3.11. Why is diffusion in crystalline solids much slower than diffusion in amorphous solids?

3.12. What is Fick's second law of diffusion? How does it compare to Fourier's second law of heat conduction?

3.13. Molecular diffusion in gases, liquids, and solids ranges from slow to extremely slow. What is the best way to increase the rate of mass transfer in fluids? What is the best way to increase the rate of mass transfer in solids?

3.14. What is the defining equation for a mass-transfer coefficient? How does it differ from Fick's law? How is it analogous to Newton's law of cooling?

3.15. For laminar flow, can expressions for the mass-transfer coefficient be determined from theory using Fick's law? If so, how?

3.16. What is the difference between Reynolds analogy and the Chilton–Colburn analogy? Which is more useful?

3.17. For mass transfer across a phase interface, what is the difference between the film, penetration, and surface-renewal theories, particularly with respect to the dependence on diffusivity?

3.18. What is the two-film theory of Whitman? Is equilibrium assumed to exist at the interface of two phases?

3.19. What advantages do the Maxwell–Stefan relations provide for multicomponent mixtures containing charged biomolecules, in comparison with Fick's law?

3.20. How do transport parameters and coefficients obtained from the Maxwell–Stefan relations compare with corresponding values resulting from Fick's law?

EXERCISES

Section 3.1

3.1. Evaporation of liquid from a beaker.

A beaker filled with an equimolar liquid mixture of ethyl alcohol and ethyl acetate evaporates at 0°C into still air at 101 kPa (1 atm). Assuming Raoult's law, what is the liquid composition when half the ethyl alcohol has evaporated, assuming each component evaporates independently? Also assume that the liquid is always well mixed. The following data are available:

	Vapor Pressure, kPa at 0°C	Diffusivity in Air m^2/s
Ethyl acetate (AC)	3.23	6.45×10^{-6}
Ethyl alcohol (AL)	1.62	9.29×10^{-6}

3.2. Evaporation of benzene from an open tank.

An open tank, 10 ft in diameter, containing benzene at 25°C is exposed to air. Above the liquid surface is a stagnant air film 0.2 in. thick. If the pressure is 1 atm and the air temperature is 25°C, what is the loss of benzene in lb/day? The specific gravity of benzene at 60°F is 0.877. The concentration of benzene outside the film is negligible. For benzene, the vapor pressure at 25°C is 100 torr, and the diffusivity in air is 0.08 cm^2/s.

3.3. Countercurrent diffusion across a vapor film.

An insulated glass tube and condenser are mounted on a reboiler containing benzene and toluene. The condenser returns liquid reflux down the wall of the tube. At one point in the tube, the temperature is 170°F, the vapor contains 30 mol% toluene, and the reflux contains 40 mol% toluene. The thickness of the stagnant vapor film is estimated to be 0.1 in. The molar latent heats of benzene and toluene are equal. Calculate the rate at which toluene and benzene are being interchanged by equimolar countercurrent diffusion at this point in the tube in lbmol/h-ft^2, assuming that the rate is controlled by mass transfer in the vapor phase.

Gas diffusivity of toluene in benzene = 0.2 ft^2/h. Pressure = 1 atm (in the tube). Vapor pressure of toluene at 170°F = 400 torr.

3.4. Rate of drop in water level during evaporation.

Air at 25°C and a dew-point temperature of 0°C flows past the open end of a vertical tube filled with water at 25°C. The tube has an inside diameter of 0.83 inch, and the liquid level is 0.5 inch below the top of the tube. The diffusivity of water in air at 25°C is 0.256 cm^2/s.

(a) How long will it take for the liquid level in the tube to drop 3 inches?

(b) Plot the tube liquid level as a function of time for this period.

3.5. Mixing of two gases by molecular diffusion.

Two bulbs are connected by a tube, 0.002 m in diameter and 0.20 m long. Bulb 1 contains argon, and bulb 2 contains xenon. The pressure

and temperature are maintained at 1 atm and 105°C. The diffusivity is 0.180 cm^2/s. At time $t = 0$, diffusion occurs between the two bulbs. How long will it take for the argon mole fraction at End 1 of the tube to be 0.75, and 0.20 at the other end? Determine at the later time the: (a) Rates and directions of mass transfer of argon and xenon; (b) Transport velocity of each species; (c) Molar-average velocity of the mixture.

Section 3.2

3.6. Measurement of diffusivity of toluene in air.

The diffusivity of toluene in air was determined experimentally by allowing liquid toluene to vaporize isothermally into air from a partially filled, 3-mm diameter, vertical tube. At a temperature of 39.4°C, it took 96×10^4 s for the level of the toluene to drop from 1.9 cm below the top of the open tube to a level of 7.9 cm below the top. The density of toluene is 0.852 g/cm^3, and the vapor pressure is 57.3 torr at 39.4°C. The barometer reading was 1 atm. Calculate the diffusivity and compare it with the value predicted from (3-36). Neglect the counterdiffusion of air.

3.7. Countercurrent molecular diffusion of H_2 and N_2 in a tube.

An open tube, 1 mm in diameter and 6 in. long, has hydrogen blowing across one end and nitrogen across the other at 75°C.

(a) For equimolar counterdiffusion, what is the rate of transfer of hydrogen into nitrogen in mol/s? Estimate the diffusivity (3-36).

(b) For part (a), plot the mole fraction of hydrogen against distance from the end of the tube past which nitrogen is blown.

3.8. Molecular diffusion of HCl across an air film.

HCl gas diffuses through a film of air 0.1 in. thick at 20°C. The partial pressure of HCl on one side of the film is 0.08 atm and zero on the other. Estimate the rate of diffusion in mol HCl/s-cm^2, if the total pressure is (a) 10 atm, (b) 1 atm, (c) 0.1 atm. The diffusivity of HCl in air at 20°C and 1 atm is 0.145 cm^2/s.

3.9. Estimation of gas diffusivity.

Estimate the diffusion coefficient for a binary gas mixture of nitrogen (A)/toluene (B) at 25°C and 3 atm using the method of Fuller et al.

3.10. Correction of gas diffusivity for high pressure.

For the mixture of Example 3.3, estimate the diffusion coefficient at 100 atm using the method of Takahashi.

3.11. Estimation of infinite-dilution liquid diffusivity.

Estimate the diffusivity of carbon tetrachloride at 25°C in a dilute solution of: (a) methanol, (b) ethanol, (c) benzene, and (d) *n*-hexane by the methods of Wilke–Chang and Hayduk–Minhas. Compare values with the following experimental observations:

Solvent	Experimental D_{AB}, cm^2/s
Methanol	1.69×10^{-5} cm^2/s at 15°C
Ethanol	1.50×10^{-5} cm^2/s at 25°C
Benzene	1.92×10^{-5} cm^2/s at 25°C
n-Hexane	3.70×10^{-5} cm^2/s at 25°C

3.12. Estimation of infinite-dilution liquid diffusivity.

Estimate the liquid diffusivity of benzene (A) in formic acid (B) at 25°C and infinite dilution. Compare the estimated value to that of Example 3.6 for formic acid at infinite dilution in benzene.

3.13. Estimation of infinite-dilution liquid diffusivity in solvents.

Estimate the liquid diffusivity of acetic acid at 25°C in a dilute solution of: (a) benzene, (b) acetone, (c) ethyl acetate, and (d) water. Compare your values with the following data:

Solvent	Experimental D_{AB}, cm^2/s
Benzene	2.09×10^{-5} cm^2/s at 25°C
Acetone	2.92×10^{-5} cm^2/s at 25°C
Ethyl acetate	2.18×10^{-5} cm^2/s at 25°C
Water	1.19×10^{-5} cm^2/s at 20°C

3.14. Vapor diffusion through an effective film thickness.

Water in an open dish exposed to dry air at 25°C vaporizes at a constant rate of 0.04 g/h-cm^2. If the water surface is at the wet-bulb temperature of 11.0°C, calculate the effective gas-film thickness (i.e., the thickness of a stagnant air film that would offer the same resistance to vapor diffusion as is actually encountered).

3.15. Diffusion of alcohol through water and N_2.

Isopropyl alcohol undergoes mass transfer at 35°C and 2 atm under dilute conditions through water, across a phase boundary, and then through nitrogen. Based on the data given below, estimate for isopropyl alcohol: (a) the diffusivity in water using the Wilke–Chang equation; (b) the diffusivity in nitrogen using the Fuller et al. equation; (c) the product, $D_{AB}\rho_M$, in water; and (d) the product, $D_{AB}\rho_M$, in air, where ρ_M is the mixture molar density.

Compare: (e) the diffusivities in parts (a) and (b); (f) the results from parts (c) and (d). (g) What do you conclude about molecular diffusion in the liquid phase versus the gaseous phase?

Data:	Component	T_c, °R	P_c, psia	Z_c	v_L, cm^3/mol
	Nitrogen	227.3	492.9	0.289	—
	Isopropyl alcohol	915	691	0.249	76.5

3.16. Estimation of liquid diffusivity over the entire composition range.

Experimental liquid-phase activity-coefficient data are given in Exercise 2.23 for ethanol-benzene at 45°C. Estimate and plot diffusion coefficients for both chemicals versus composition.

3.17. Estimation of the diffusivity of an electrolyte.

Estimate the diffusion coefficient of NaOH in a 1-M aqueous solution at 25°C.

3.18. Estimation of the diffusivity of an electrolyte.

Estimate the diffusion coefficient of NaCl in a 2-M aqueous solution at 18°C. The experimental value is 1.28×10^{-5} cm^2/s.

3.19. Estimation of effective diffusivity in a porous solid.

Estimate the diffusivity of N_2 in H_2 in the pores of a catalyst at 300°C and 20 atm if the porosity is 0.45 and the tortuosity is 2.5. Assume ordinary molecular diffusion in the pores.

3.20. Diffusion of hydrogen through a steel wall.

Hydrogen at 150 psia and 80°F is stored in a spherical, steel pressure vessel of inside diameter 4 inches and a wall thickness of 0.125 inch. The solubility of hydrogen in steel is 0.094 $lbmol/ft^3$, and the diffusivity of hydrogen in steel is 3.0×10^{-9} cm^2/s. If the inner surface of the vessel remains saturated at the existing hydrogen pressure and the hydrogen partial pressure at the outer surface

is assumed to be zero, estimate the: (a) initial rate of mass transfer of hydrogen through the wall; (b) initial rate of pressure decrease inside the vessel; and (c) time in hours for the pressure to decrease to 50 psia, assuming the temperature stays constant at 80°F.

3.21. Mass transfer of gases through a dense polymer membrane.

A polyisoprene membrane of 0.8-μm thickness is used to separate methane from H_2. Using data in Table 14.9 and the following partial pressures, estimate the mass-transfer fluxes.

	Partial Pressures, MPa	
	Membrane Side 1	Membrane Side 2
Methane	2.5	0.05
Hydrogen	2.0	0.20

Section 3.3

3.22. Diffusion of NaCl into stagnant water.

A 3-ft depth of stagnant water at 25°C lies on top of a 0.10-in. thickness of NaCl. At time < 0, the water is pure. At time = 0, the salt begins to dissolve and diffuse into the water. If the concentration of salt in the water at the solid–liquid interface is maintained at saturation (36 g NaCl/100 g H_2O) and the diffusivity of NaCl is 1.2×10^{-5} cm^2/s, independent of concentration, estimate, by assuming the water to act as a semi-infinite medium, the time and the concentration profile of salt in the water when: (a) 10% of the salt has dissolved; (b) 50% of the salt has dissolved; and (c) 90% of the salt has dissolved.

3.23. Diffusion of moisture into wood.

A slab of dry wood of 4-inch thickness and sealed edges is exposed to air of 40% relative humidity. Assuming that the two unsealed faces of the wood immediately jump to an equilibrium moisture content of 10 lb H_2O per 100 lb of dry wood, determine the time for the moisture to penetrate to the center of the slab (2 inches from each face). Assume a diffusivity of water of 8.3×10^{-6} cm^2/s.

3.24. Measurement of moisture diffusivity in a clay brick.

A wet, clay brick measuring $2 \times 4 \times 6$ inches has an initial uniform water content of 12 wt%. At time = 0, the brick is exposed on all sides to air such that the surface moisture content is maintained at 2 wt%. After 5 h, the average moisture content is 8 wt%. Estimate: (a) the diffusivity of water in the clay in cm^2/s; and (b) the additional time for the average moisture content to reach 4 wt%. All moisture contents are on a dry basis.

3.25. Diffusion of moisture from a ball of clay.

A spherical ball of clay, 2 inches in diameter, has an initial moisture content of 10 wt%. The diffusivity of water in the clay is 5×10^{-6} cm^2/s. At time $t = 0$, the clay surface is brought into contact with air, and the moisture content at the surface is maintained at 3 wt%. Estimate the time for the average sphere moisture content to drop to 5 wt%. All moisture contents are on a dry basis.

Section 3.4

3.26. Diffusion of oxygen in a laminar-flowing film of water.

Estimate the rate of absorption of oxygen at 10 atm and 25°C into water flowing as a film down a vertical wall 1 m high and 6 cm in width at a Reynolds number of 50 without surface ripples. Diffusivity of oxygen in water is 2.5×10^{-5} cm^2/s and the mole fraction of oxygen in water at saturation is 2.3×10^{-4}.

3.27. Diffusion of carbon dioxide in a laminar-flowing film of water.

For Example 3.13, determine at what height the average concentration of CO_2 would correspond to 50% saturation.

3.28. Evaporation of water from a film on a flat plate into flowing air.

Air at 1 atm flows at 2 m/s across the surface of a 2-inch-long surface that is covered with a thin film of water. If the air and water are at 25°C and the diffusivity of water in air is 0.25 cm^2/s, estimate the water mass flux for the evaporation of water at the middle of the surface, assuming laminar boundary-layer flow. Is this assumption reasonable?

3.29. Diffusion of a thin plate of naphthalene into flowing air.

Air at 1 atm and 100°C flows across a thin, flat plate of subliming naphthalene that is 1 m long. The Reynolds number at the trailing edge of the plate is at the upper limit for a laminar boundary layer. Estimate: (a) the average rate of sublimation in kmol/s-m^2; and (b) the local rate of sublimation 0.5 m from the leading edge. Physical properties are given in Example 3.14.

3.30. Sublimation of a circular naphthalene tube into flowing air.

Air at 1 atm and 100°C flows through a straight, 5-cm i.d. tube, cast from naphthalene, at a Reynolds number of 1,500. Air entering the tube has an established laminar-flow velocity profile. Properties are given in Example 3.14. If pressure drop is negligible, calculate the length of tube needed for the average mole fraction of naphthalene in the exiting air to be 0.005.

3.31. Evaporation of a spherical water drop into still, dry air.

A spherical water drop is suspended from a fine thread in still, dry air. Show: (a) that the Sherwood number for mass transfer from the surface of the drop into the surroundings has a value of 2, if the characteristic length is the diameter of the drop. If the initial drop diameter is 1 mm, the air temperature is 38°C, the drop temperature is 14.4°C, and the pressure is 1 atm, calculate the: (b) initial mass of the drop in grams; (c) initial rate of evaporation in grams per second; (d) time in seconds for the drop diameter to be 0.2 mm; and (e) initial rate of heat transfer to the drop. If the Nusselt number is also 2, is the rate of heat transfer sufficient to supply the required heat of vaporization and sensible heat? If not, what will happen?

Section 3.5

3.32. Dissolution of a tube of benzoic acid into flowing water.

Water at 25°C flows turbulently at 5 ft/s through a straight, cylindrical tube cast from benzoic acid, of 2-inch i.d. If the tube is 10 ft long, and fully developed, turbulent flow is assumed, estimate the average concentration of acid in the water leaving the tube. Physical properties are in Example 3.15.

3.33. Sublimation of a naphthalene cylinder to air flowing normal to it.

Air at 1 atm flows at a Reynolds number of 50,000 normal to a long, circular, 1-in.-diameter cylinder made of naphthalene. Using the physical properties of Example 3.14 for a temperature of 100°C, calculate the average sublimation flux in kmol/s-m^2.

3.34. Sublimation of a naphthalene sphere to air flowing past it.

For the conditions of Exercise 3.33, calculate the initial average rate of sublimation in kmol/s-m^2 for a spherical particle of 1-inch

initial diameter. Compare this result to that for a bed packed with naphthalene spheres with a void fraction of 0.5.

Section 3.6

3.35. Stripping of CO_2 from water by air in a wetted-wall tube.

Carbon dioxide is stripped from water by air in a wetted-wall tube. At a location where pressure is 10 atm and temperature 25°C, the flux of CO_2 is 1.62 lbmol/h-ft^2. The partial pressure of CO_2 is 8.2 atm at the interface and 0.1 atm in the bulk gas. The diffusivity of CO_2 in air at these conditions is 1.6×10^{-2} cm^2/s. Assuming turbulent flow, calculate by film theory the mass-transfer coefficient k_c for the gas phase and the film thickness.

3.36. Absorption of CO_2 into water in a packed column.

Water is used to remove CO_2 from air by absorption in a column packed with Pall rings. At a region of the column where the partial pressure of CO_2 at the interface is 150 psia and the concentration in the bulk liquid is negligible, the absorption rate is 0.017 lbmol/h-ft^2. The CO_2 diffusivity in water is 2.0×10^{-5} cm^2/s. Henry's law for CO_2 is $p = Hx$, where $H = 9{,}000$ psia. Calculate the: (a) liquid-phase mass-transfer coefficient and film thickness; (b) contact time for the penetration theory; and (c) average eddy residence time and the probability distribution for the surface-renewal theory.

3.37. Determination of diffusivity of H_2S in water.

Determine the diffusivity of H_2S in water, using penetration theory, from the data below for absorption of H_2S into a laminar jet of water at 20°C. Jet diameter = 1 cm, jet length = 7 cm, and solubility of H_2S in water = 100 mol/m^3. Assume the contact time is the time of exposure of the jet. The average rate of absorption varies with jet flow rate:

Jet Flow Rate, cm^3/s	Rate of Absorption, mol/s $\times 10^6$
0.143	1.5
0.568	3.0
1.278	4.25
2.372	6.15
3.571	7.20
5.142	8.75

Section 3.7

3.38. Vaporization of water into air in a wetted-wall column.

In a test on the vaporization of H_2O into air in a wetted-wall column, the following data were obtained: tube diameter = 1.46 cm; wetted-tube length = 82.7 cm; air rate to tube at 24°C and 1 atm = 720 cm^3/s; inlet and outlet water temperatures are 25.15°C and 25.35°C, respectively; partial pressure of water in inlet air is 6.27 torr and in outlet air is 20.1 torr. The diffusivity of water vapor in air is 0.22 cm^2/s at 0°C and 1 atm. The mass velocity of air is taken relative to the pipe wall. Calculate: (a) rate of mass transfer of water into the air; and (b) K_G for the wetted-wall column.

3.39. Absorption of NH_3 from air into aq. H_2SO_4 in a wetted-wall column.

The following data were obtained by Chamber and Sherwood [*Ind. Eng. Chem.*, **29,** 1415 (1937)] on the absorption of ammonia from an ammonia-air mixture by a strong acid in a wetted-wall column 0.575 inch in diameter and 32.5 inches long:

Inlet acid (2-N H_2SO_4) temperature, °F	76
Outlet acid temperature, °F	81
Inlet air temperature, °F	77
Outlet air temperature, °F	84
Total pressure, atm	1.00
Partial pressure NH_3 in inlet gas, atm	0.0807
Partial pressure NH_3 in outlet gas, atm	0.0205
Air rate, lbmol/h	0.260

The operation was countercurrent, the gas entering at the bottom of the vertical tower and the acid passing down in a thin film on the vertical, cylindrical inner wall. The change in acid strength was negligible, and the vapor pressure of ammonia over the liquid is negligible because of the use of a strong acid for absorption. Calculate the mass-transfer coefficient, k_p, from the data.

3.40. Overall mass-transfer coefficient for a packed cooling tower.

A cooling-tower packing was tested in a small column. At two points in the column, 0.7 ft apart, the data below apply. Calculate the overall volumetric mass-transfer coefficient $K_y a$ that can be used to design a large, packed-bed cooling tower, where a is the mass-transfer area, A, per unit volume, V, of tower.

	Bottom	Top
Water temperature, °F	120	126
Water vapor pressure, psia	1.69	1.995
Mole fraction H_2O in air	0.001609	0.0882
Total pressure, psia	14.1	14.3
Air rate, lbmol/h	0.401	0.401
Column cross-sectional area, ft^2	0.5	0.5
Water rate, lbmol/h (approximation)	20	20

Section 3.8

3.41. Thermal diffusion.

Using the thermal diffusion apparatus of Example 3.22 with two bulbs at 0°C and 123°C, respectively, estimate the mole-fraction difference in H_2 at steady state from a mixture initially consisting of mole fractions 0.1 and 0.9 for D_2 and H_2, respectively.

3.42. Separation in a centrifugal force field.

Estimate the steady-state concentration profile for an aqueous ($\hat{V}_B = 1.0$ cm^3/g) solution of cytochrome C (12×10^3 Da; $x_{A_0} = 1 \times 10^{-6}$; $\hat{V}_A = 0.75$ cm^3/g) subjected to a centrifugal field 50×10^3 times the force of gravity in a rotor held at 4°C.

3.43. Diffusion in ternary mixture.

Two large bulbs, A and B, containing mixtures of H_2, N_2, and CO_2 at 1 atm and 35°C are separated by an 8.6-cm capillary. Determine the quasi-steady-state fluxes of the three species for the following conditions [77]:

	$x_{i,A}$	$x_{i,B}$	D'_{AB}, cm^2/s
H_2	0.0	0.5	$D'_{H_2\text{-}N_2} = 0.838$
N_2	0.5	0.5	$D'_{H_2\text{-}CO_2} = 0.168$
CO_2	0.5	0.0	$D'_{N_2\text{-}CO_2} = 0.681$